PENNSTATE

DOE/PC/92162--T7

THE DEVELOPMENT OF COAL-BASED TECHNOLOGIES FOR DEPARTMENT OF DEFENSE FACILITIES

Semiannual Technical Progress Report for the Period 03/28/1995 to 09/27/1995

By

Bruce G. Miller, Patrick Hatcher, Heike Knicker, and Alan W. Scaroni
Energy and Fuels Research Center;
Richard Hogg, Subhash Chander, Heechan Cho, M. Thaddeus Ityokumbul, Mark S. Klima, and Peter T. Luckie
Mineral Processing Section;
Adam Rose, Timothy J. Considine, Richard L. Gordon, Ahmet E. Kocagil, Jeffrey Lazo, and Katherine McClain
Department of Mineral Economics; and
Paul C. Painter and Boris Veytsman
Polymer Science Program

October 21, 1996

Work Performed Under Cooperative Agreement No. DE-FC22-92PC92162

For
U.S. Department of Energy
Pittsburgh Energy Technology Center
P.O. Box 10940
Pittsburgh, Pennsylvania 15236

By
The Consortium for Coal-Water Slurry Fuel Technology
The Pennsylvania State University
C211 Coal Utilization Laboratory
University Park, Pennsylvania 16802

DISCLAIMER

THE DEVELOPMENT OF COAL-BASED TECHNOLOGIES FOR DEPARTMENT OF DEFENSE FACILITIES

Semiannual Technical Progress Report for the Period 03/28/1995 to 09/27/1995

By

Bruce G. Miller, Patrick Hatcher, Heike Knicker and Alan W. Scaroni
Energy and Fuels Research Center;
Richard Hogg, Subhash Chander, Heechan Cho, M. Thaddeus Ityokumbul,
Mark S. Klima, and Peter T. Luckie
Mineral Processing Section;
Adam Rose, Timothy J. Considine, Richard L. Gordon, Ahmet E. Kocagil, Jeffrey Lazo,
and Katherine McClain,
Department of Mineral Economics; and
Paul C. Painter and Boris Veytsman
Polymer Science Program

October 21, 1996

Work Performed Under Cooperative Agreement No. DE-FC22-92PC92162

For
U.S. Department of Energy
Pittsburgh Energy Technology Center
P.O. Box 10940
Pittsburgh, Pennsylvania 15236

By
The Consortium for Coal-Water Slurry Fuel Technology
The Pennsylvania State University
C211 Coal Utilization Laboratory
University Park, Pennsylvania 16802

DISCLAIMER

EXECUTIVE SUMMARY

The U.S. Department of Defense (DOD), through an Interagency Agreement with the U.S. Department of Energy (DOE), has initiated a three-phase program with the Consortium for Coal-Water Mixture Technology, with the aim of decreasing DOD's reliance on imported oil by increasing its use of coal. The program is being conducted as a cooperative agreement between the Consortium and DOE.

Activities this reporting period are summarized by phase.

PHASE I

During this reporting period, preparation of the Phase I final report continued. The report is undergoing final review and will be submitted during the next reporting period.

PHASE II

Work in Phase II focused on emissions reductions, coal benefication/preparation studies, and economic analyses of coal use.

Emissions reductions investigations included initiating a study to indentify appropriate SO_2 and NO_x control technologies for coal-fired industrial boilers. In addition, work started on the design of a ceramic filtering device for installation on the demonstration boiler. The ceramic filtering device will be used to demonstrate a more compact and efficient filtering device for retrofit applications.

Coal preparation and utilization activities, and the economic analysis were completed and work focused on preparing the final report.

PHASE III

Work in Phase III focused on coal preparation studies and economic analyses of coal use.

Coal preparation studies were focused on continuing activities on particle size control, physical separations, surface-based separation processes, and dry processing.

The economic study focused on selecting incentives for commercialization of coal using technologies, community sensitivity to coal usage, regional economic impacts of new coal utilization technologies, and constructing a national energy portfolio.

TABLE OF CONTENTS

TABLE OF CONTENTS

LIST OF FIGURES

LIST OF TABLES

1.0 INTRODUCTION

The U.S. Department of Defense (DOD), through an Interagency Agreement with the U.S. Department of Energy (DOE), has entered into a cooperative agreement with the Consortium for Coal-Water Slurry Fuel Technology, with the aim of decreasing DOD's reliance on imported oil by increasing its use of coal.

To achieve the objectives of the program, the Consortium assembled a team of researchers from Penn State (Energy and Fuels Research Center (EFRC), Mineral Processing Section, Department of Mineral Economics, and Polymer Science Program) Energy and Environmental Research Corporation (EER), AMAX Research and Development Center and ABB Combustion Engineering.

Phase I activities focused on developing clean, coal-based combustion technologies for the utilization of both micronized coal-water mixtures (MCWMs) and dry, micronized coal (DMC) in fuel oil-designed industrial boilers. Phase II research and development activities continue to focus on industrial boiler retrofit technologies by developing ultra-low emissions control strategies when firing coal-based fuels in industrial boilers. Phase III activities are evaluating current DOD boiler operation and emissions, and examine coal-based fuel combustion systems that cofire wastes. Each phase includes an engineering cost analysis and technology assessment. The activities and status of the phases are described below.

The objective in Phase I was to deliver fully engineered retrofit options for a fuel oil-designed watertube boiler located on a DOD installation to fire either MCWM or DMC. This was achieved through a program consisting of the following five tasks: 1) Coal Beneficiation and Preparation; 2) Combustion Performance Evaluation; 3) Engineering Design; 4) Engineering and Economic Analysis; and 5) Final Report/Submission of Design Package. Outlines of the Phase I project tasks follow:

Task 1: Coal Beneficiation/Preparation

- Subtask 1.1 Identify/Procure Coals
- Subtask 1.2 Determine Liberation Potential
- Subtask 1.3 Produce Laboratory-Scale Quantities of Micronized Coal-Water Mixtures (MCWMs)
- Subtask 1.4 Develop Dry Coal Cleaning Technique
- Subtask 1.5 Produce MCWMs and Dry, Micronized Coal (DMC) From Dry Clean Coal
- Subtask 1.6 Produce MCWM and DMC for the Demonstration Boiler
- Subtask 1.7 Project Management and Support

Task 2: Combustion Performance Evaluation

- Subtask 2.1 Boiler Retrofit
- Subtask 2.2 Fuel Evaluation in the Research Boiler
- Subtask 2.3 Performance Evaluation of the MCWM and DMC in the Demonstration Boiler

Subtask 2.4 Evaluate Emissions Reductions Strategies
Subtask 2.5 Project Management and Support

Task 3: Engineering Design

Subtask 3.1 MCWM/DMC Preparation Facilities
Subtask 3.2 Fuel Handling
Subtask 3.3 Burner System
Subtask 3.4 Ash Removal, Handling, and Disposal
Subtask 3.5 Air Pollution Control
Subtask 3.6 Integrate Engineering Design
Subtask 3.7 Project Management and Support

Task 4: Engineering and Economic Analysis

Subtask 4.1 Survey Boiler Population/Identify Boilers for Conversion
Subtask 4.2 Identify Appropriate Cost-Estimating Methodologies
Subtask 4.3 Estimate Basic Costs of New Technologies
Subtask 4.4 Process Analysis of MCWM and DMC
Subtask 4.5 Analyze/Identify Transportation Cost of Commercial Sources of MCWM and Cleaned Coal for DMC Production
Subtask 4.6 Determine Community Spillovers
Subtask 4.7 Regional Market Considerations and Impacts
Subtask 4.8 Integrate the Analysis
Subtask 4.9 Project Management and Support

Task 5: Final Report/Submission of Design Package

Phase I activities included:

Task 1: The coal beneficiation and preparation effort was conducted by Penn State's Mineral Processing Section with assistance from Penn State's Polymer Science Program. This task involved identifying and procuring six coals that could be cleaned to <1.0 wt.% sulfur and <5.0 wt.% ash, which have been, or possess the characteristics to enable them to be, made into MCWMs. The coals were subjected to detailed characterization and used to produce laboratory-scale quantities of MCWM. A fundamental study of MCWM stabilization was conducted. Additional activities included developing a dry coal cleaning technique and producing MCWMs and DMC from the resulting cleaned coal.

Task 2: Penn State's EFRC conducted the combustion performance evaluation with assistance from EER and Penn State's Fuel Science Program. The technical aspects of converting a fuel oil-designed boiler at a DOD facility were identified in this task. All appropriate components were evaluated, including the fuel, the fuel storage, handling and delivery equipment, the burner, the boiler, the ash handling and disposal equipment, the emissions control system, and the boiler control system. Combustion performance as indicated by flame stability, completeness of combustion, and related issues such as system derating, changes in system maintenance, the occurrence of slagging, fouling, corrosion and erosion, and air pollutant emissions were determined. As part of this task, MCWM

and DMC were evaluated in EFRC's 15,000 lb steam/h watertube boiler. EER provided a coal-designed burner for retrofitting Penn State's boiler. In addition, EER designed a burner for the DOD boiler identified for retrofitting.

Task 3: An engineering study was conducted for a complete retrofit of a DOD boiler facility to fire either MCWM or DMC. The designs were performed by EER with input from the other project participants. The designs included the coal preparation, the fuel handling, the burner, the ash removal, handling, and disposal, and the air pollution control systems. The two designs were for the DOD boiler identified in Task 4. The retrofits were designed for community/societal acceptability. The deliverables for this task were detailed designs that could be used for soliciting bids from engineering/construction firms to retrofit the candidate DOD boiler.

Task 4: An engineering cost analysis and technology assessment of MCWM and DMC combustion were performed by Penn State's Department of Mineral Economics and EFRC with assistance from the industrial participants. The effort involved surveying the DOD boiler population, identifying boilers for conversion, identifying appropriate cost-estimating methodologies, estimating basic costs for new technologies, developing a process model, analyzing and identifying transportation costs for commercial sources of MCWM and cleaned coal, determining community spillovers, and determining regional market considerations and impacts.

Task 5: The results from each of the tasks were summarized in a final report. In addition, the design packages for the boiler retrofits were submitted. These included the engineering designs and economic analyses.

The original objectives of Phase II were to: (a) extend the Phase I boiler retrofit options by including designs to achieve further reductions in gaseous and particulate emissions, (b) prepare and characterize fuels compatible with coal precombustors, and (c) investigate precombustion as a means of using high ash, high sulfur coals. Upon investigating precombustion options for installing a system on either Penn State's demonstration boiler (15,000 lb steam/h) or research boiler (1,000 lb steam/h), it became apparent that there were limited viable options and that system complexity would likely preclude their use on small-scale, industrial boilers. A similar conclusion was drawn by the U.S. Army Corps of Engineers, regarding the use of slagging combustors in the Army[1]. Consequently, the Phase II work statement has been revised by eliminating the precombustion fundamental, pilot-scale, and demonstration-scale studies and focusing on fundamental, pilot-scale, and demonstration-scale emissions reduction strategies. An economic analysis of precombustion strategies was conducted, as originally planned, in

order to compare precombustion strategies with (low ash) MCWM and DMC combustion retrofits. The revised Phase II consists of four tasks as outlined below:

Task 1. Emissions Reduction

- Subtask 1.1 Evaluation of Emissions Reduction Strategies
- Subtask 1.2 Fundamental Emissions Studies
- Subtask 1.3 Installation of an Emissions Reduction System on the Demonstration Boiler
- Subtask 1.4 Evaluation of an Emissions Reduction System

Task 2. Coal Preparation/Utilization

- Subtask 2.1 Optimization of Particle Size Consist for CWM Formulation
- Subtask 2.2 Fine Grinding/Classification/Liberation
- Subtask 2.3 Fine Gravity Concentration
- Subtask 2.4 Agglomeration/Flotation Studies
- Subtask 2.5 Fundamental Studies of Surface-Based Processes
- Subtask 2.6 Column Flotation
- Subtask 2.7 Dry Cleaning of Fine Coal
- Subtask 2.8 CWM Density Control
- Subtask 2.9 Stabilization of CWM

Task 3. Engineering Design and Cost; and Economic Analysis

- Subtask 3.1 Determination of Basic Cost Estimation of Boiler Retrofits
- Subtask 3.2 Determination of Process Analysis
- Subtask 3.3 Determination of Environmental and Regulatory Impacts
- Subtask 3.4 Determination of Transportation Cost Analysis
- Subtask 3.5 Determination of Technology Adoption
- Subtask 3.6 Determination of Regional Economic Impacts
- Subtask 3.7 Determination of Public Perception of Benefits and Costs
- Subtask 3.8 Determination of Social Benefits
- Subtask 3.9 Determination of Coal Market Analysis
- Subtask 3.10 Engineering Design
- Subtask 3.11 Integration of Analyses

Task 4. Final Report/Submission of Design Package

Portions of Phase II have been completed. Phase II activities include:

Task 1: Task 1 activities are ongoing. In Task 1, strategies are being developed to provide for ultra-low emissions when firing coal-based fuels in industrial boilers. Emissions being addressed are SO_2, NO_x, fine particulate matter (<10 μm), air toxics (volatile organic compounds and trace metals), and CO_2. Post-combustion and during-combustion technologies to reduce SO_2 and NO_x emissions from coal-fired industrial boilers are being investigated. Novel technologies that are under development but are not commercially available are being evaluated, as well as proven technologies such as limestone/lime injection, selective catalytic reduction, and nonselective catalytic reduction. Options to remove submicron particulates are also being investigated.

Task 2: Task 2 activities are completed. Emphasis in Task 2 was on the refinement and optimization of coal grinding and CWM preparation procedures, and on the

development of advanced processes for beneficiating high ash, high sulfur coals. CWM formulation involved determining the optimum particle size distribution, how and why the optimum particle size distribution varies from coal to coal, and the specific roles of chemical dispersing and stabilizing agents. The extensive, physical coal pre-cleaning effort built on work conducted in Phase I.

Task 3: Economic analysis activities are complete and focused on determining the basic cost estimation of boiler retrofits, evaluating environmental, regulatory, and regional economic impacts, and analyzing the coal market.

Task 4: The results from each of the tasks will be summarized in a final report.

The objectives in Phase III are to: (a) develop coal-based fuel/waste cofiring technologies, and (b) assist DOD in improving the combustion performance and reducing emissions from existing stoker-fired boilers. This will be achieved through a combination of fundamental, pilot-scale, and demonstration-scale studies, field testing, and an engineering design and cost analysis of a stoker retrofit. Phase III consists of six tasks outlined below:

Task 1. Coal Preparation/Utilization

- Subtask 1.1 Particle Size Control
- Subtask 1.2 Physical Separations
- Subtask 1.3 Surface-Based Separation Process
- Subtask 1.4 Dry Processing
- Subtask 1.5 Stabilization of Coal-Water Mixtures

Task 2. Stoker Combustion Performance Analysis and Evaluation

- Subtask 2.1 Determine DOD Stoker Operability and Emissions Concerns
- Subtask 2.2 Conduct Field Test of a DOD Stoker
- Subtask 2.3 Provide Performance Improvement Analysis to DOD
- Subtask 2.4 Evaluate Pilot-Scale Stoker Retrofit Combustion
- Subtask 2.5 Perform Engineering Design of Stoker Retrofit

Task 3. Emissions Reduction

- Subtask 3.1 Demonstrate Advanced Pollution Control System
- Subtask 3.2 Evaluate Carbon Dioxide Mitigation and Heavy Metal Removal in a Slipstream System
- Subtask 3.3 Study VOC and Trace Metal Occurrence and Capture

Task 4. Coal-Based Fuel/Waste Cofiring

- Subtask 4.1 Coal Fines Combustion
- Subtask 4.2 Coal/Rocket Propellant Cofiring

Task 5. Economic Evaluation

- Subtask 5.1 Cost and Market Penetration of Coal-Based Fuel Technologies

Subtask 5.2	Selection of Incentives for Commercialization of the Coal-Using Technology
Subtask 5.3	Community Sensitivity to Coal Fuel Usage
Subtask 5.4	Regional Economic Impacts of New Coal Utilization Technologies
Subtask 5.5	Economic Analysis of the Defense Department's Fuel Mix
Subtask 5.6	Constructing a National Energy Portfolio which Minimizes Energy Price Shock Effects
Subtask 5.7	Proposed Research on the Coal Markets and their Impact on Coal-Based Fuel Technologies
Subtask 5.8	Integrate the Analysis

Task 6. Final Report/Submission of Design Package

Phase III activities include:

Task 1: Research conducted under Phase I and Phase II of this project has revealed a number of specific areas where continued and/or more focused effort is required in order to develop more effective and more reliable coal processing systems. Specific objectives of Task 1 are centered around:

- focused investigations into specific coal-cleaning options and their associated ancillary operations; and
- integration of processing/cleaning operations for overall system optimization.

As in the previous phases, emphasis will be on fine-coal processing for the production of high-quality, micronized coal for dry coal and coal-water mixture (CWM) applications.

Task 2: DOD operates several large World War II-vintage stoker-fired boilers for steam production. The objective in Task 2 is to address DOD's concern that they are difficult to operate properly, which results in poor combustion performance and excessive emissions. Ultimately, there is the possibility that the boilers may be converted from coal to another fuel form. The objective will be achieved by surveying the operability of the stoker-fired boilers, identifying a candidate boiler for improvement, conducting field testing to determine the combustion performance and emissions, providing a performance improvement analysis to DOD, if applicable, evaluating pilot-scale stoker retrofit combustion technologies, and performing an engineering design of a stoker retrofit to fire coal in a form that is most conducive to achieve operability and environmental goals.

Task 3: In Task 3, three levels of effort investigating emissions reductions will be performed. An advanced pollution control system will be tested at the demonstration level, CO_2 mitigation and heavy metal removal will be evaluated at the pilot-scale level, and fundamental studies of VOC and trace metal occurrence and capture will be conducted.

Task 4: The activities in Task 4 will address advanced/novel combustion techniques. This involves coal fines combustion and cofiring wastes with coal-based fuels.

Task 5: The activities in Task 5 will focus on determining cost and market penetration, selection of incentives, and regional economic impacts of coal-based fuel

technologies. In addition, DOD's fuel mix will be determined and a national energy portfolio constructed.

Task 6: The results from each of the tasks will be summarized in a final report. In addition, the design package for the stoker retrofit will be submitted. This will include the engineering design and economic analysis.

The accomplishments and status of Phase I, Tasks 1, 2, 3, 4, and 5 are presented in Sections 2.0, 3.0, 4.0, 5.0, and 6.0, respectively. The accomplishments and status of Phase II, Tasks 1, 2, 3, and 4 are presented in Sections 7.0, 8.0, 9.0, and 10.0, respectively. The accomplishments and status of Phase III, Tasks 1, 2, 3, 4, 5, and 6 are presented in Sections 11.0, 12.0, 13.0, 14.0, 15.0, and 16.0, respectively. Section 17.0 discusses miscellaneous activities that were conducted. Activities planned for the next semiannual period are listed in Section 18.0. References and acknowledgments are contained in Sections 19.0 and 20.0, respectively. The project schedule for Phases II and III is given in Figures 1-1 and 1-2, respectively, with a description of the milestones contained in Tables 1-1 and 1-2, respectively.

2.0 PHASE I, TASK 1: COAL BENEFICIATION/PREPARATION

Activities in Phase I, Task 1 focused on preparing the final report.

3.0 PHASE I, TASK 2: COAL COMBUSTION PERFORMANCE

Activities in Phase 1, Task 2 focused on preparing the final report.

4.0 PHASE I, TASK 3: ENGINEERING DESIGN

Activities in Phase I, Task 3 focused on preparing the final report.

5.0 PHASE I, TASK 4: ENGINEERING AND COST ANALYSIS

Activities in Phase I, Task 4 focused on preparing the final report.

6.0 PHASE I, TASK 5: FINAL REPORT/SUBMISSION OF DESIGN PACKAGE

The Phase I final report is undergoing final revision and will be completed on November 1, 1995.

7.0 PHASE II, TASK 1: EMISSIONS REDUCTION

The objectives of this task are to develop strategies to provide for ultra-low emissions when firing coal-based fuels in industrial-scale boilers. Emissions to be addressed include SO_2, NO_x, fine particulate matter (<10 μm), air toxics (volatile organic compounds and trace metals), and CO_2.

7.1 Subtask 1.1 Evaluation of Emissions Reduction Strategies

It is the objective of this subtask to evaluate emissions reduction strategies for the installation of commercial NO_x and SO_2 systems on the demonstration boiler. The work in

Task 1. Emissions Reductions

Subtask 1.1 - Evaluate Emissions Reductions Strategies

Subtask 1.2 - Conduct Fundamental Emissions Studies

Subtask 1.3 - Install System on Demonstration Boiler

Subtask 1.4 - Evaluate Emissions Reduction System

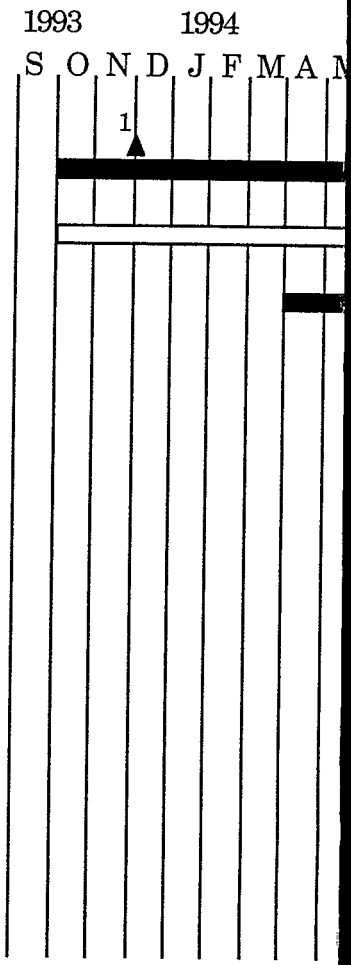

Figure 1-1. DOD Phase I

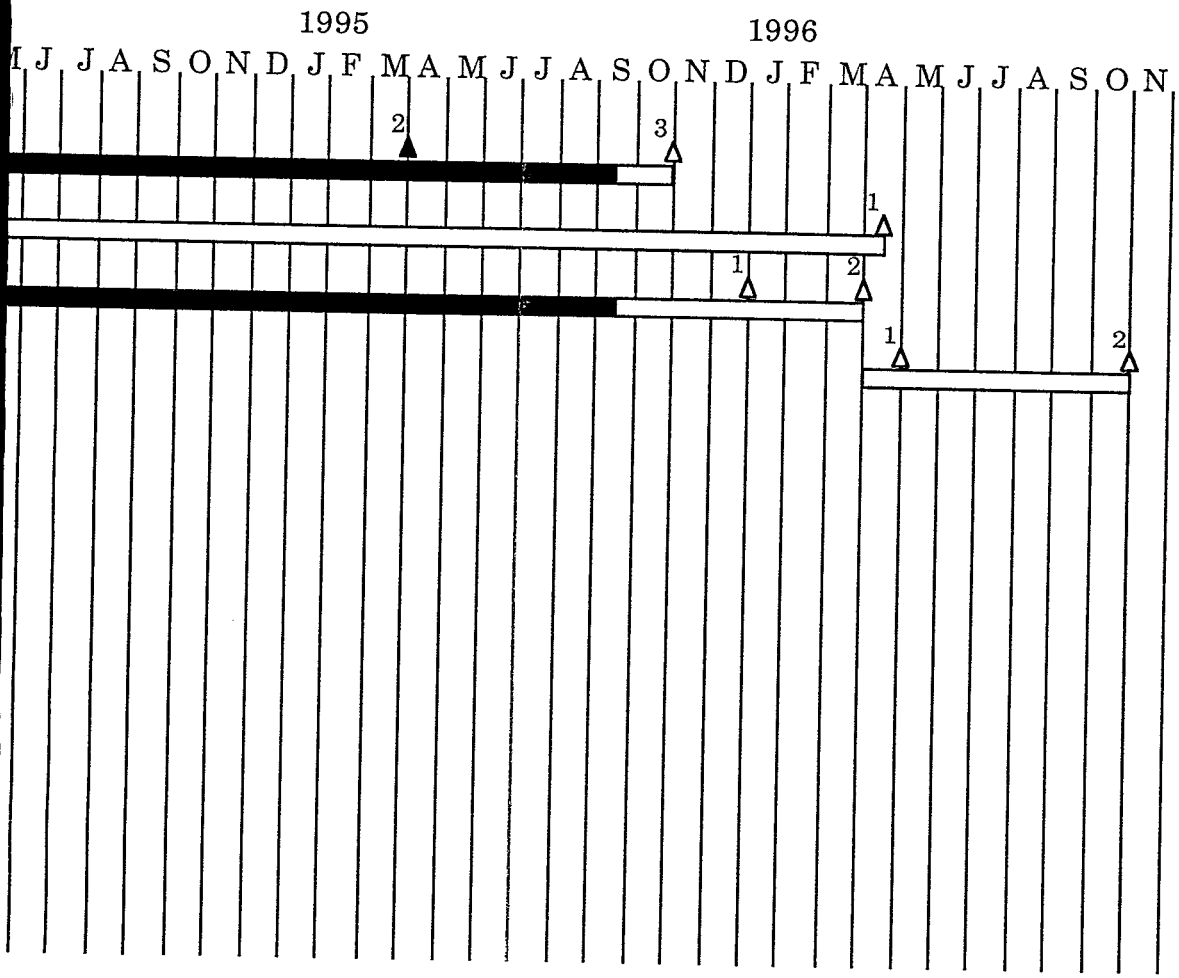

Milestone Schedule

Task 2. Coal Preparation / Utilization

Subtask 2.1 - Optimization of Particle Size Consist for Slurry Formulation

Subtask 2.2 - Fine Grinding / Classification / Liberation

Subtask 2.3 - Fine Gravity Concentration

Subtask 2.4 - Agglomeration / Flotation Studies

Subtask 2.5 - Fundamental Studies of Surface-Based Processes

Subtask 2.6 - Column Flotation

Subtask 2.7 - Dry Cleaning of Fine Coal

Subtask 2.8 - Slurry Density Control

Subtask 2.9 - Stabilization of CWSF

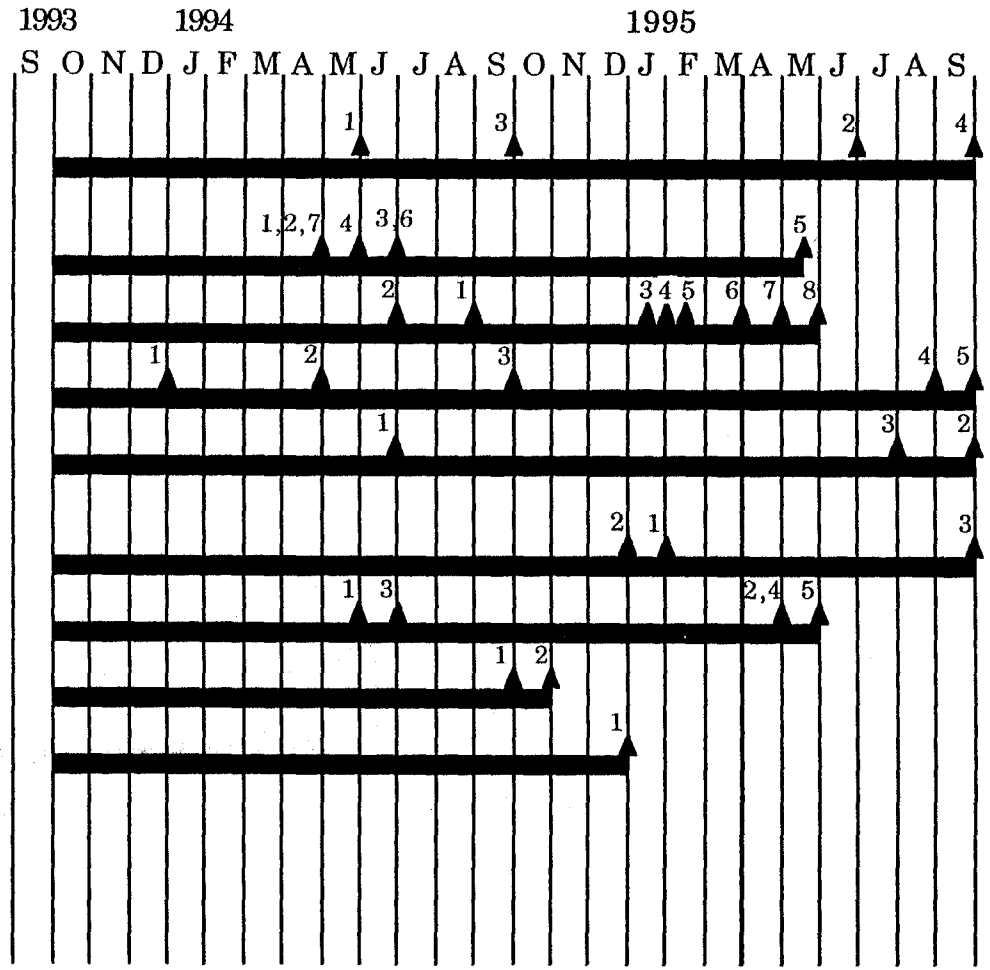

Task 3. Engineering Design and Cost and Economic Analysis

Subtask 3.1 - Basic Cost Estimation of Boiler Retrofits

Subtask 3.2 - Process Analysis

Subtask 3.3 - Environmental and Regulatory Impacts

Subtask 3.4 - Transportation Cost Analysis

Subtask 3.5 - Technology Adoption

Subtask 3.6 - Regional Economic Impacts

Subtask 3.7 - Public Perception of Benefits and Costs

Subtask 3.8 - Social Benefits

Subtask 3.9 - Coal Market Analysis

Subtask 3.10 - Integration of Analyses

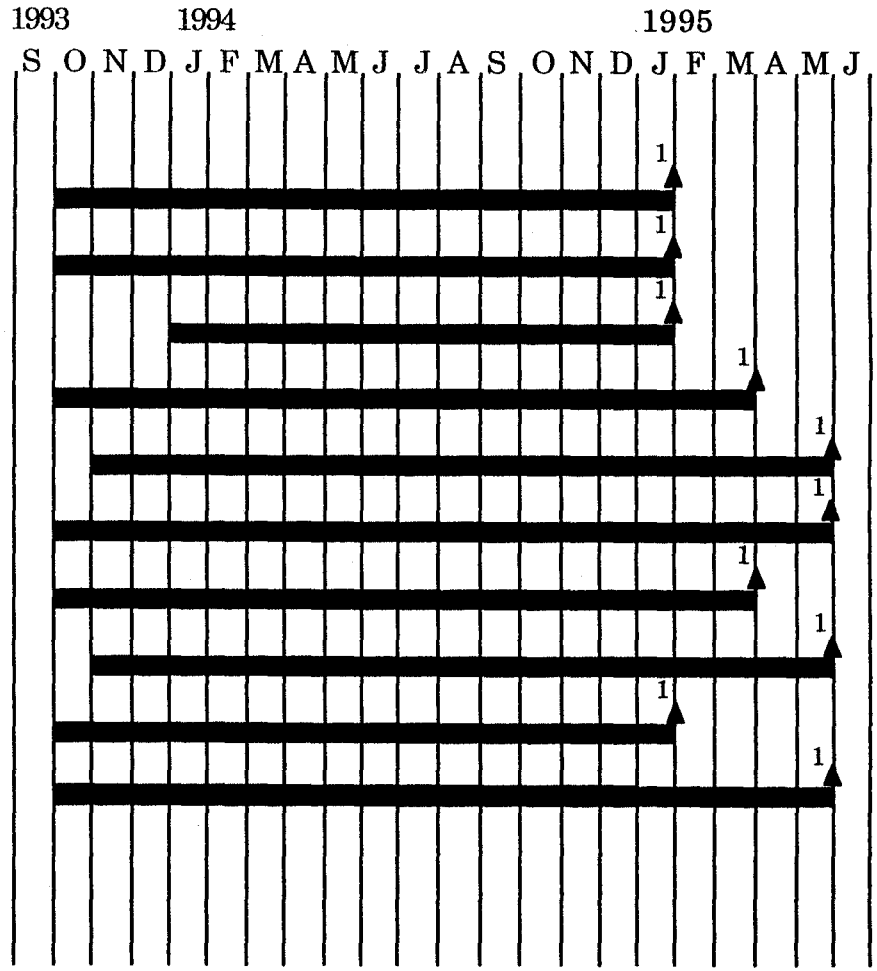

Task 4. Final Report

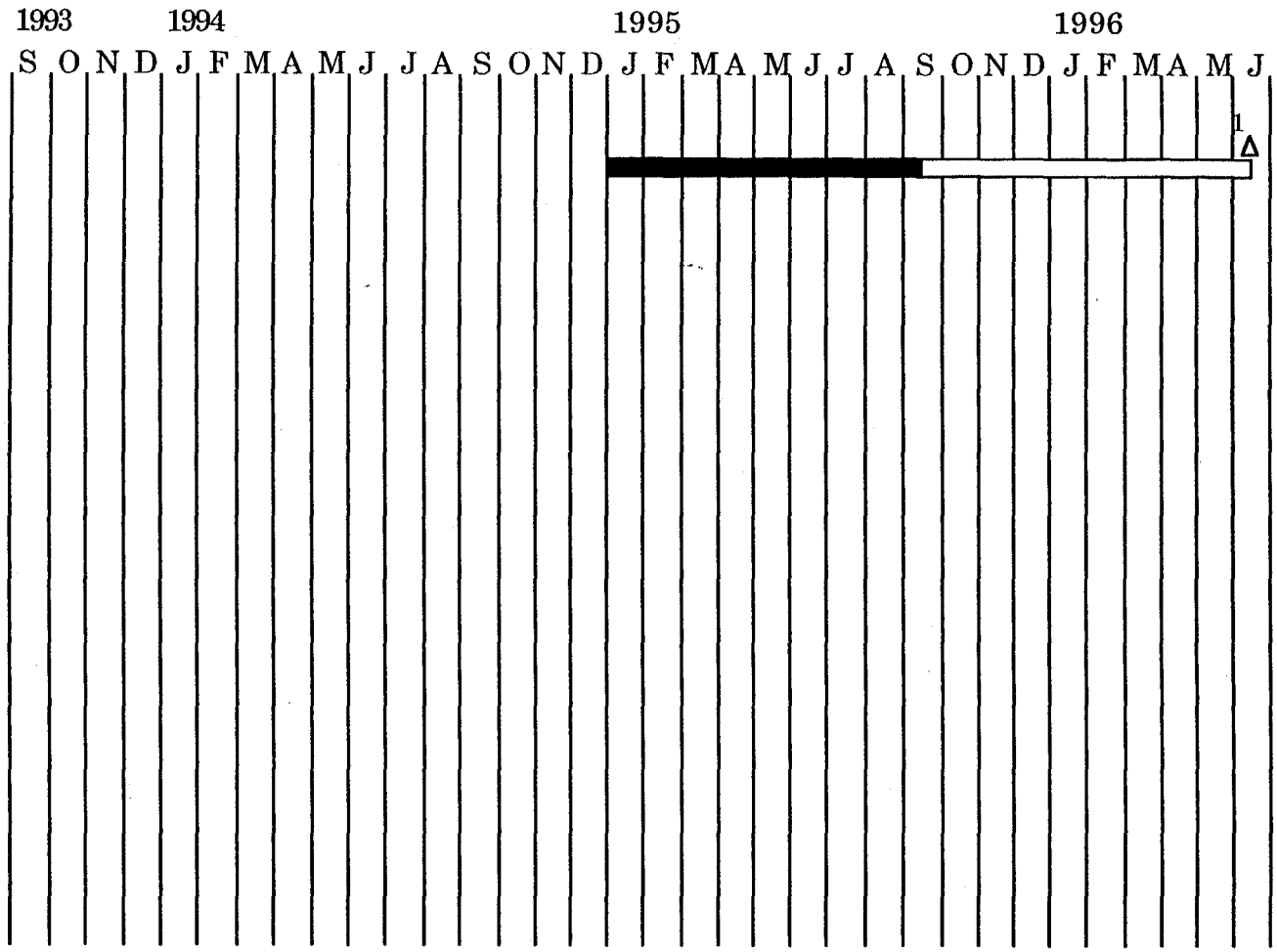

Task 1. Coal Preparation Utilization

Subtask 1.1 - Particle Size Control

Subtask 1.2 - Physical Separations

Subtask 1.3 - Surface-Based Separation Process

Subtask 1.4 - Dry Processing

Subtask 1.5 - Stabilization of Coal-Water Mixtures

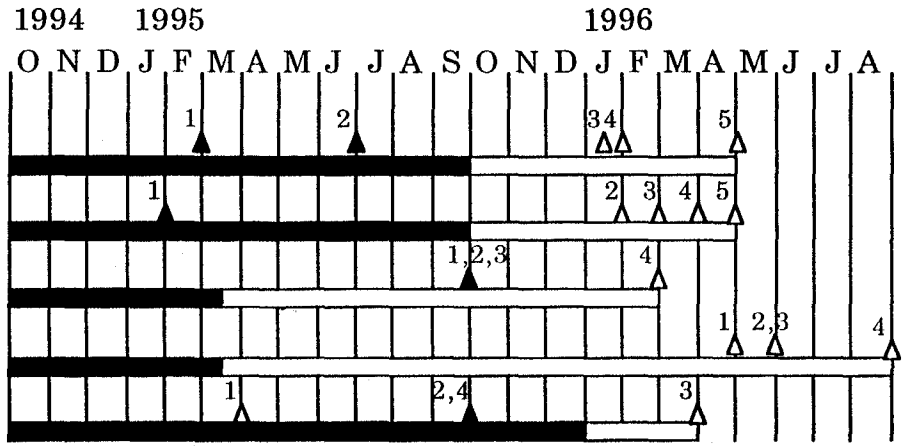

Task 2. Stoker Combustion Performance Analysis and Evaluation

Subtask 2.1 - Determine DOD Stoker Operability and Emissions

Subtask 2.2 - Conduct Field Test of a DOD Stoker

Subtask 2.3 - Provide Performance Improvement Analysis to DOD

Subtask 2.4 - Evaluate Pilot-Scale Stoker Retrofit Combustion

Subtask 2.5 - Perform Engineering Design of Stoker Retrofit

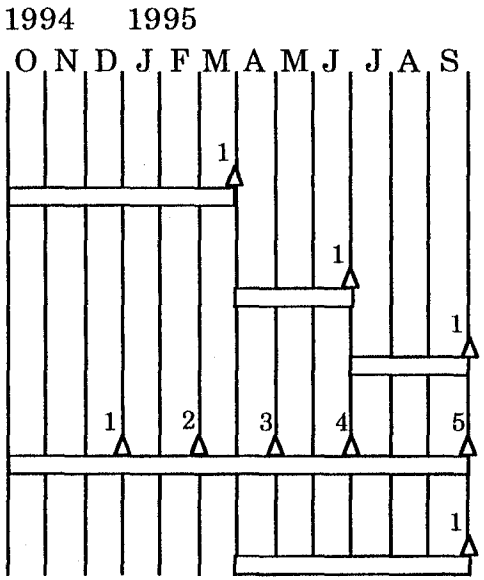

Figure 1-2. DOD Phase III Milestone Schedule

Task 3. Emissions Reduction

Subtask 3.1 - Demonstrate Advanced Pollution Control System

Subtask 3.2 - Evaluate CO_2 Mitigation and Heavy Metal Removal in a Slipstream System

Subtask 3.3 - Study VOC and Trace Metal Occurrence and Capture

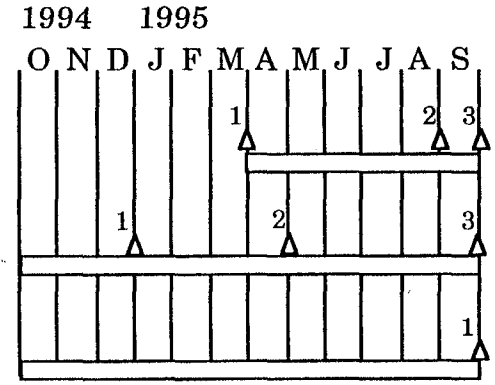

Task 4. Coal-Based Fuel Waste Cofiring

Subtask 4.1 - Coal Fines Combustion

Subtask 4.2 - Coal/Rocket Propellant Cofiring

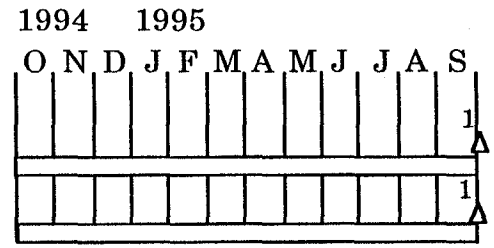

Task 5. *Economic Evaluation*

Subtask 5.1 - Cost and Market Penetration of Coal-Based FuelTechnologies

Subtask 5.2 - Selection of Incentives for Commercialization of the Coal Using Technology

Subtask 5.3 - Community Sensitivity of Coal Fuel Usage

Subtask 5.4 - Regional Economic Impacts of New Coal UtilizationTechnologies

Subtask 5.5 - Economic Analysis of the Defense Department's Fuel Mix

Subtask 5.6 - Constructing a National Energy Portfolio which Minimizes Energy Price Shock Effects

Subtask 5.7 - Proposed Research on the Coal Markets and their Impact on Coal-Based Fuel Technologies

Subtask 5.8 - Integration of Economic Analysis

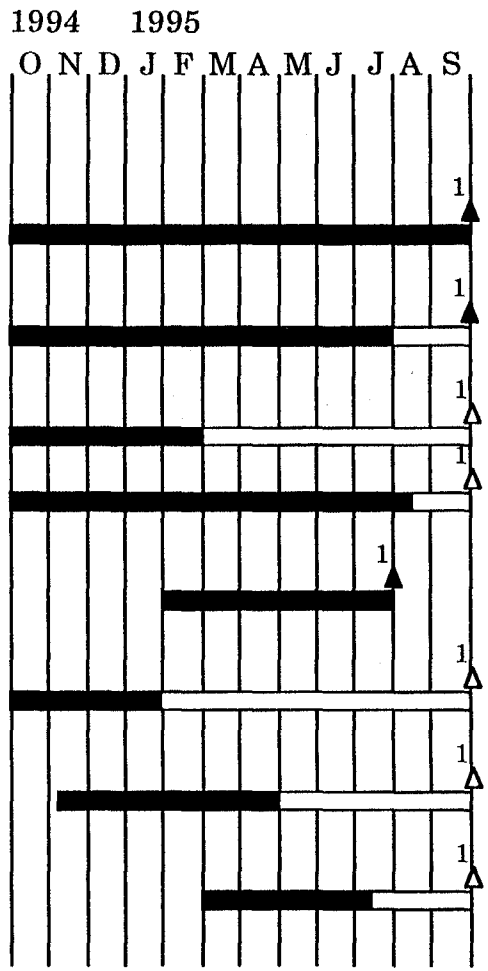

Task 6. Final Report / Submission of Design Package

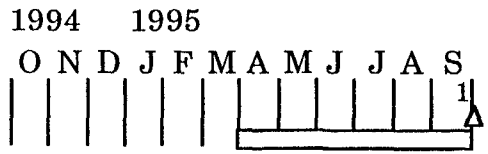

Table 1-1. Phase II. Milestone Description

Milestone	Description	Planned Completion Date	Actual Completion Date
Task 1. Emissions Reduction			
Subtask 1.1. Evaluation of Emissions Reduction Strategies			
Subtask 1.1, No. 1	Receive proposals for pollution control system	12/01/93	12/01/93
Subtask 1.1, No. 2	Complete summary report of pollution control technologies	03/31/95	03/31/95
Subtask 1.1, No. 3	Select pollution control system	10/31/95	
Subtask 1.2. Conduct Fundamental Emissions Studies			
Subtask 1.2, No. 1	Prepare summary of emissions studies	04/15/96	
Subtask 1.3. Install System on Demonstration Boiler			
Subtask 1.3, No. 1	Design pollution control system	12/31/95	
Subtask 1.3, No. 2	Complete installation of system	04/01/96	
Subtask 1.4. Evaluate Emissions Reduction System			
Subtask 1.4, No. 1	Shakedown system	05/01/96	
Subtask 1.4, No. 2	Complete system evaluation	11/01/96	
Task 2. Coal Preparation/Utilization			
Subtask 2.1. Optimization of Particle Size Consist for Slurry Formulation			
Subtask 2.1, No. 1	Samples of fine and coarse slurry components prepared	04/30/94	05/30/94
Subtask 2.1, No. 2	Rheological characterization of components completed	04/30/95	06/30/95
Subtask 2.1, No. 3	Models for rheology of binary mixtures developed	09/30/94	09/30/94
Subtask 2.1, No. 4	Optimization studies complete	06/30/95	09/30/95
Subtask 2.2. Fine Grinding/Classification Liberation			
Subtask 2.2, No. 1	Grinding kinetics data for wet ball milling obtained	04/30/94	04/30/94
Subtask 2.2, No. 2	Wet classifier performance evaluated	04/30/95	04/30/95
Subtask 2.2, No. 3	Dry classifier performance evaluated	04/30/94	06/30/94
Subtask 2.2, No. 4	Grinding kinetics data for stirred media milling obtained	05/31/94	05/31/94
Subtask 2.2, No. 5	Closed-circuit jet-milling data obtained	05/15/95	05/15/95
Subtask 2.2, No. 6	Slurry production simulations initiated	06/30/94	06/30/94
Subtask 2.2, No. 7	Liberation data on Type III coal obtained	04/30/94	04/30/94
Subtask 2.3. Fine Gravity Concentration			
Subtask 2.3, No. 1	Initiate magnetic fluid separation of Type III coal	07/31/94	08/15/94
Subtask 2.3, No. 2	Complete batch centrifuge testing	04/30/94	06/30/94
Subtask 2.3, No. 3	Continuous centrifuge test rig set-up	09/30/94	01/15/95
Subtask 2.3, No. 4	Initiate magnetite classification studies	10/15/94	01/31/95
Subtask 2.3, No. 5	Initiate separations of Type III coals	02/28/95	02/28/95

Milestone	Description	Planned Completion Date	Actual Completion Date
Subtask 2.3, No. 6	Initiate micronized coal classification studies	04/30/95	03/31/95
Subtask 2.3, No. 7	Evaluate dense-medium separation data	04/30/95	04/30/95
Subtask 2.3, No. 8	Evaluate size classification data	05/31/95	05/31/95
Subtask 2.4. Agglomeration/Flotation Studies			
Subtask 2.4, No. 1	Set-up device to size separate flotation products of micronized coal	12/31/93	12/31/93
Subtask 2.4, No. 2	Set-up equipment for larger scale tests using 2.2 cu.ft. flotation cells	04/30/94	04/30/94
Subtask 2.4, No. 3	Conduct agglomeration-flotation tests for micronized Type III coal	09/30/94	09/30/94
Subtask 2.4, No. 4	Conduct agglomeration-flotation tests in larger cells	03/31/95	08/31/95
Subtask 2.4, No. 5	Determine parameters for scale-up	06/30/95	09/30/95
Subtask 2.5. Fundamental Studies of Surface-Based Processes			
Subtask 2.5, No. 1	Conduct interface characterization studies to determine flotation reagent-coal interactions	06/30/94	06/30/94
Subtask 2.5, No. 2	Measure contact angles in the coal-oil-surfactant-water system	06/30/95	09/30/95
Subtask 2.5, No. 3	Determine effect of surfactants on slurry stability	05/31/95	07/31/95
Subtask 2.6. Column Flotation			
Subtask 2.6, No. 1	Test work on Type II coals	11/30/94	01/31/95
Subtask 2.6, No. 2	Test work on Type III coals	09/30/94	12/31/94
Subtask 2.6, No. 3	Determine scale-up parameters	05/31/95	09/30/95
Subtask 2.7. Dry Cleaning of Fine Coal			
Subtask 2.7, No. 1	Complete evaluation of Type III coal in batch separator	04/30/94	05/31/94
Subtask 2.7, No. 2	Integration of closed dry grinding circuit with TES	04/30/95	04/30/95
Subtask 2.7, No. 3	Initiate investigation of continuous TES	04/01/94	06/30/94
Subtask 2.7, No. 4	Complete charge measurements on Type II coal	04/30/95	04/30/95
Subtask 2.7, No. 5	Complete charge measurements on Type III	05/31/95	05/31/95
Subtask 2.8. Slurry Density Control			
Subtask 2.8, No. 1	Evaluate procedures for reversible flocculation of fine coal	09/30/94	09/30/94
Subtask 2.8, No. 2	Establish process engineering for thickening of fine-coal slurries	10/31/94	10/31/94
Subtask 2.9. Stabilization of CWSF			
Subtrask 2.9, No. 1	Complete stabilization study	12/31/94	12/31/94

Milestone	Description	Planned Completion Date	Actual Completion Date
Task 3.	**Engineering Design and Cost; and Economic Analysis**		
Subtask 3.1.	Determine Basic Cost Estimation of Boiler Retrofits	02/01/95	02/01/95
Subtask 3.2.	Determine Process Analysis	02/01/95	02/01/95
Subtask 3.3.	Determine Environmental and Regulatory Impacts	02/01/95	02/01/95
Subtask 3.4.	Determine Transportation Cost Analysis	04/01/95	04/01/95
Subtask 3.5.	Determine Technology Adoption	06/01/95	06/01/95
Subtask 3.6.	Determine Regional Economic Impacts	06/01/95	06/01/95
Subtask 3.7.	Determine Public Perception of Benefits and Costs	04/01/95	04/01/95
Subtask 3.8.	Determine Social Benefits	06/01/95	06/01/95
Subtask 3.9.	Determine Coal Market Analysis	02/01/95	02/01/95
Subtask 3.10.	Complete Integration of Analyses	06/01/95	06/01/95
Task 4.	**Final Report**	06/15/96	

Table 1-2. Phase III. Milestone Description

Milestone	Description	Planned Completion Date	Actual Completion Date
Task 1. Coal Preparation/Utilization			
Subtask 1.1. Particle Size Control			
Subtask 1.1, No. 1	Evaluate conventional ball milling circuit	02/28/95	02/28/95
Subtask 1.1, No. 2	Evaluate stirred-media milling circuit	06/30/95	06/30/95
Subtask 1.1, No. 3	Complete baseline testing of attrition milling for the production of broad size distributions	01/31/96	
Subtask 1.1, No. 4	Complete preliminary evaluation of dry grinding/ cleaning circuit	01/31/96	
Subtask 1.1, No. 5	Initiate investigation of an integrated grinding/cleaning circuit	04/30/96	
Subtask 1.2. Physical Separations			
Subtask 1.2, No. 1	Complete preliminary investigation of magnetic fluid-based separation for fine coal cleaning	01/31/95	01/31/95
Subtask 1.2, No. 2	Complete baseline testing of dense-medium separation using the continuous, solid-bowl centrifuge	01/31/96	
Subtask 1.2, No. 3	Initiate investigation of magnetic fluid cyclone separations	02/29/96	
Subtask 1.2, No. 4	Complete baseline testing of solid-bowl centrifuge for micronized coal classification	03/31/96	
Subtask 1.2, No. 5	Initiate testing of integrated centrifugal/flotation system	04/30/96	
Subtask 1.3. Surface-Based Separation Processes			
Subtask 1.3, No. 1	Set up and evaluate continuous flotation circuit	05/31/95	09/30/95
Subtask 1.3, No. 2	Evaluate effectiveness of alternative bubble generators in flotation column	06/30/95	09/30/95
Subtask 1.3, No. 3	Baseline testing on selected coal	08/31/95	09/30/95
Subtask 1.3, No. 4	Evaluate flotation system performance	02/29/96	
Subtask 1.4 Dry Processing			
Subtask 1.4, No. 1	Complete deagglomeration testing using the batch triboelectrostatic separator	04/30/96	
Subtask 1.4, No. 2	Complete baseline testing of continuous triboelectrostatic separator unit	05/31/96	
Subtask 1.4, No. 3	Initiate investigation of alternative approaches to charging/deagglomeration	05/31/96	
Subtask 1.4, No. 4	Complete preliminary testing of integrated grinding and triboelectrostatic separator unit	08/31/96	

Milestone	Description	Planned Completion Date	Actual Completion Date
Subtask 1.5 Stabilization of Coal-Water Mixtures			
Subtask 1.5, No. 1	Complete PSD model extension	04/01/95	04/01/95
Subtask 1.5, No. 2	Complete construction of computer program	09/27/95	09/27/95
Subtask 1.5, No. 3	Complete PSD model comparison to experimental results	09/27/95	
Subtask 1.5, No. 4	Complete coal oxidation study	09/27/95	09/27/95
Task 2. Stoker Combustion Performance Analysis and Evaluation			
Subtask 2.1. Determine DOD Stoker Operability and Emissions			
Subtask 2.1, No. 1	Complete stoker survey, identify stoker for evaluation	03/31/95	
Subtask 2.2. Conduct Field Test of a DOD Stoker			
Subtask 2.2, No. 1	Complete stoker field test	07/01/95	
Subtask 2.3 Provide Performance Improvement Analysis to DOD			
Subtask 2.3, No. 1	Complete performance improvement analysis	09/27/95	
Subtask 2.4. Evaluate Pilot-Scale Stoker Retrofit Combustion			
Subtask 2.4, No. 1	Complete modifications to stoker system	12/31/94	
Subtask 2.4, No. 2	Complete evaluation of anthracite micronized coal	02/28/95	
Subtask 2.4, No. 3	Complete evaluation of anthracite/water mixtures	04/30/95	
Subtask 2.4, No. 4	Complete evaluation of bituminous micronized coal	06/30/95	
Subtask 2.4, No. 5	Complete evaluation of bituminous/water mixtures	09/27/95	
Subtask 2.5. Perform Engineering Design of Stoker Retrofit			
Subtask 2.5, No. 1	Complete retrofit design	09/27/95	
Task 3. Emissions Reduction			
Subtask 3.1. Demonstrate Advanced Pollution Control System			
Subtask 3.1, No. 1	Identify low-temperature catalysts	03/31/95	
Subtask 3.1, No. 2	Install catalyst-coated filter and SO_2 removal system	08/31/95	
Subtask 3.1, No. 3	Complete demonstration of unit	09/27/95	
Subtask 3.2. Evaluate Carbon Dioxide Mitigation and Heavy Metal Removal in a Slipstream System			
Subtask 3.2, No. 1	Identify CO_2 mitigation technique	01/01/95	
Subtask 3.2, No. 2	Install slipstream	05/01/95	

Milestone	Description	Planned Completion Date	Actual Completion Date
Subtask 3.2, No. 3	Complete evaluation of CO_2 mitigation/heavy metal removal	09/27/95	
Subtask 3.3. Study VOC and Trace Metal Occurrence and Capture			
Subtask 3.3, No. 1	Complete evaluation of VOC and trace metals	09/27/95	
Task 4. Coal-Based Fuel Waste Cofiring			
Subtask 4.1. Coal Fines Combustion			
Subtask 4.1, No. 1	Complete coal fines combustion evaluation	09/27/95	
Subtask 4.2. Coal/Rocket Propellant Cofiring			
Subtask 4.2, No. 1	Complete cofiring testing	09/27/95	
Task 5. Economic Evaluation			
Subtask 5.1. Cost and Market Penetration of Coal-Based Fuel Technologies			
Subtask 5.1, No. 1	Complete study of cost and market penetration of coal-based fuel technologies	06/01/95	09/27/95
Subtask 5.2. Selection of Incentives for Commercialization of the Coal Using Technology			
Subtask 5.2, No. 1	Complete selection of incentives for commercialization of the coal-using technology	09/27/95	
Subtask 5.3. Community Sensitivity to Coal Fuel Usage			
Subtask 5.3, No. 1	Complete evaluation of community sensitivity to coal fuel usage	09/27/95	
Subtask 5.4 Regional Economic Impacts of New Coal Utilization Technologies			
Subtask 5.4, No. 1	Complete study of regional economic impacts of new coal utilization technologies	09/27/95	
Subtask 5.5 Economic Analysis of the Defense Department's Fuel Mix			
Subtask 5.5, No. 1	Complete economic analysis of the defense department's fuel mix	09/27/95	06/30/95

Milestone	Description	Planned Completion Date	Actual Completion Date
Subtask 5.6 Constructing a National Energy Portfolio which Minimizes Energy Price Shock Effects			
Subtask 5.6, No. 1	Complete construction of a national energy portfolio which minimizes energy price shock effects	09/27/95	
Subtask 5.7 Proposed Research on the Coal Markets and their Impact on Coal-Based Fuel Technologies			
Subtask 5.7, No. 1	Complete research on the coal markets and their impact on coal-based fuel technologies	09/27/95	
Subtask 5.8 Integrate the Analysis		09/27/95	
Subtask 5.8, No.1	Complete integration of the analysis	09/27/95	
Task 6. Final Report/Submission of Design Package		09/27/95	

this subtask is being conducted primarily by literature searches and discussions with manufacturers of flue gas cleanup equipment and with other researchers in the field.

Literature searches were conducted on NO_x, SO_2, volatile organic compounds, and trace metals removal systems during the previous reporting period[2]. The literature searches were for all coal-fired boilers and were not limited to industrial-size boilers. The information from the literature searches is being used with that received from the vendors and engineering firms to select appropriate control systems for installation on the demonstration boiler (Section 7.3).

Discussions with Vendors and Engineering Firms

NO_x and SO_2 Emissions Control Technologies

Vendors and engineering firms were contacted to identify the appropriate NO_x and SO_2 emissions control technologies. Of the firms contacted, Raytheon Constructors and Contractors was selected to provide a summary report reviewing the operational data on the demonstration boiler, and identifying the appropriate NO_x and SO_2 technologies for installation on the industrial boiler. A summary of the report will be presented in the next semiannual report.

Particulate Removal

Activity is underway to install a ceramic filtering device on the demonstration boiler to remove ultrafine particulates and to increase the particulate collection efficiency. The ceramic filtering device will be installed adjacent to the existing baghouse and will be capable of filtering the entire flue gas stream. The system will be engineered such that the flue gas stream can be passed either through the baghouse or ceramic filtering device. An application for plan approval to modify the system has been prepared by Penn State and submitted to the Pennsylvania Department of Environmental Protection (DEP). While the application is under review, Penn State is beginning the design of the new system, which includes the ceramic filtering device, ducting, valves, induced draft fan, and associated controls.

The ceramic filtering device is being designed by Penn State and CeraMem Separations, Inc. The ceramic filters are being procured from CeraMem Separations, Inc. The design criteria of the filters are:

Design face velocity (A/C ratio)	4.00
Volume (acfm)	8,150
Temperature (F)	400
Grain loading to filters (gr/acf)	3.0
Operating pressure drop (" water column)	7-10
Filter area (sq.ft.)	2,000

The ceramic filtering device will be installed upon approval from DEP and the completion of the modification design. It will contain 80 filters, 7" in diameter and 15" long. The

current baghouse contains 120 bags, 4.5" in diameter and 10' long. It is the intent of this portion of the program to demonstrate the applicability of a more compact and efficient filtering device for retrofit applications.

7.2 Subtask 1.2 Conduct Fundamental Emissions Reduction Studies

The combustion of fossil fuels releases NO_X into the atmosphere. NO_X is known to be related to the problems of acid precipitation and ozone formation. Although, technologies effort have decreased the amount of NO_X released into the atmosphere during combustion of fossil fuels, further improvements in combustion and mitigation technologies are necessary.

During combustion, NO_X is mainly formed by the interactions of released nitrogen with atmospheric oxygen. Optimized combustion conditions and post combustion cleanup have already led to a major decrease in NO_X-emissions. For further decreases in NO_X emissions, however, a better understanding of the N-functionality in fossil fuels and the chemistry occurring during their combustion are necessary.

Unfortunately, N-functionality and N-chemistry during combustion are still not well understood. This is mainly due to the low nitrogen concentration in coal, but also to the fact that a major part of the nitrogen in coal is bound in the insoluble macromolecular fraction. This fraction is very often difficult, and sometimes impossible, to characterize with standard analytical approaches. An alternative approach to characterizing Nitrogen in coal is the use of non-degradative analytical methods, i.e. ^{15}N NMR spectroscopy. This approach was recently successfully applied to the determination of N-functionality in degrading plant material and natural soils. Unfortunately, the application of ^{15}N NMR to fossil fuels involves sensitivity problems, due to the very low N-concentration of these samples. One task of our research was, therefore, to test whether ^{15}N NMR could be a useful analytical approach in coal science, first for the examination of the coals themselves, then for their diagenetic formation and N-chemistry during their combustion.

The second task of the research involved an evaluation of the feasibility of a new biomitigation strategy. This strategy proposes the mitigation of NO_X emissions from coal combustion via refossilization of algal material. The idea is to grow specific algae containing exceptionally high amounts of refractory biopolymers on combustion flue gases, which are bubbled through an algal pond. These flue gases deliver CO_2, which can be converted by the algae into biomass via photosynthesis and NO_X, which will dissolve in the aquarious phase as nitrate. Nitrate is known to be an important algal nutrient and can be used by the algae for the build up of N-containing biomass. After the death of the algae, their labile compounds will be quickly microbiologically degraded, while a huge part of the

biomass will be selectively preserved and after its deposition, may refossilize. In our research, we concentrated on the examination of the chemical structure of such refractory algal-derived biomass and its potential as a precursor for fossilized organic material by means of ^{13}C and ^{15}N NMR spectroscopy.

Characterization of Nitrogen in Coal by ^{15}N NMR Spectroscopy.

Solid-state ^{15}N NMR spectroscopy was successfully applied to non- ^{15}N-enriched coal samples[3]. These ^{15}N NMR spectra were the first ever obtained from coals at natural ^{15}N abundance. Although these spectra suffer from a low signal-to-noise ratio (Figure 7-1), the successful application of ^{15}N NMR spectroscopy to coal samples may help to provide a new level of understanding of coal-nitrogen chemistry. Ongoing research in this area involves ways to improve the spectrum quality. These solid-state ^{15}N NMR spectra of the examined bituminous and subbituminous coals (Table 7-1) reveal that pyrrolic-N is the major N-form. Signals typical of pyridinic-N were not identified. This contradicts the common belief that pyridinic-N comprises the major form of nitrogen in coal. A comparison of solid-state ^{15}N NMR spectra of the coals to those obtained from several plant composts and peats[4-6] reveals that the shift in N-functionality from refractory amides to pyrrolic-N occurs during the early stage of coalification, shortly after peatification.

The ^{15}N NMR spectroscopic investigation of N-functionality was extended to vitrinites of different rank, from the lignite stage to the anthracite stage (Figure 7-2). These data are being prepared for publication, and will be presented at the International Chemical Congress of Pacific Basin Societies, Dec. 17-22, 1995. Due to the low N-content of the lignite (0.3 %), its spectra is hampered by a low signal-to-noise ratio. Only one broad signal, which is most likely assigned to pyrrolic-N, was identified. With increasing rank, a shift in the main ^{15}N NMR signal towards indolic- and carbazolic-N can be observed. In the anthracite spectrum a weak signal in the chemical shift region of pyridinic-N was identified. These results indicate that chemical changes in the N-functionality occur as result of maturation and that the N-functionality shifts from mainly pyrrolic-N towards more stable compounds such as indoles or carbazoles. Proving the latter hypothesis is the task of ongoing research.

To evaluate the application of solid-state ^{15}N NMR spectroscopy to investigate chemistry during combustion, a series of coal were analyzed. These chars were produced at aslow heating up to 700 ° C under oxidizing conditions. Compared to fossil sediments with similar N-content (1 to 2%), the signal-to-noise ratios of the char spectra were very low. Chars of PSOC 1517 and 1362 could not be analyzed, due to their high conductivity, which can lead to a destruction of the NMR-probe during repetitive NMR-pulse irradition.

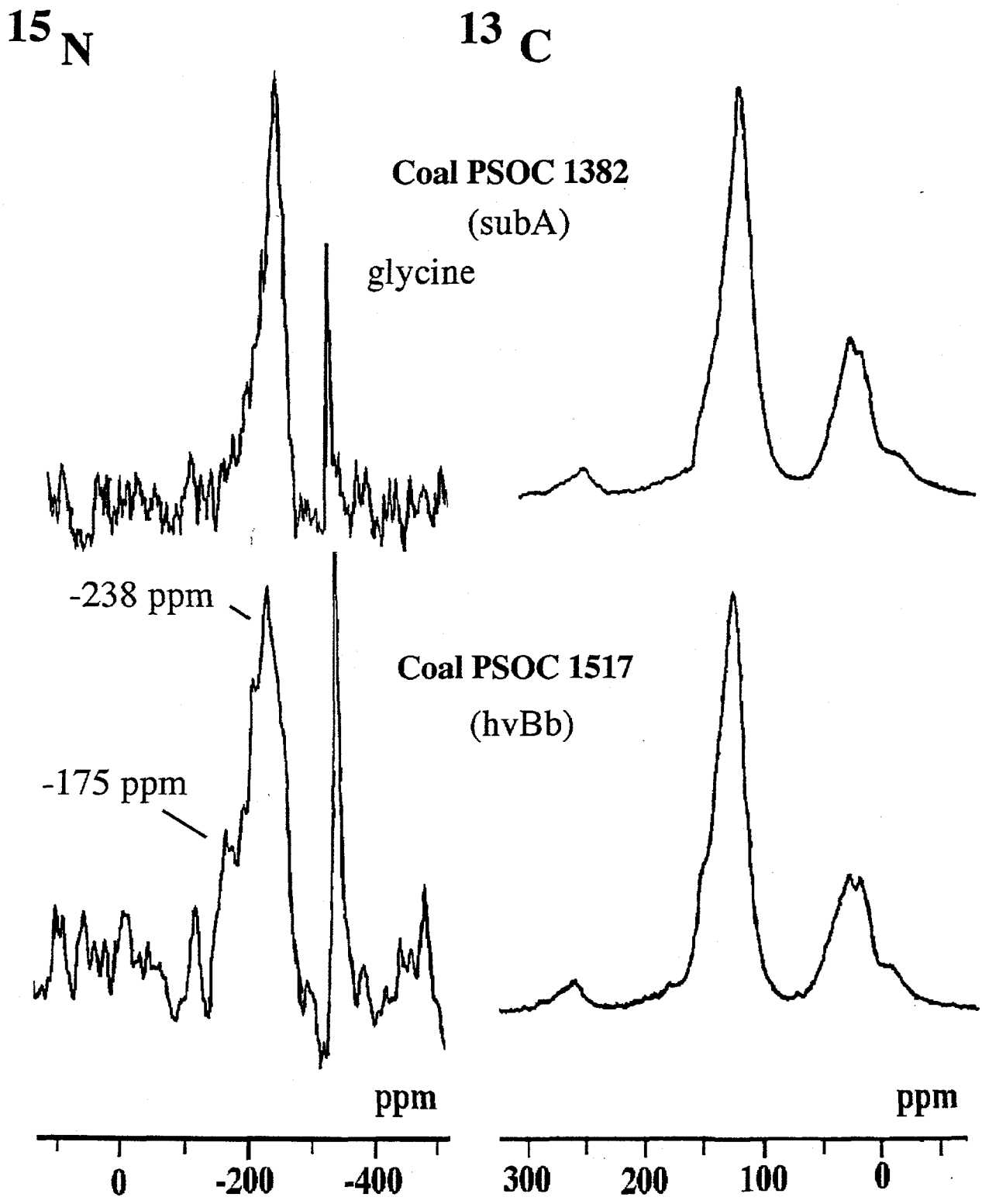

Figure 7-1. SOLID-STATE ^{15}N AND ^{13}C NMR SPECTRA OF VARIOUS COALS (Reference: Glycine = -345 ppm)

Table 7-1: Description of the coal samples from the Penn State Coal Sample Bank:

Sample	Location	Formation	Age	Carbon (%)	Hydrogen (%)	Nitrogen (%)	Rank
PSOC 1362	Lawrence County, Pennsylvania, USA	Allegheny Group, Freeport Formation	Middle Pennsylvanian	84.0	6.0	2.0	high volatile A bituminous (hvAb)
PSOC 1517	Mahoning County, Ohio #5, USA	Allegheny Group, Kittanning Formation	Middle Pennsylvanian	83.6	5.4	1.9	high volatile B bituminous (hvBb)
PSOC 1382	Moffat County, Colorado, USA	Mesaverde Group Williams Fork Formation	Late Cretaceous	75.8	5.0	2.0	subbituminous A (SubA)

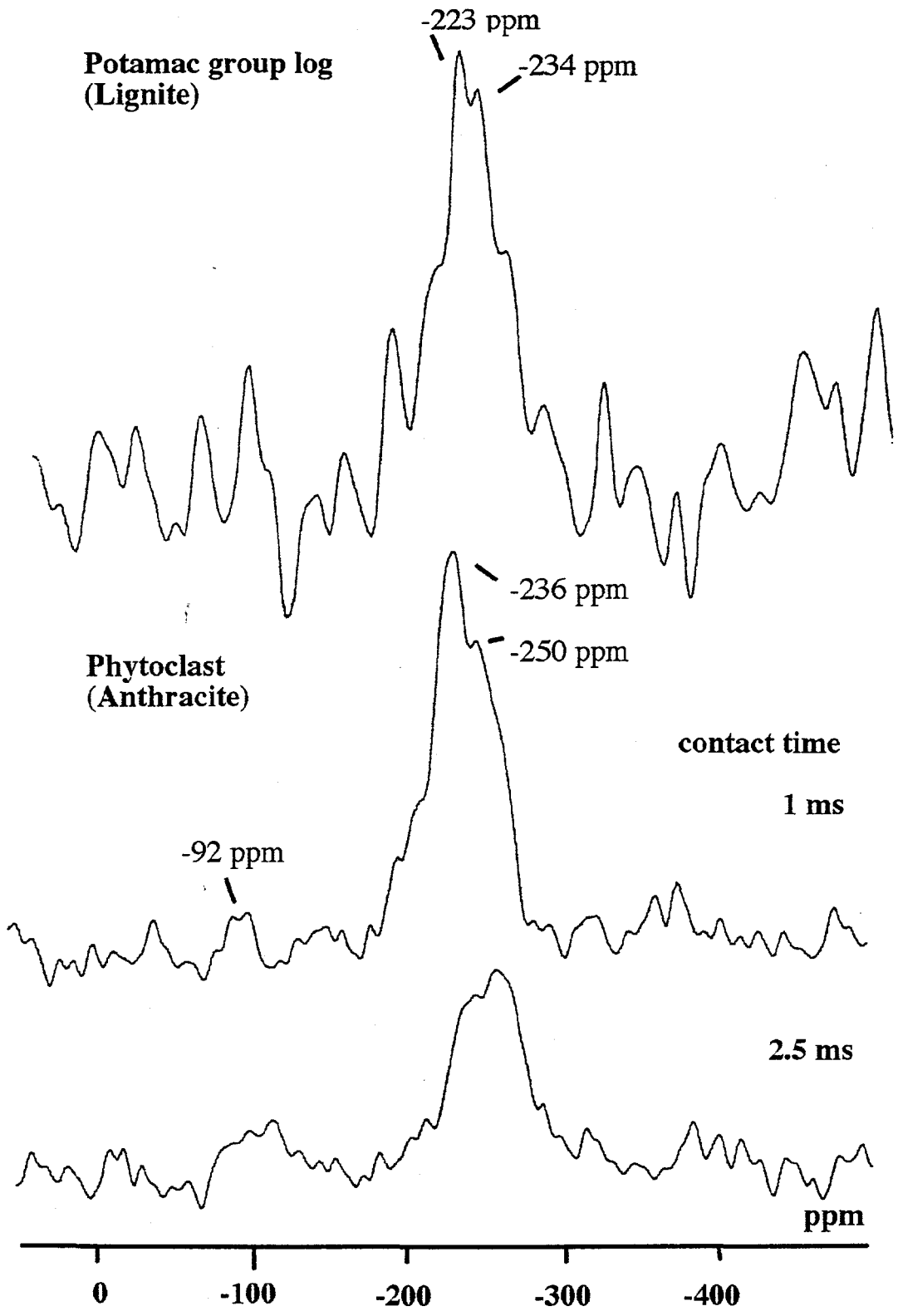

Figure 7-2. SOLID-STATE ^{15}N NMR SPECTRA OF VITRINITES (Lignite and Anthracite)

After HF-treatment of these samples, their high conductivitywas lost, which made acquisition of spectra possible. The signal-to-noise ratio of the spectra was doubled by using a NMR probe built for rotors of twice the volume of those previously used. An example of the spectra obtained is given in Figure 7-3. The main signal intensity can be assigned to carbazolic-N. The relative intensities in the region of pyrrolic-N are weaker than for the uncombusted samples. A signal in the region of pyridinic-N (-71 ppm) might be present. The weakness of these signals, however, makes identification rather difficult.

The conclusion to be drawn from this study is that a break-down of the less stable pyrrolic-N and a relative enrichment of carbazolic-N occurs during combustion. The latter might be selectively enriched due to the loss of other more labile N-components or newly formed during combustion. Although it was shown for the first time that ^{15}N NMR spectroscopy can help in understanding and examining chemical processes during combustion, a more detailed and expanded investigation of such processes is necessary and is part of the ongoing research. Time-dependency experiments, where chars are produced in a commercial boiler are sampled and analyzed as a function of combustion time are planned. From these experiments, it is hoped to obtain information on the kinetic behavior of the organic nitrogen in coal during combustion.

Refossilization of Algal Biomass as a Means of Biomitigation of Flue Gas Emissions during Coal Combustion.

Improvement and Testing of Techniques for the Isolation of Algaenans

One problem with comparing literature data obtained from the analysis of algaenan is that, although the basic steps of the extraction procedures are similar, specific steps are different. The basic steps include the removal of lipids with organic solvents, saponification and acid hydrolysis. In general, it is assumed that these procedures do not alter the chemical structure of the residue. However, it is well known that strong acid hydrolysis of a heterogeneous mixture containing amino acids and sugars can cause Maillard reactions. During such reactions, the free amino group of amino acids condenses with the OH-groups of the sugars and form, after rearrangement, dark insoluble polymers. Although the exact mechanism of this reaction is still not completely understood, it has been shown, that the insoluble polymers contain heterocyclic compounds, such as pyridines and pyrroles. In order to get information of the original structure of the algaenan, we started to examine how the extraction procedure influences the chemical structure of the Algaenan. Changes of the chemical structure of algal material during different extraction procedures of algaenan, which have been reported in the literature[7] and have been developed recently in our laboratory, were systematically investigated by solid-state ^{13}C

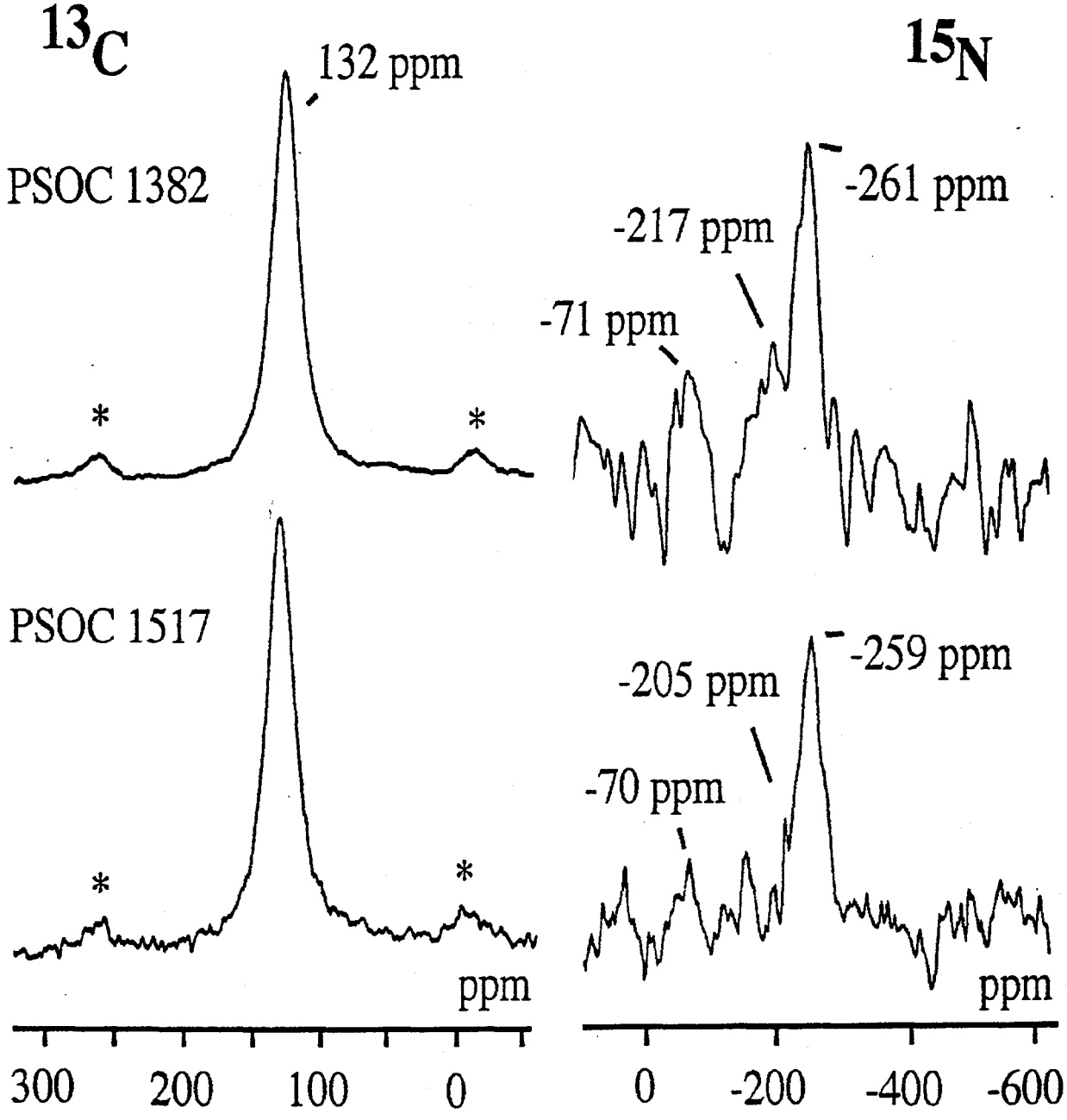

Figure 7-3. SOLID-STATE ^{15}N AND ^{13}C NMR SPECTRA OF VARIOUS COAL CHARS

NMR spectroscopy. Further ^{15}N NMR spectroscopic investigation on these materials are planned. Although the different extraction methods ask for different solvents to remove the lipid content, the ^{13}C NMR spectra of the extraction residue obtained after removal of lipids, and a following saponification of the algal material, showed spectra with comparable intensity distribution and a strong decrease in the chemical shift region of alkane and carboxylic-C, indicating the relatively efficiently removal of lipids. The procedure of removing lipids suggested by Berkaloff, et al.[7], however, is approximately 4 times more time consuming than the one suggested by Hatcher et al., and the one developed in our laboratory. The ^{13}C NMR spectroscopic analysis of the acid hydrolyzed algaenan residues obtained with the different methods, however, has yet to be finished.

Growing of algae on combustion flue gas:

The intention of this task was to test and optimize algal growth on simulated flue gas emissions. To date the research has focused on growing algal material for preliminary tests on the extraction of algaenan and on improvement of the extraction methods. Up to now, not enough biomass could be cultivated to begin extensive growth experiments.

Examination of the formation of algal-derived fossil sediments.

^{13}C- and ^{15}N NMR were applied to a maturation series of modern and ancient algal residues for the purpose of establishing the forms of nitrogen in algal remains and to evaluate their long-term stability. Samples were taken from different horizons of the sapropel of Mangrove Lake (Bermuda) and their NMR spectra were compared to those obtained from modern algal material (Fig 7-4, 7-5). In many respects, Mangrove Lake is a miniature Holocene analogue of ancient anoxic basins of the type leading to the formation of petroleum-generating kerogen[8]. This provides an ideal location for studies of diagenetic processes. Figure 7-4 shows the NMR spectra of the whole sediments as a function of sediment depth. The spectra are dominated by a strong amide signal at -256 ppm, indicating that some amides resist sediment maturation up to the deepest horizons at 9.8 m. At this sediment depth the organic matter was found to be 4000 yrs of age. A signal at -346 ppm, assigned to free amino groups, i.e. in amino acids and sugars and weak signals between -145 and -220 ppm and -285 to -325 ppm, both regions where amino acids components are expected, no other resonance lines can be identified. This strongly suggests, that in these sediments, organic-N survives mainly as amide, most probably in proteinaceous material. This contradicts most general beliefs, that nitrogen in soil and sediments resists maturation in the form of heterocyclic compounds, such as pyrroles or pyridines, formed by abiotic repolymerization and condensation of small degradation products.

Proteins, believed to be labile, but protected by interaction with the mineral phase, were found even in matured sediments[8]. They are normally extracted with base or acid

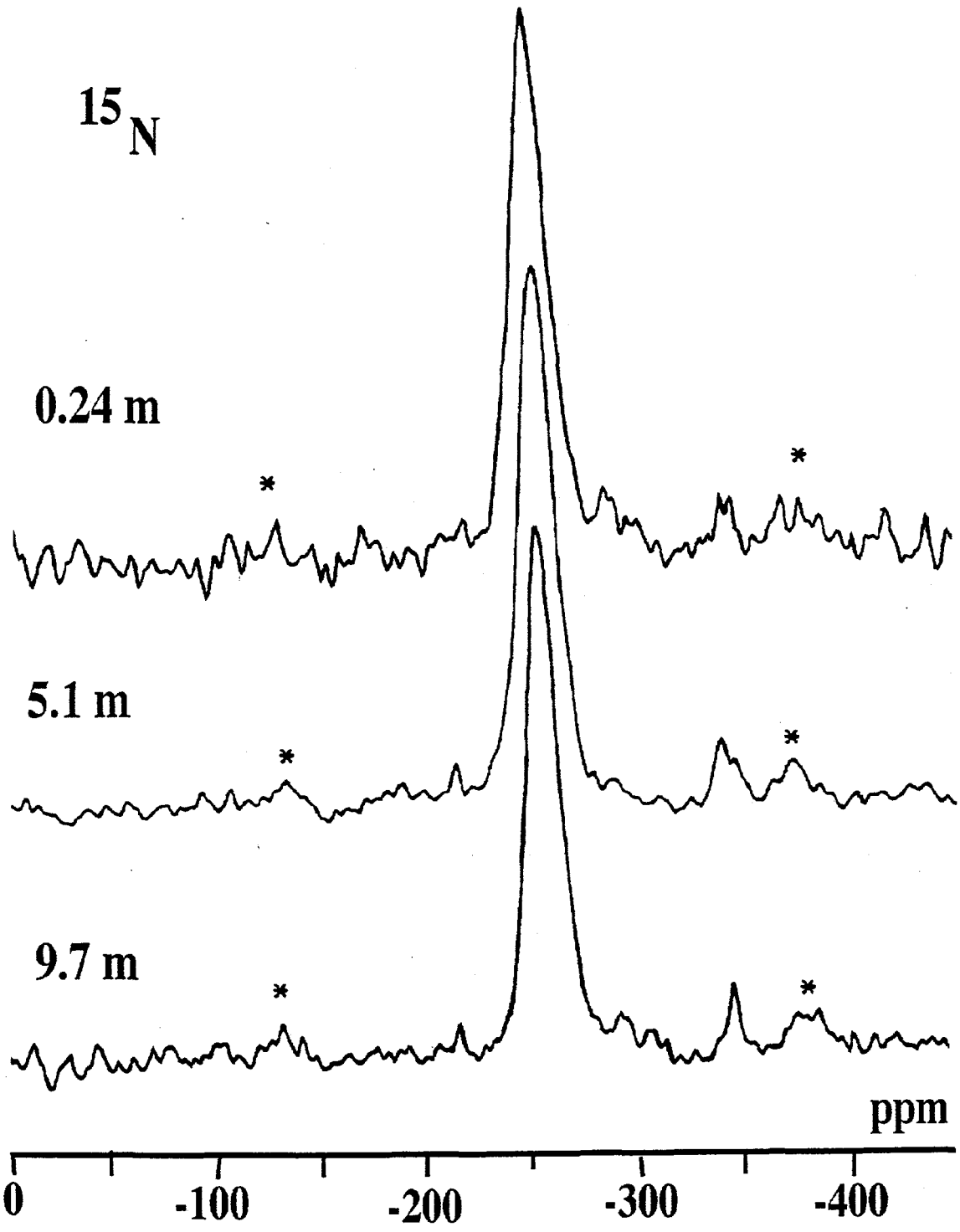

Figure 7-4. SOLID-STATE ^{15}N NMR SPECTRA OF AN ALGAL SAPROPEL (Mangrove Lake, Bermuda) OBTAINED FROM SEDIMENT DEPTH AT 0.24 m, 5.1 m AND 9.7 m.
Asteriks indicate spinning sidebands.

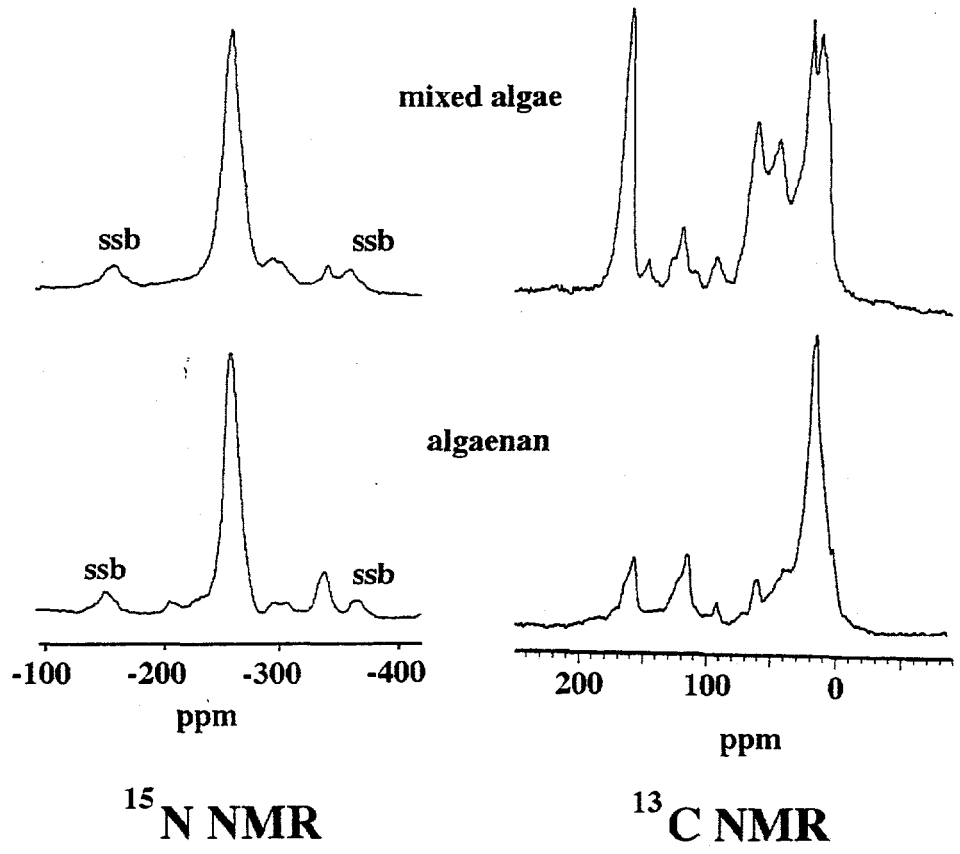

Figure 7-5. SOLID-STATE ^{15}N AND ^{13}C NMR SPECTRA A ^{15}N-ENRICHED MIXED ALGAL CULTURE AND ITS ALGAENAN. SSB INDICATES SPINNING SIDE BANDS

hydrolysis, methods, believed to be strong enough to extract all amino acids and proteins. It was found that less than 10 % of the nitrogen in such sediments can be assigned to such proteinaceous material[8]. On the other hand, this amount can only explain approximately 10 % of the nitrogen found in the amide region of the ^{15}N NMR spectra of the Mangrove Lake sapropel. The NMR spectroscopic analysis of extraction residues, obtained after strong basic and acid hydrolysis revealed the dominance of the amide signal even in those insoluble. Their resistance against chemical degradation may have been the reason why the role of such proteinaceous components in refractory organic matter formation of soils and sediments has been underestimated. The fact that up to 80 % of the examined sediments are organic, suggests that protection of the identified amides against microbial and chemical degradation is not only due to interactions with the mineral phase. The protection of proteinaceous material may result fromtheir encapsulation into the macromolecular network of the insoluble and recalcitrant algal biopolymer, the algaenan. The similarity of the ^{15}N NMR spectra of the sediments with that obtained from isolated algaenan supports this conclusion (Figure 7-5). However, also a lot of evidence was found for this assumption further experiments have to be conducted to prove this new hypothesis.

The next step in the investigation of the fate of refractory organic nitrogen during the formation of algal-derived fossil fuels was the NMR spectroscopic analysis of Torbanites and a sample of the Green River Shale (Figure 7-6). Both sediments are known to derive from the refractory residues of the algae *Botryococcus braunii,* the algae intended to use for our biomitigation strategy via refossilization of algal material. The ^{15}N NMR spectra reveal that during coalification the N-functionality shifts from amides to pyrrolic- and indolic-N. In contrast to the vitrinites examined above a signal in the chemical shift range of pyridinic-N can be identified as a weak resonance line[9]. The relative enrichment of pyrrolic-N in these sample may be due to their selective preservation or due to abiotic processes caused by the influence of heat and pressure. Such reactions may be the formation of melanoidins or the cyclization of proteinaceous material. Evidence for both pathways have been found in previous experiments[10, 11]. However, a more explicit investigation of this process is planned and involves an artificial coalification of algal material and the systematic investigation of samples at different stages of the artificial coalification process.

The overall conclusion of all these experiments is that nitrogen, once incorporated into algal biomass can survive prolonged microbial degradation. This is shown by the spectra of ancient and fossilized algal sediments. Therefore, nitrogen released during coal combustion and incorporated into algae may be a feasible strategy for sequestering NOx from its fast reentering into the atmosphere over a prolonged time scale.

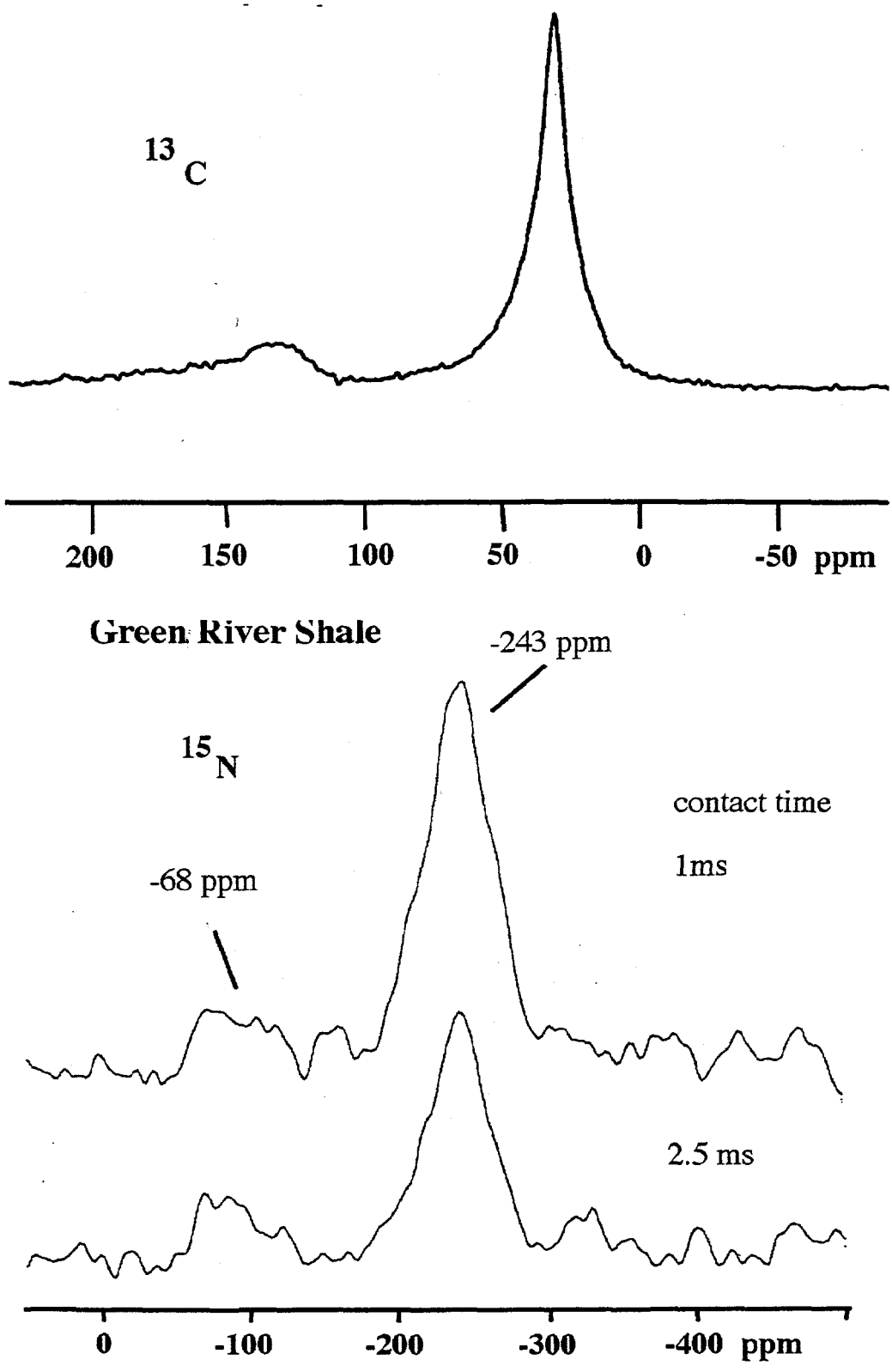

Figure 7-6. SOLID-STATE ^{13}C AND ^{15}N NMR SPECTRA OF ALGAL-DERIVED FOSSIL SEDIMENT (Green River Shale)

7.3 Subtask 1.3 Install System on the Demonstration Boiler

No work was conducted on this subtask.

7.4 Subtask 1.4 Evaluate Emissions Reduction System

No work was conducted on this subtask.

8.0 PHASE II, TASK 2: COAL PREPARATION/UTILIZATION

Activities in Phase II, Task 2 focused on preparing the final report.

9.0 PHASE II, TASK 3 ENGINEERING DESIGN AND COST; AND ECONOMIC ANALYSIS

Phase II, Task 3 has been completed except for Subtask 3.10, engineering design. Activities focused on preparing the final report for the remainder of the subtasks.

9.1 Subtask 3.10 Engineering Design

No work was conducted.

10.0 PHASE II, TASK 4 FINAL REPORT/SUBMISSION OF DESIGN PACKAGE

Work in preparing the final report continued. Tasks 2 and 3 (except for Subtask 3.10) have been completed.

11.0 PHASE III, TASK 1 COAL PREPARATION/UTILIZATION

11.1 Subtask 1.1 Particle Size Control

Grinding Circuit Simulation

It was shown in the previous report[2] that single-stage grinding in a conventional ball mill did not produce the shape of the size distribution required for a stable coal-water mixture. Stirred ball milling was also unable to produce the shape of size distribution needed for coal-water mixtures, although the size distribution was much finer than that produced in the ball mill. It was concluded, therefore, that a circuit arrangement involving two-stage grinding was required to produce slurry with the proper size consist. One such circuit arrangement is shown in Figure 11-1.

In the first stage, crushed coal (e.g., -12 mesh), water and dispersant are introduced into a ball mill, where it is ground in closed circuit. The product from the first stage grinding product is then classified. The fine stream is further ground in a closed stirred ball mill circuit to produce an ultrafine fraction. This product is then combined with the coarser size fraction, producing a bimodal size distribution.

The ideal mixing ratio of coarse and fine particles for maximum packing is 60:40. Therefore, the production rate of the coarse and fine size fraction must be controlled accordingly. At the same time, the maximum size of the coarse fraction must be controlled for proper combustion while keeping the size ratio of the coarse and the fine fraction sufficiently large (at least ten) for maximum solid loading and low viscosity.

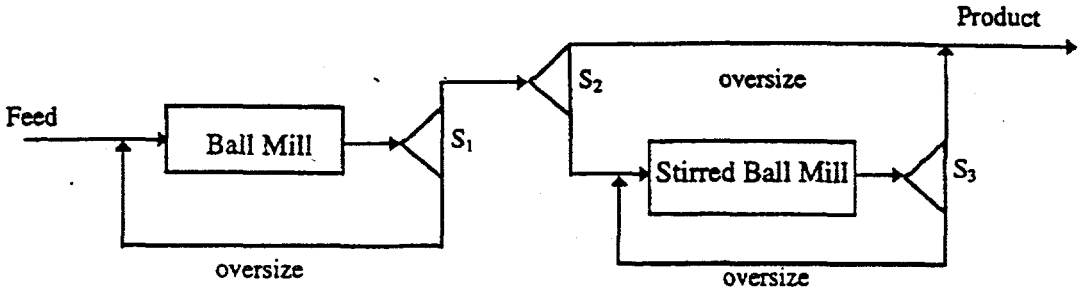

S_1 = Post-classifier for the first stage
S_2 = Pre-classifier for the second stage
S_3 = Post-classifier for the second stage

Figure 11-1. TWO STAGE GRINDING CIRCUIT FOR PRODUCING COAL-WATER MIXTURES WITH A BIMODAL SIZE DISTRIBUTION

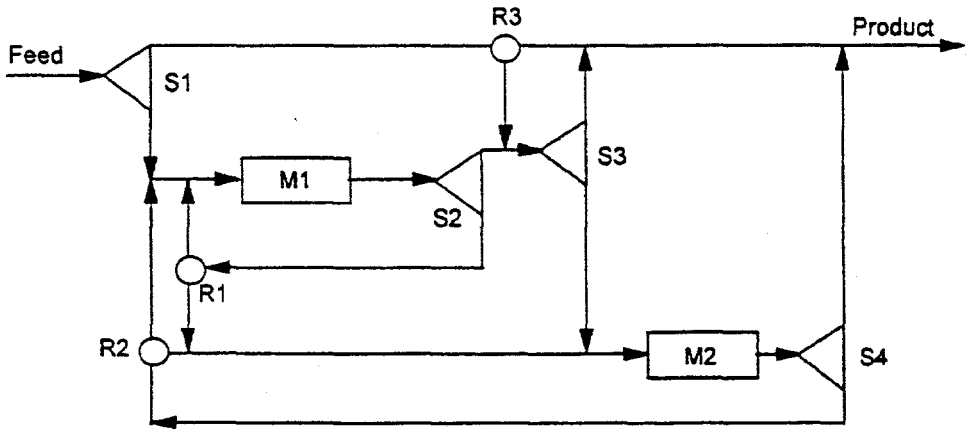

M1 = First Mill
M2 = Second Mill
S1 = Preclassifier
S2 = First Mill Classifier
S3 = Intermediate Preclassifier
S4 = Second Mill Classifier
R1 = First Mill Splitter
R2 = Second Mill Splitter
R3 = Third Splitter

Figure 11-2. GENERAL TWO-MILL GRINDING CIRCUIT

It can be expected that the mean residence time, τ, for each mill determines the characteristics of the final circuit product. The mill residence time (and hence the extent of size reduction) is controlled by material flow rates and mill operating conditions. However, the operating variables are not completely independent of the design variables. Let Ω be the ratio of the hold-up of the first stage (W_1) to the hold-up of the second stage (W_2), that is, $\Omega=W_1/W_2$. For a simple two-stage closed circuit at steady state, the mass flow rate into the first stage (G_1) equals the mass flow rate into the second stage (G_2): then, since the actual flow rate to the first mill is $F_1=G_1(1+C_1)$, to the second mill is $F_2=G_2(1+C_2)$, and $\tau_1= W_1/F_1, \tau_2=W_2/F_2$,

$$\Omega=[\tau_1 (1+C_1) G_1/ \tau_2 1+C_2) G_2]$$

where C_1 and C_2 are the circulation ratios of the first and the second stage, respectively.

Thus for a fixed set of breakage parameters, mill residence time distributions, (RTD), and classifier settings, a particular value of τ_1 fixes the entire system for a given Ω. Therefore, the design criteria involving two mills in series, are the mean residence time for the first mill, the classifier settings and the relative size of the two mills. Designing such a grinding circuit requires a simulator to evaluate the performance of a two mill grinding circuit under various operating conditions.

For this purpose, a general two-mill grinding circuit simulator was developed at Penn State. The complete circuit scheme is shown in Figure 11-2. In its original form, the circuit consists of two ball mills in normal closed circuit, with a circuit pre-classifier and a pre-classifier before the second mill. Additionally, the circuit has three dividers so that the streams of the first and second mill can be connected. By assigning the appropriate values to the classifiers and dividers, the general two-stage circuit can be reduced to any desired circuit varying from a simple single-stage open circuit to a very complicated two-stage circuit. Evaluating the performance of a grinding circuit is achieved by combining the mill model and the classifier model via the appropriate mass balance equations. A detailed description of the computational procedure can be found elsewhere[12].

However, before the simulator can be used to evaluate the circuit shown in Figure 11-1, several modifications are needed. The scale-up procedure involving the mill sizes and operating conditions for ball milling is well established as described in the previous report. However, the design procedure for stirred ball milling has not been completely established. It is often assumed that the specific energy is constant between the test and large mill for the same reduction ratios. The power draw of a stirred ball mill is a function of mill diameter and operating conditions. If operating conditions are selected for large

mills to consume the same specific energy as the test mill, the simulation can be performed using the same breakage parameters as those determined by the laboratory milling tests.

Classification is done extensively throughout the coal industry. In most cases, separations are made at sizes coarser than approximately 40 μm using hydrocyclones. Such operations are common and existing data are available to model the size separations. However, classification of particles down to 10 μm and perhaps finer will be required for coal-water slurry production. Although separations in this size range are often done in various mineral applications, they are not generally done in the coal industry. Therefore, selected tests were conducted using hydrocyclones to develop the appropriate parameters for the classification devices used in the circuit simulator.

The make-up feed size distribution (i.e., crushed product) was chosen as 80% passing 700 μm with Gaudin-Schuhmann slope 0.9. The parameters for the breakage rates and the breakage distribution were obtained through laboratory testing. The complete list of these parameters was reported previously[13]. The ball mill was assumed to have a residence time distribution equivalent to one-large/two-small fully mixed tanks-in-series with relative hold-up ratios of 0.5, 0.25, 0.25, whereas the stirred ball mill was assumed to be fully mixed. The simulations were conducted for a 1 meter diameter by 1.5 meter long wet-overflow ball mill operating at 70 wt. % solids, a fractional ball load of 0.35, rotational speed 70% of critical, with a make-up ball size of 31.75 mm (1.25 inches). The relative size of the stirred ball mill to the ball mill was 1:10, operating at 40 wt. % solids, 0.6 fractional ball loading and a total charge volume (balls and slurry) of 0.9.

The classifiers were assumed to be hydrocyclones. The characteristic parameters for the selectivity values at various cut sizes were determined by the laboratory testing and are shown in Table 11-1. It was assumed that an appropriate operation could be obtained to give suitable underflow and overflow slurry densities and the flow rates for the desired cut sizes.

Figure 11-3 shows the size distributions of the various streams when grinding the Taggart seam coal operated at 4 minutes residence time for the first mill and cut sizes for the first, second and third cyclones at 150 μm, 40 μm, and 17 μm, respectively. The mean residence time for the second mill was determined as 3.8 minutes. It can be seen that the final product size distribution has a bimodal shape resulting from combining the first stage and the second stage product. The bimodal shape, though, is less well defined than in the batch grinding system due to the imperfect separation of the cyclones and the back-mixing occurring in the continuous mill. The median sizes for each stage product are 52 μm and 3.3 μm, receptively, with the size ratio of the coarse and finer sizes being 16. The proportion of the coarser and the finer size fraction is about 60:40, which is an ideal

Table 11-1. Characteristic Parameters for the Size Selectivity Values at Various Cut Sizes.

Cyclone dia. inch	O/F dia. inch	U/F dia. inch	Cut size μm	Sharpness Index	Bypass	Flow rate liter/min
1	0.28	0.06	25.2	0.56	0.04	16.2
1	0.28	0.09	17.3	0.44	0.06	16.2
1	0.28	0.13	14.2	0.43	0.06	16.5
2	0.38	0.13	39.8	0.51	0.08	37.7
2	0.38	0.19	26.7	0.36	0.12	35.6
2	0.38	0.38	14.8	0.33	0.50	35.9
10	4.00	3.00	148.0	0.53	0.20	1128.0

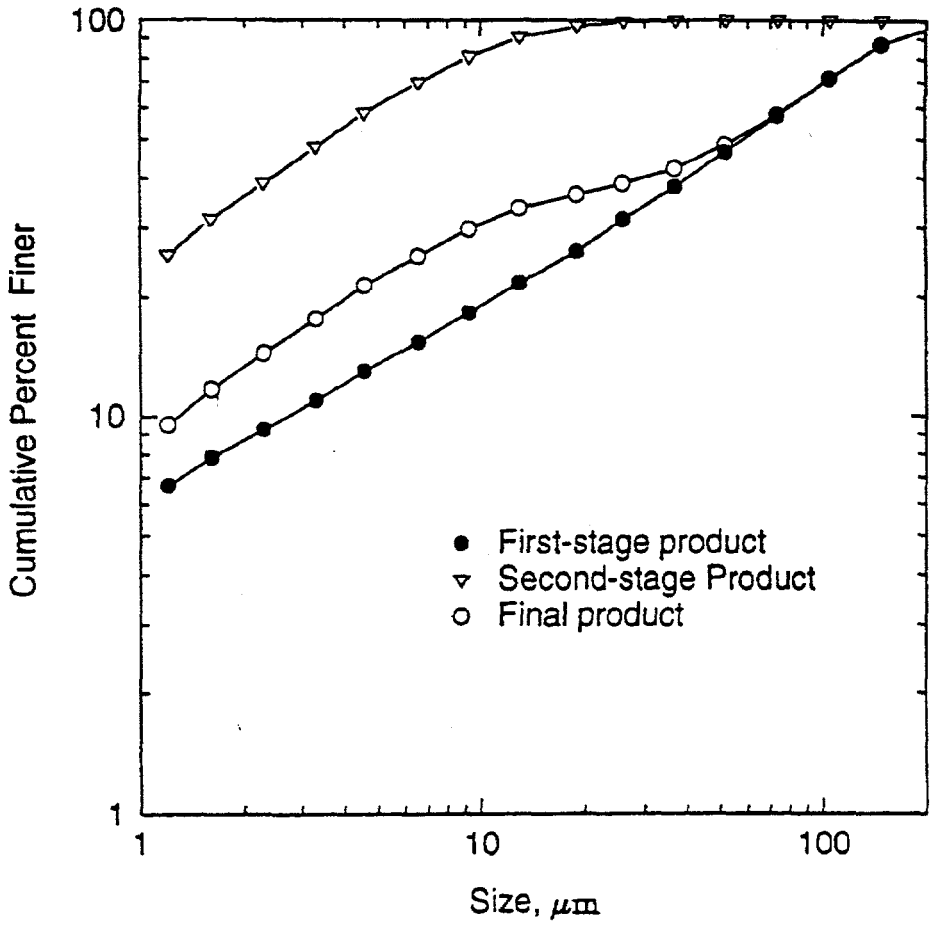

Figure 11-3. PRODUCT SIZE DISTRIBUTIONS AROUND TWO-STAGE GRINDING CIRCUIT

composition. The size ratio can be increased by reducing the cut size for the second stage post-classifier. This will produce a more distinct bimodal shape for the final product size distribution. However, this will also result in a decrease in the production rate for the second stage grinding, and hence, require a larger stirred ball mill. This effect will be further investigated.

Attrition Milling

Attrition milling operates on the same basic principle as stirred-media milling, but the size reduction is accomplished by the using the coal itself as the media. However, there is a major difference between the stirred-media mills and attrition mills. First, the power input is substantially less for the attrition milling, since the coal is lighter than the media and hence, less energy is required to agitate the slurry. More importantly, the breakage process in attrition milling is totally different. Large coal particles act as grinding media for smaller particles, giving breakage mechanisms similar to those obtained by normal grinding media. But they also break themselves by particle-particle contact. The breakage in any grinding mill is generally achieved by three different mechanisms - fracture, chipping and abrasion. Fracture refers to complete disintegration of a particle by massive impact, chipping involves cutting off corners, while abrasion results from the wearing of surfaces by a rubbing action. The fragments produced by fracture are distributed over a broad range of sizes. On the other hand, chipping and abrasion lead to production of fine material and a residual "core" close to the original particle size. Therefore, the shape of the product size distribution is greatly influenced by the type of the breakage mechanism. In attrition milling, chipping and abrasion will play bigger roles and the resulting products are likely to be composed of two main populations - coarse (remaining cores) and fines (chipped or abraded material). This is quite appropriate for coal-water slurry feed stock. Therefore, attrition milling potentially offers a great advantage for coal-water slurry preparation over other grinding procedures from both economic and engineering viewpoints.

Tests are being conducted to explore such a potential advantage using a vertical type stirred-media mill. The mill has been constructed with a stainless steel cylinder of 3" width and 4" height. The stirrer shaft carries 3-perforated disks. The rotation of the stirrer is provided by a 2-hp variable speed motor. A torque sensor, mounted on the drive shaft between the motor and the mill, provides an indication to the power input of the mill.

Test Plan

Obviously, the performance of the attrition mill depends on the composition of the material being ground. Large pieces must be available to use as grinding media. However, there is an optimum condition for the particle size and quantity ratio between the large and small particles for effective grinding. Therefore, tests are being conducted to determine the

breakage characteristics of large particles alone, and of small particles of various sizes when ground together with large particles at various blending ratios. Since the rheological properties are likely to play an important part in determining the breakage mechanisms, the effect of overall solids content is being examined as well as other operating parameters such as agitation speed.

Dry Grinding/Classification

Experimental data on dry grinding and classification of Upper Freeport seam coal were obtained as part of the Phase II research. Analysis of the results is currently in progress.

11.2 Subtask 1.2 Physical Separations

Dense-Medium Separation

The investigation of centrifugal dense-medium separation continued. Baseline testing was carried out using the continuous, solid-bowl centrifuge to determine the effect of operating conditions such as bowl and scroll speeds and weir height on dense-medium separation. All tests were run using -100 mesh Upper Freeport seam coal. Samples of the clean coal (weir overflow) and refuse (scroll discharge) streams were taken. Wet screening was used to remove the -500 mesh material. The clean coal yield was calculated by ash balance. The operating conditions and test results are summarized in Table 11-2.

For selected samples, a float-sink analysis was done at several relative densities on both centrifuge products. Using these data, along with the clean coal yield, the partition values for each relative density fraction were calculated. These values give the fraction of feed in a given relative density fraction that reports to the clean coal.

Figure 11-4 shows the centrifuge results for various main drive (bowl) speeds at a constant back drive speed (tests 1-3), along with the washability curve, for the 100x500 mesh Upper Freeport seam coal. The results approached the washability curve for the lower two bowl speeds but deviated at the higher speed. No separation was obtained at a bowl speed of 2400 rpm (Table 11-2). Tests 2, 4 and 5 show the effect of changing the weir height and in turn, pond depth for constant bowl and back drive speeds. In both cases, the results indicate that the centrifuge made very good separations at relative densities above about 1.5 even though the relative density of the medium was 1.3. Testing of the solid-bowl centrifuge will continue.

Magnetic Fluid Separation

Magnetic-fluid testing of the modified Frantz separator continued. Continuous separations were made with the flow-through separator and the test circuit as shown in Figure 11-5 using 28x32 mesh Upper Freeport seam coal. The coal was added to tank 1 containing the magnetic fluid and stirred for several minutes to ensure adequate mixing.

Table 11-2. Summary of the Operating Conditions and Test Results for the Solid-Bowl Centrifuge (Medium relative density = 1.3, feed rate = 11.3 L/min (3 gpm), medium-to-coal ratio = 10:1).

Test	Weir Setting*	Main Drive Speed, rpm	Back Drive Speed, rpm	O/F Ash, %	U/F Ash, %	Yield, %
1	2	800	300	6.9	63.0	91.7
2	2	1200	300	5.4	56.1	87.9
3	2	1500	300	4.9	27.5	70.7
4	2	2400	300	-	11.5	0.0
5	1	800	300	5.6	46.0	85.3
6	3	800	300	5.8	37.2	81.7

* Lower weir setting corresponds to a shallower pond depth.

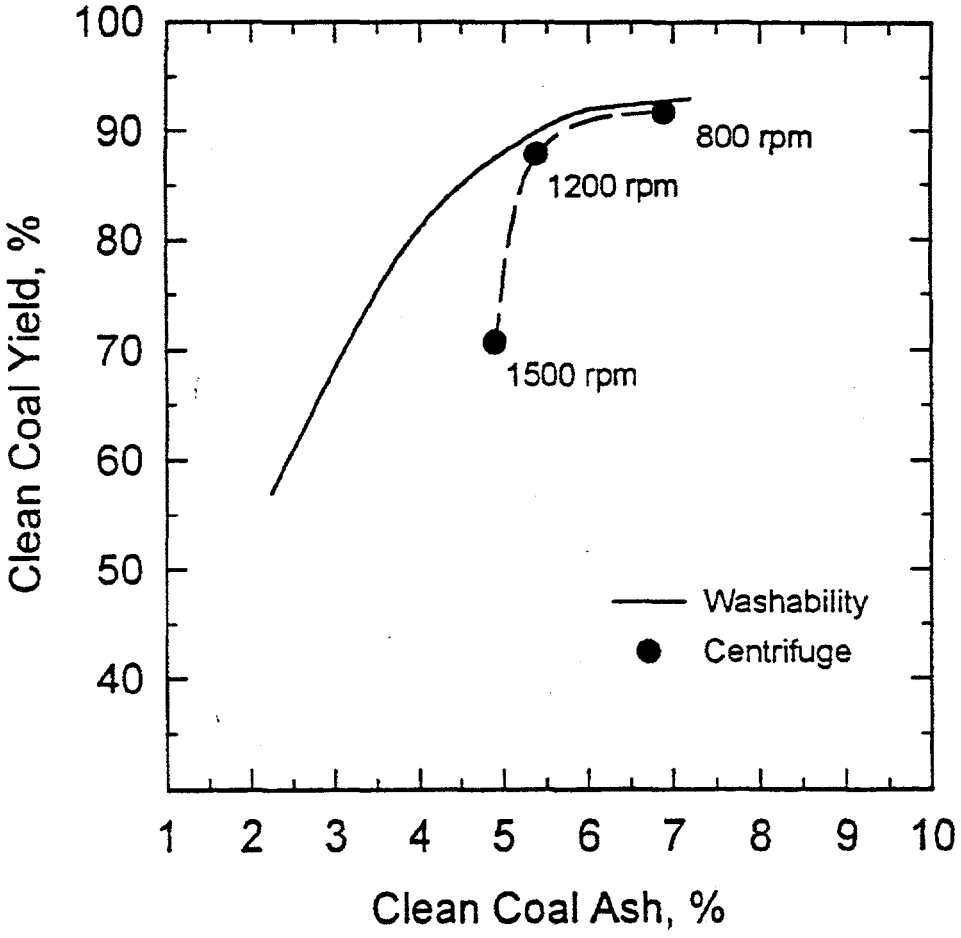

Figure 11-4. EFFECT OF MAIN DRIVE SPEED ON THE GRADE-YIELD VALUES FOR THE SOLID-BOWL CENTRIFUGE AT A CONSTANT BACK DRIVE SPEED OF 300 RPM AND A MEDIUM RELATIVE DENSITY OF 1.30 FOR THE 100 x 500 MESH UPPER FREEPORT SEAM COAL

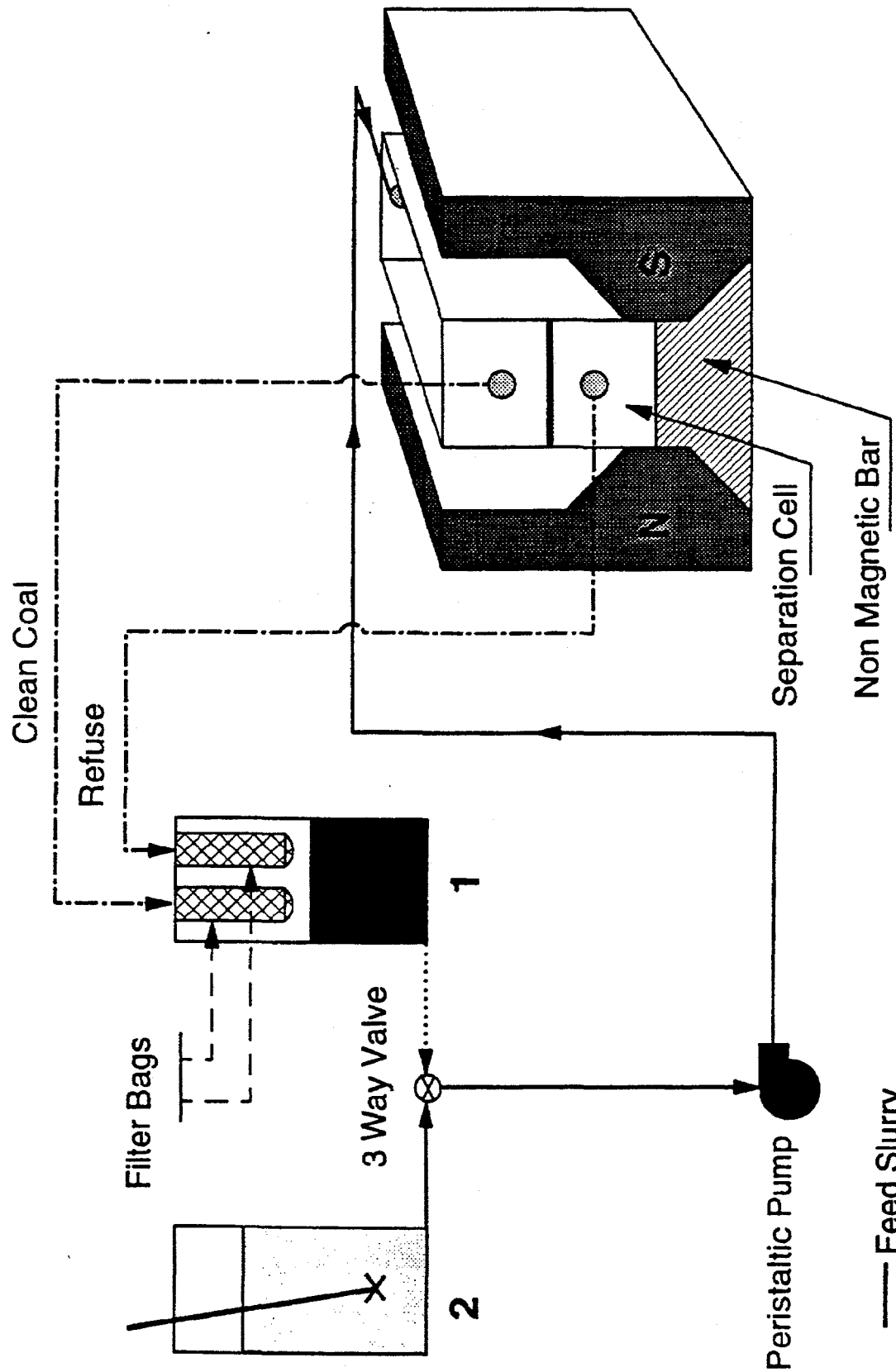

Figure 11-5. MAGNETIC FLUID SEPARATOR TEST CIRCUIT

The solids concentration was fixed at 2% solids by weight. The magnet was turned on and set to the appropriate setting to produce the desired relative density. The peristaltic pump was started and set to the desired speed. The flow rate and hence, the retention time in the device, were set by adjusting the pump speed. The valve was set to tank 2 so that only the magnetic fluid was pumped through the separator. This was done to fill the unit prior to feeding the coal slurry. Care was taken to dispel any air bubbles from the separator. Once filled, the valve was set to pump the coal slurry from tank 2. The float and sink products were split at the discharge end and collected continuously over the test period.

Upon completion of the test, the valve was set to pump the recirculated fluid from tank 2 to flush out the remaining solids in the system. After all of the float material was removed, the pump and the magnet were shut off. Any solids remaining on the bottom of the separator were combined with the sink material. The test procedure was repeated using a new pump speed or new magnet (i.e., relative density) setting.

The products were subjected to float-sink separation at several relative densities using organic liquids. Using these data, along with the clean coal yield, the partition values were calculated for each of the test conditions. These values were then fitted to the logistic function to determine the relative density of separation and the probable error (Table 11-3).

Tests were run with the 28x32 mesh coal using the continuous separator at a relative density of 1.3 for a flow rates of 1.7, 2.4, and 3.3 L/m. This gave retention times in the device of 5.2, 3.6, and 2.7 seconds, respectively. Figure 11-6 shows the partition curves obtained as a function of flow rate. As expected, the curves steepen with an increase in retention time, indicating a sharper separation. This is expected since a horizontal line that corresponds to the volumetric split of slurry to the overflow stream would be indicative of splitting rather than separation. For these tests, the volumetric split was approximately 0.5 for all flow rates.

Additional tests were run at relative densities of 1.4 and 1.6 at a flow rate of 1.7 L/m. Figure 11-7 shows the variation of the partition curves as a function of the relative density of the medium. As expected, the curves shifted to the right with an increase in the medium density. For densities of 1.3 and 1.4, the probable errors were similar (Table 11-3) but increased at 1.6.

Figure 11-8 compares the grade-yield curves for each flow rate and medium density to the washability curve for the 28x32 mesh coal. As can be seen, magnetic fluid separation approached the theoretical curve at the lower flow rates (longer retention times) and for the higher densities of separation. Additional work in this area is continuing.

Table 11-3. Partition Parameters when Separating 28x32 Mesh Upper Freeport Seam Coal in the Magnetic Fluid Separator.

Flow Rate, L/min	Medium Relative Density	Mean Retention Time, s	Relative Density of Separation	Probable Error
3.3	1.3	2.7	1.35	0.30
2.4	1.3	3.6	1.37	0.22
1.7	1.3	5.2	1.39	0.11
1.7	1.4	5.2	1.47	0.12
1.7	1.6	5.2	1.78	0.17

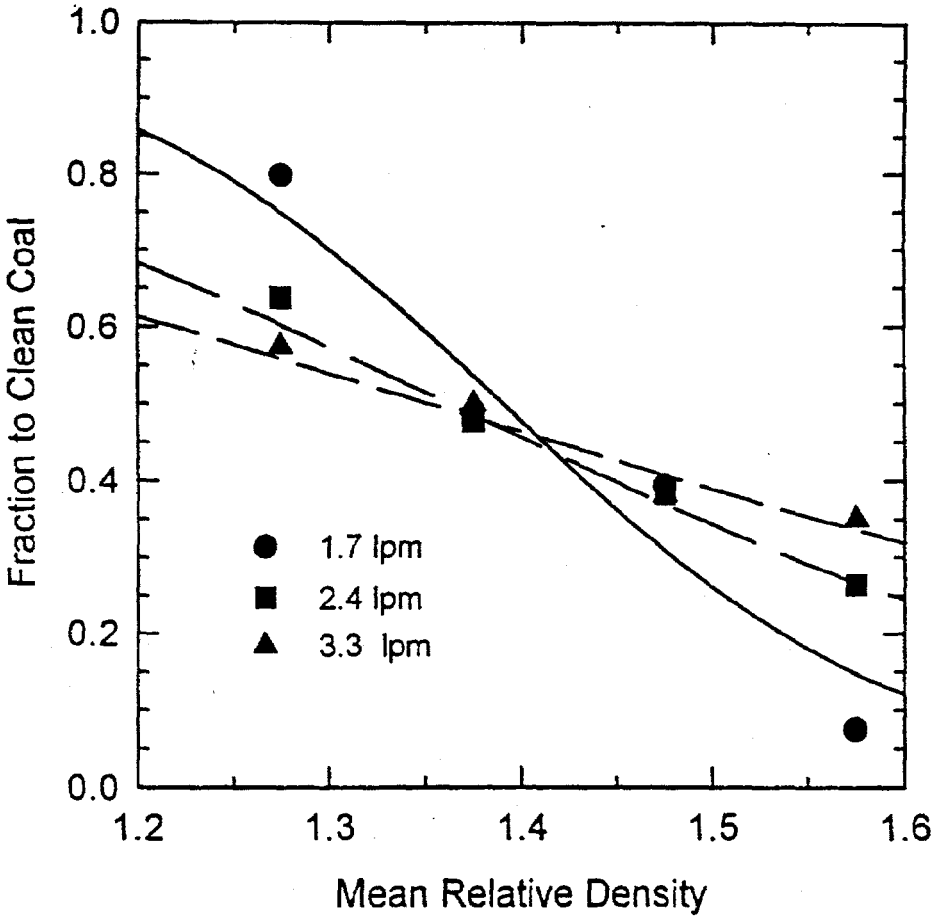

Figure 11-6. FRACTIONAL RECOVERY CURVES FOR THE MAGNETIC FLUID SEPARATOR AS A FUNCTION OF FLOW RATE AT A MEDIUM RELATIVE DENSITY OF 1.3 FOR THE 28 x 32 MESH UPPER FREEPORT SEAM COAL

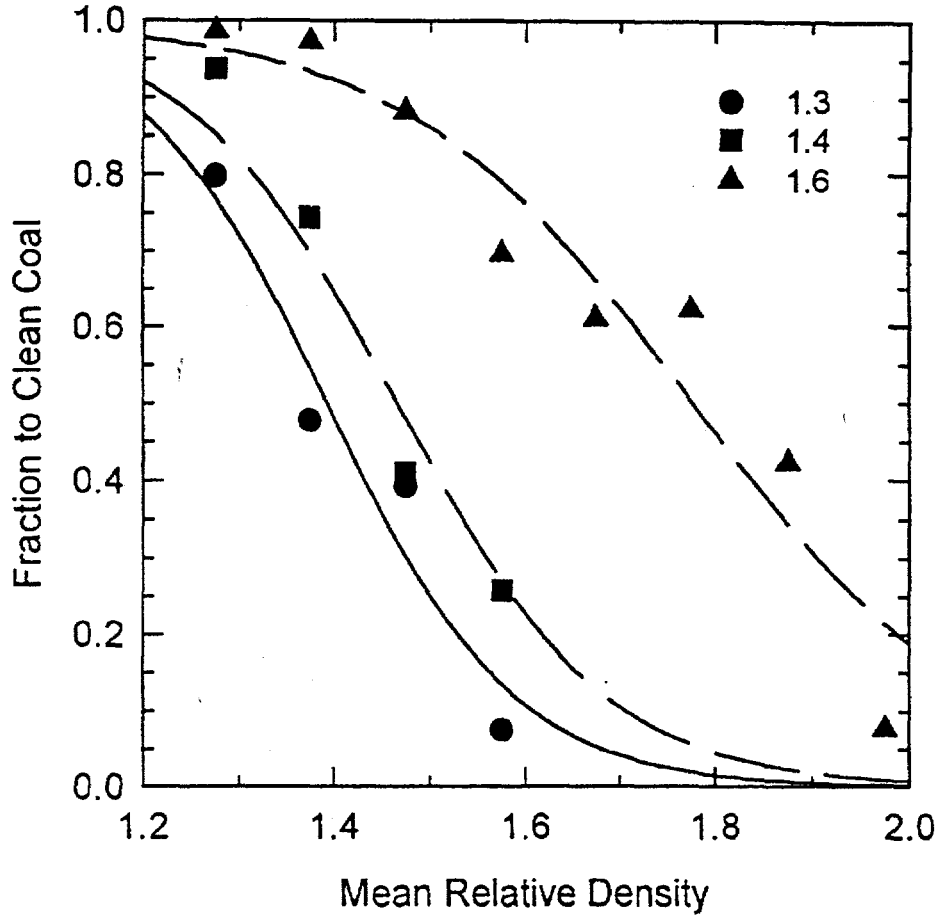

Figure 11-7. FRACTIONAL RECOVERY CURVES FOR THE MAGNETIC FLUID SEPARATOR AS A FUNCTION OF MEDIUM RELATIVE DENSITY AT A FLOW RATE OF 1.7 L/min FOR THE 28 x 32 MESH UPPER FREEPORT SEAM COAL

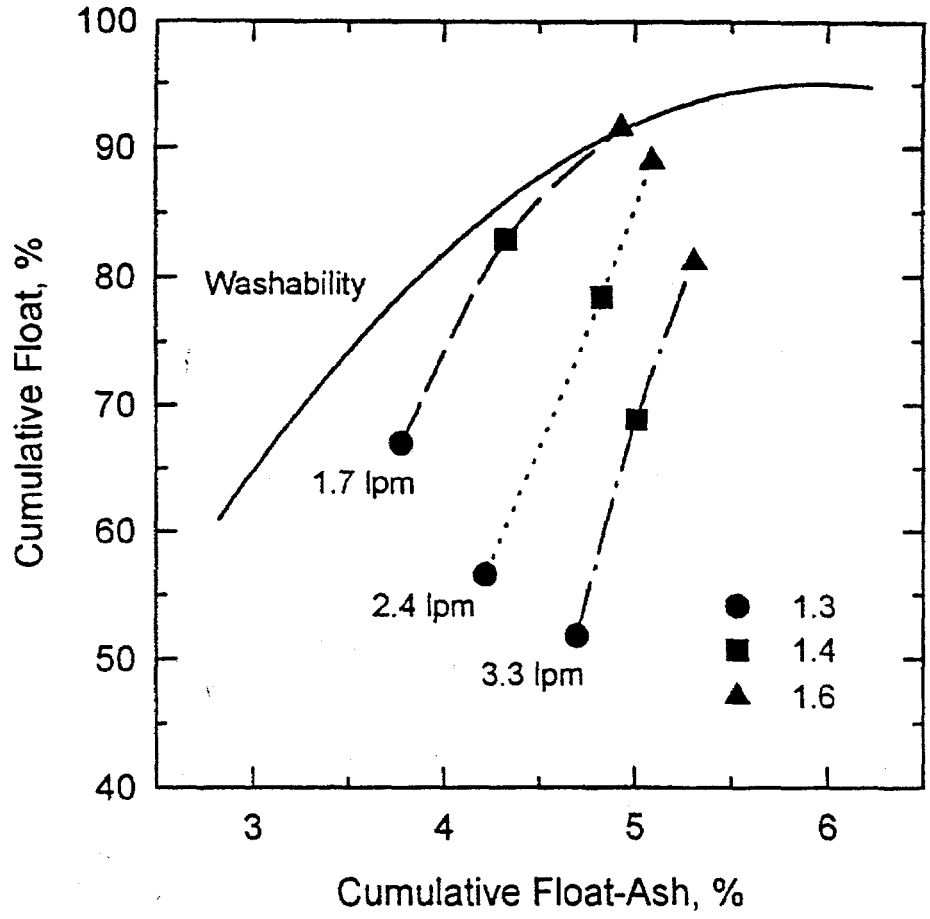

Figure 11-8. EFFECT OF FLOW RATE AND MEDIUM DENSITY ON THE GRADE-YIELD VALUES FOR THE 28 x 32 MESH UPPER FREEPORT SEAM COAL

11.3 Subtask 1.3 Surface-Based Separation Processes

Continuous Froth Flotation

Experimental

The continuous flotation tests were conducted on a pilot plant scale froth flotation circuit which was described in a previous semi-annual report. The flowsheet of the continuous circuit with a capacity of about 8 gpm, located at the EFRC is given in Figure 11-9. The flotation circuit was designed for cleaning coal in two stages. The coal to be fed to the flotation circuit was ground in a stirred ball mill which had a total capacity of 30 gallons and a working capacity of about 20 gallons. The operating conditions were selected so as to produce a size distribution of about 100% passing 28 mesh; a typical size distribution is shown in Figure 11-10. The ground slurry, containing about 20-35% solids was transferred to the 500 gallon capacity head tank, shown in Figure 11-9. The slurry from the head tank was pumped by a Moyno pump at a flow rate that was set depending on the circuit requirements and the percent solids in the feed slurry. A flow meter was connected after the pump to monitor the slurry flow rate from the head tank.

The rougher circuit consisted of :

1. 20 gallon feed tank with mixer
2. Four, WEMCO cells of 1.4 cubic feet capacity each
3. 5 gallon frother tank
4. 1 gallon collector tank with mixer
5. Quinn froth pump, with a flow meter
6. Sampling system

The coal-water slurry from the head tank was fed into the rougher feed tank where it was diluted with water to make a slurry containing about 5% solids. The amount of water added to the feed tank depended on the solids content of the feed slurry from the head tank. A rotameter was used in series with the water line to measure the flow rate which was adjusted so as to obtain the desired total flow rate.

The MIBC frother, and dodecane collector were each mixed with water in a ratio of 1 to 400, in the frother and collector tanks respectively. The frother and the collector were pumped into the rougher feed tank where the contents were mixed. In some tests the collector was fed to cells 3 and 4 only, to avoid overloading of the froth in cells 1 and 2, thereby increasing recovery in cells 3 and 4. In these tests, collector addition in the head tank resulted in high froth stability and poor recovery in cells 3 and 4.

The coal-water slurry containing 5% solids, and frother and collector were fed to the series of four cells. The impellers in the cells were rotated at a fixed speed of about 1000 rpm, and the aeration was set to the maximum value. The froth containing clean coal flowed above the weir of the cells and was removed into the launders on each side of the

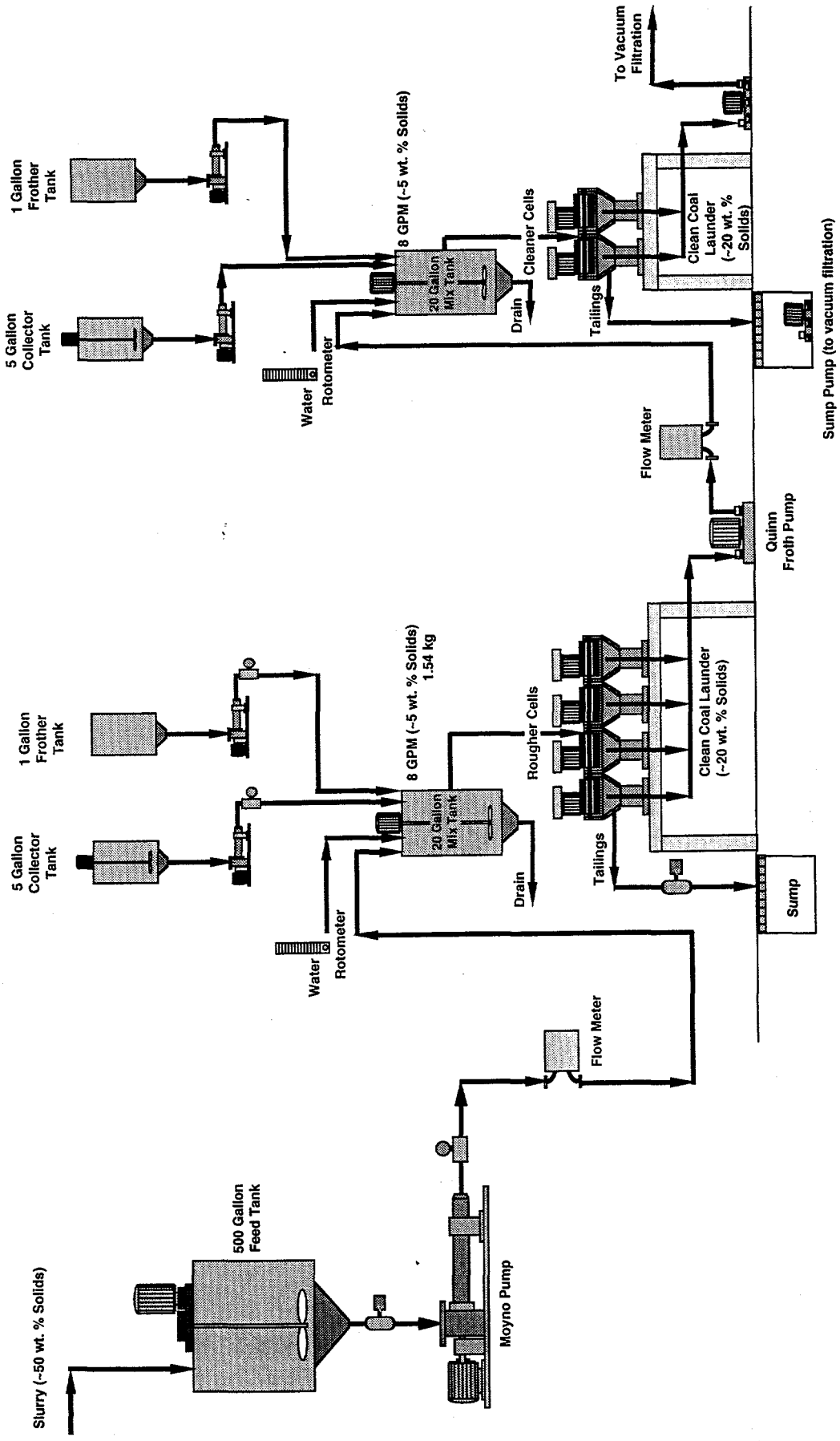

Figure 11-9. ROUGHER-CLEANER FLOTATION CIRCUIT USED IN CONTINUOUS FLOTATION TESTS

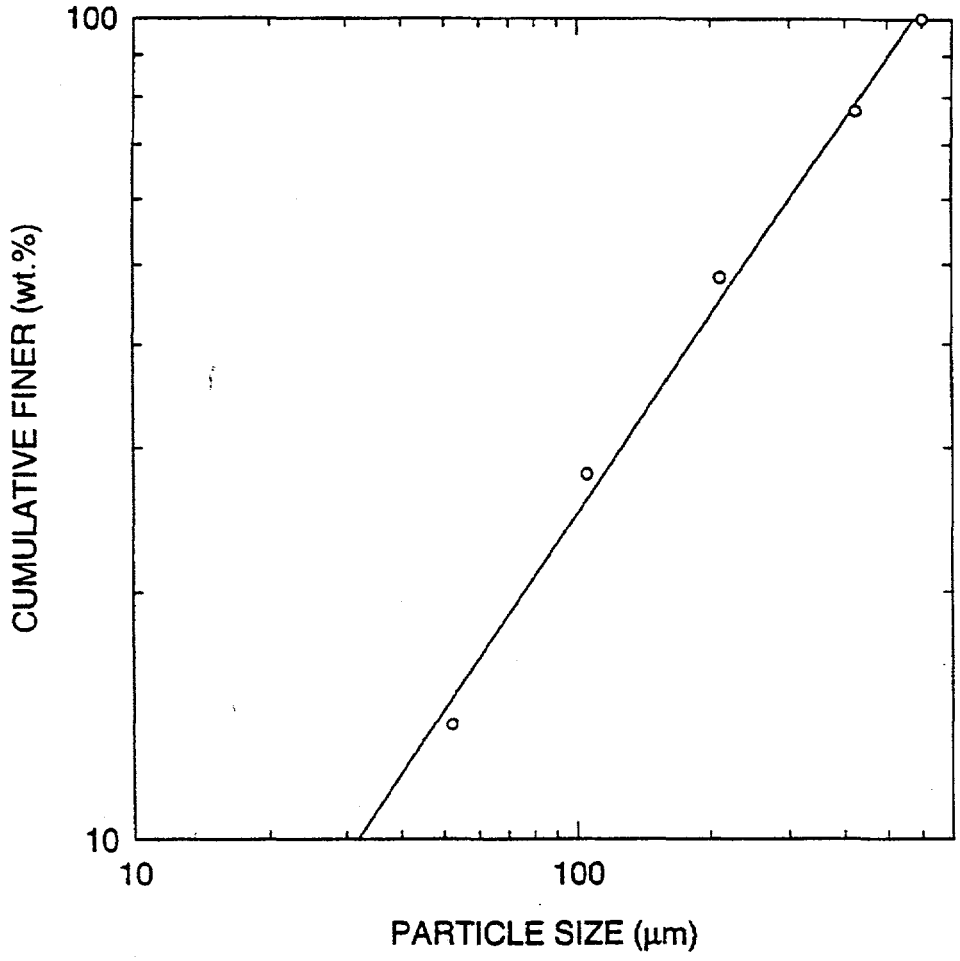

Figure 11-10. SIZE DISTRIBUTION OF THE FEED

cells by rotating paddles. The froth in the launders was washed down by the wash water. The wash water flow rate was about 1 gpm, and was monitored by a rotameter.

The froth product from the circuit was collected in plastic storage drums, and was subsequently filtered and stored. In those tests in which the cleaner circuit was used, the froth was allowed to flow down into a froth sump, from where it was pumped to the cleaner circuit. The tailings from the last cell in the rougher circuit were discharged into a sump.

The cleaner circuit consisted of:

1. 20 gallon feed tank with mixer
2. Two flotation cells of 1.4 cubic feet capacity each
3. 5 gallon frother tank
4. 1 gallon collector tank with mixer

The froth product from the rougher circuit was diluted to about 5% solids with water. The water flow rate into the feed tank was adjusted to get the desired total flow rate, and was monitored using a rotameter. The frother and collector could be fed into the feed tank as desired. The froth product from the cleaner cells was collected in drums, and the tailings from the last cell flowed down into a sump. If required, the cleaner tailings could be recycled to the rougher cells.

The product from the cleaner circuit was filtered on a vacuum filter. The tailings in the trench sump, now containing very low percent solids were pumped using the trench pump to a overhead tank, where it was mixed with a solution of calcium chloride, and the solids were allowed to flocculate and settle overnight. The clear water on the top was decanted, and the slurry with settled solids was pumped to a vacuum filter.

For the Lower Kittanning seam coal tested in this part of the investigation, the ash analysis of samples taken from the rougher and cleaner circuits during preliminary tests showed that the froth product from the rougher circuit satisfied the ash content requirement for subsequent combustion tests. Therefore most of the tests with this coal sample were performed using only the rougher circuit.

To evaluate the performance of the circuit slurry samples were taken from the froth product from all the four cells, and the feed and the tailings streams. To maximize the probability of representative sampling the whole streams at each circuit sampling point were diverted into sampling containers and samples were taken simultaneously from every stream. The samples collected were subsequently filtered, dried, weighed and analyzed for ash content. Two sets of samples were collected for each test to determine whether the circuit was operating at steady state. The samples collected from one test were sieved using 28, 48, 100, 200, and 400 mesh sieves to obtain the size distribution of each stream. From

the weight and ash analysis of various samples, the flotation response of various size fractions could be determined.

Results And Discussion

Lag Time

During laboratory tests it is often observed that the froth flows over the weir of the cell only after a finite time has elapsed after the air is turned on. This time lapse is called 'lag time'. The time when the froth starts flowing over the weir is often set as flotation time 'zero'.

The mean residence time of the slurry in a cell or a bank of cells is calculated by the relation

$$\tau = V/Q$$

where V is the effective volume and Q is the flowrate of the slurry. Here, it is assumed that that the slurry acts as a liquid, and the liquid mean residence time would represent that of the whole slurry. Assuming that about 15% of the cell volume is occupied by air, the mean residence time for a 1.4 ft^3 cell at a flow rate of 6 gpm, is calculated to be 1.50 minutes.

The cumulative weight percent of material remaining in the each cell is plotted in Figure 11-11. It is assumed that the mean residence time is the same for each cell, and the residence time of the material at any cell is the cell number multiplied by the mean residence time for one cell. The curves joining the recovery points at different conditions do not merge to 100 percent at time 0 or cell 0. The lag time is different, ranging from 0.2 cell to 0.5 cell, under different operating conditions. To calculate the lag time, the following equation was used:

$$R = R_\infty\left(1-e^{-k(t+t_L)}\right)$$

where t_L is the lag time. The lag time for the rougher circuit was estimated to be 0.4 times the mean residence time of a cell, which is 0.6 minutes.

Effect of Frother Concentration

Figures 11-12 and 11-13 show the effect of frother concentration on the recovery from each cell in the bank of flotation cells. Figure 11-12 shows the cumulative recovery at each cell. As expected, the cumulative recovery curves shifted to higher values as the cell number increased. In each curve the cumulative recovery attains a maximum in the frother concentration range of 0.4 kg/T to 0.45 kg/T. Figure 11-13 shows the fractional recovery from each cell as a function of frother concentration. In the first two cells the recovery

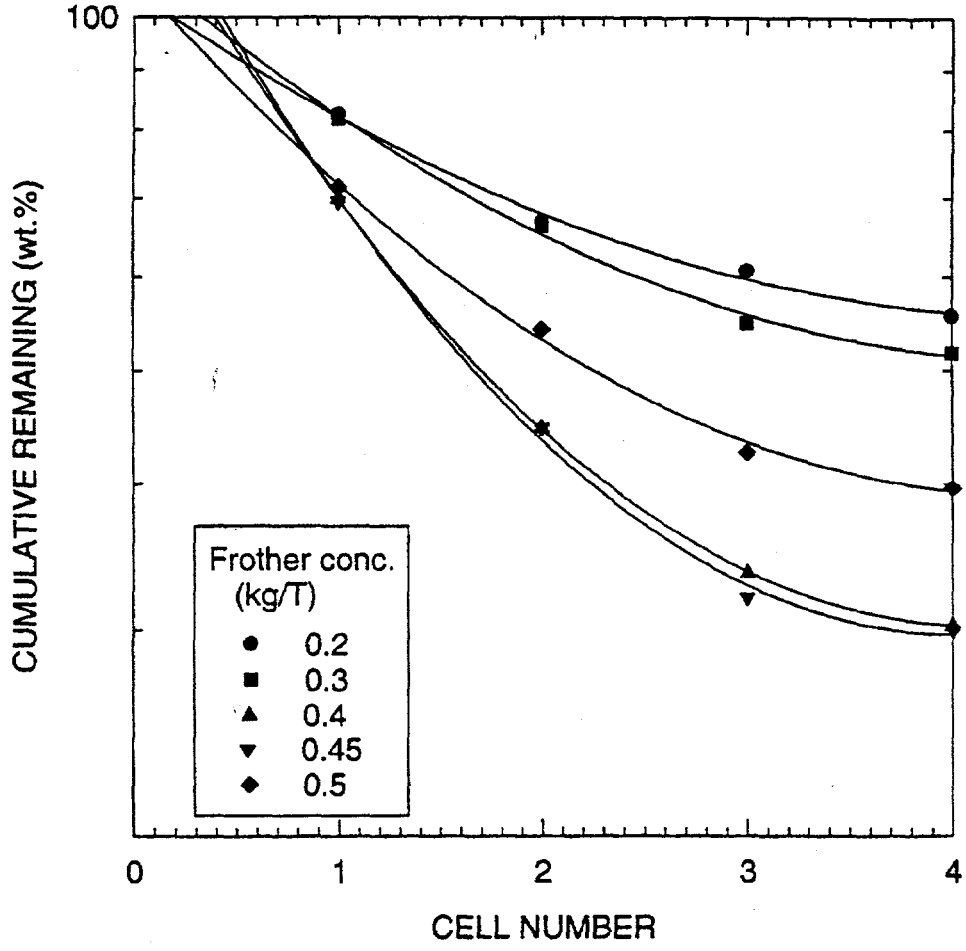

Figure 11-11. ESTIMATION OF INDUCTION TIME

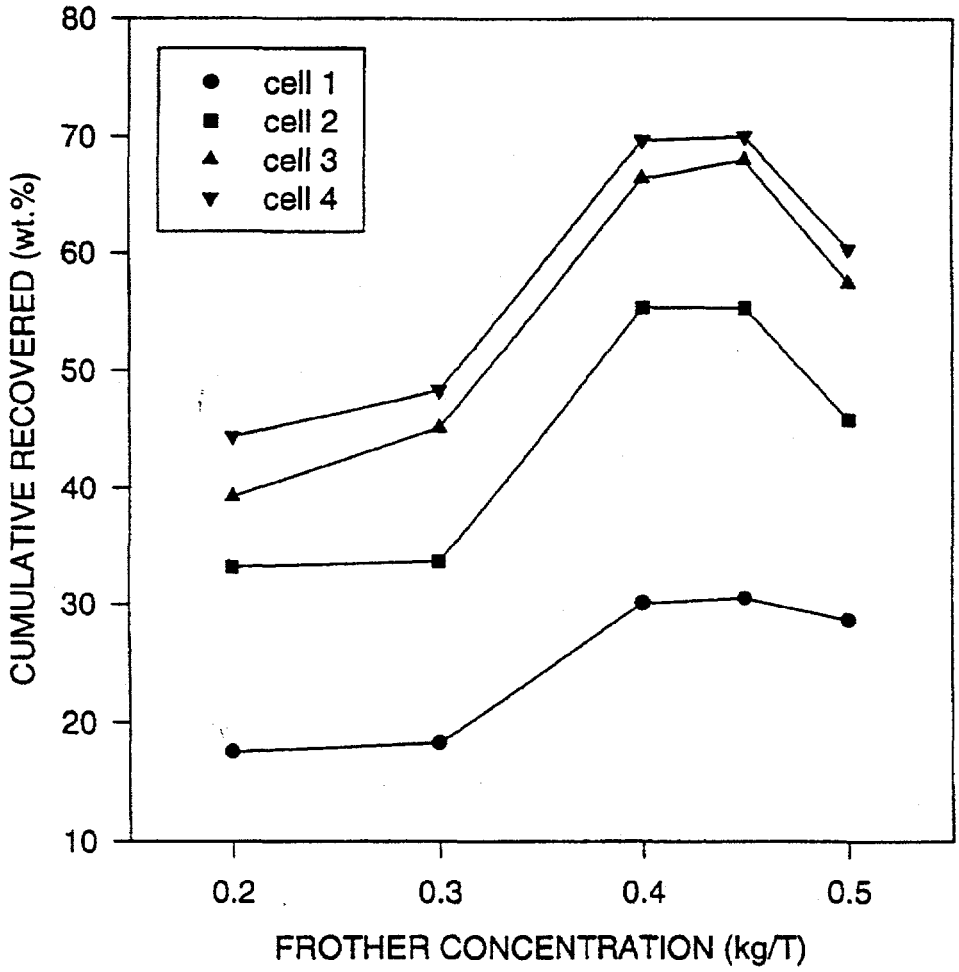

Figure 11-12. CUMULATIVE RECOVERY FROM EACH CELL AT DIFFERENT FROTHER CONCENTRATIONS

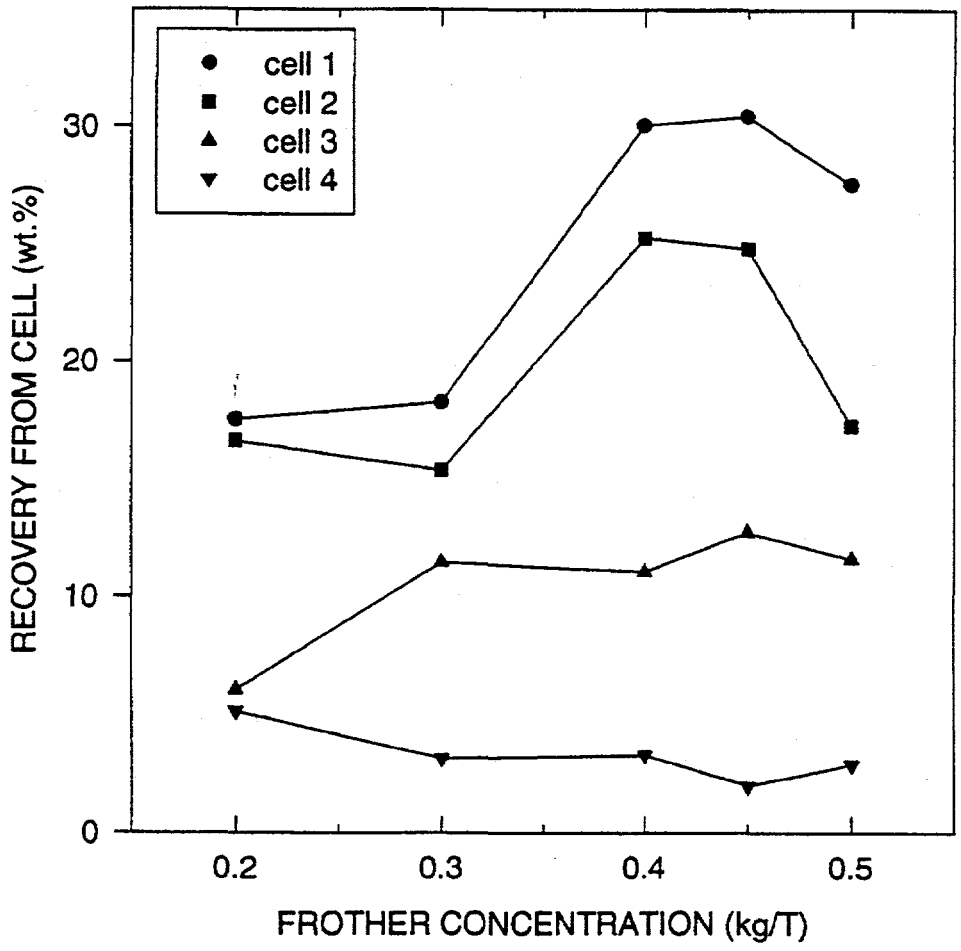

Figure 11-13. FRACTIONAL RECOVERY FROM EACH CELL AT DIFFERENT FROTHER CONCENTRATIONS

increased with increase in frother concentration in the range of 0.2 kg/T to 0.4 kg/T. The recovery remained fairly constant in the range 0.4 to 0.45 kg/T, and then decreased as the frother concentration was increased further. In cell # 3, the recovery increased when the frother concentration was increased from 0.2 kg/T to 0.3 kg/T, and remained relatively constant. In cell # 4, the fractional recovery decreased slightly when the frother concentration was increased at low concentrations. The recovery remained relatively constant at higher frother concentrations. The flotation recovery from each cell is maximum at a frother concentration in the range 0.4 kg/T to 0.45 kg/T. It is concluded that this frother concentration range is optimum for the flotation of Lower Kittanning coal in the pilot plant flotation circuit.

Kinetics

The flotation results are plotted in Figure 11-14 after incorporating the lag time. Since the data fits the first order model only in the initial stages, the data up to cell 3 was used to estimate the rate constants and the first-order plots are given in Figure 11-15. The flotation rate increased with frother concentration in the range of 0.2 kg/T to 0.4 kg/T. The rate remained constant in range of 0.4 kg/T to 0.45 kg/T. The flotation rate decreased with further increase in frother concentration. The flotation rate constant are given in Table 11-4.

Effect of collector concentration

The kinetics plots for tests performed with a fixed frother concentration of 0.3 kg/T and varying the collector concentration from 0 to 0.1 kg/T are shown in Figure 11-16. Most of the coal that floated was recovered in the first two cells. Though the flotation rate increased with the addition of collector, the froth in cells 3 and 4 became very stable resulting in a stagnant froth. As a result, the particles in the froth fell back into the cell, and the recovery decreased. Since the cells 1 to 4 were connected as one unit, it was not possible to separately adjust pulp level in each cell. An independent control of the pulp level in each cell and a method to add frother and collector to cells 3 and 4 could have improved recovery. This approach was not pursued due to time constants, however.

The corresponding flotation rate constants are given in Table 11-5.

Flotation rates of various size fractions

To determine the behavior of coal in various size fractions, this series of tests were conducted. Various samples obtained from the test conducted with a frother concentration of 0.5 kg/T were sieved to obtain the size distribution in each stream. The kinetics plots for the different size fractions are plotted in Figure 11-17. The flotation rate and final recovery increased as the particle size decreased from 600 μm to 37 μm. The flotation rate

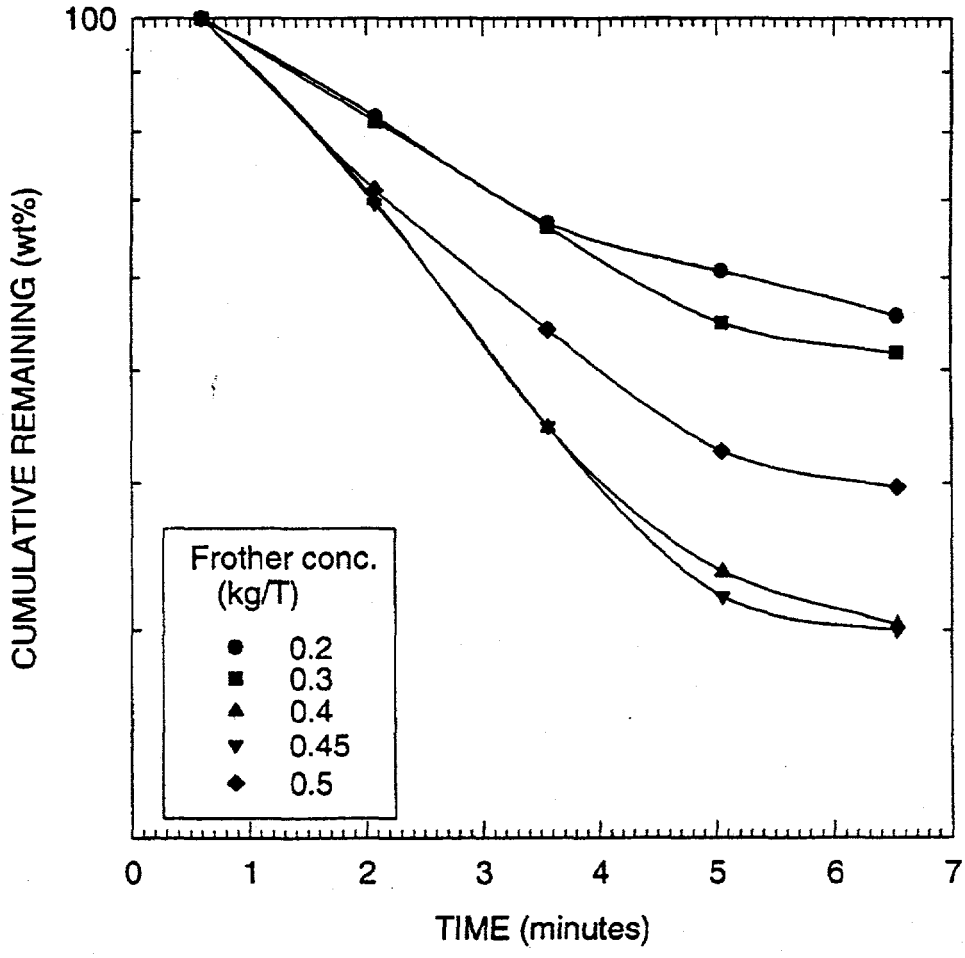

Figure 11-14. KINETICS PLOTS AT DIFFERENT FROTHER CONCENTRATIONS

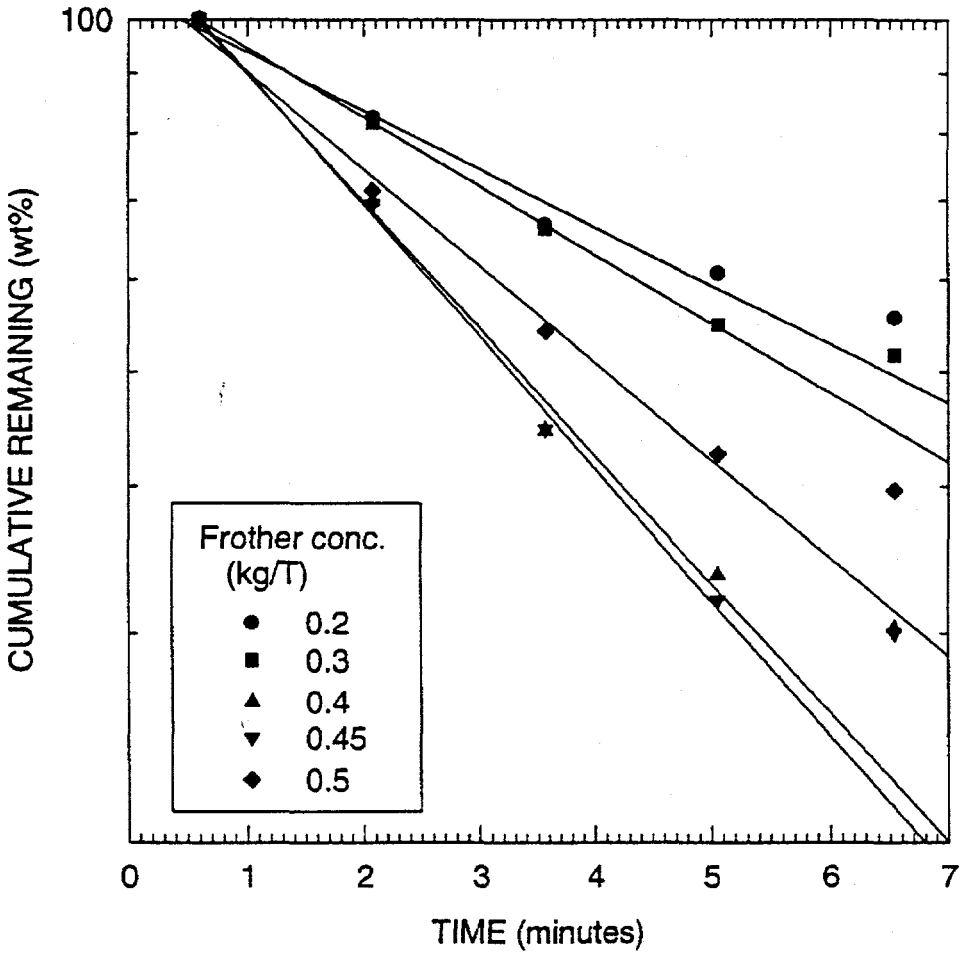

Figure 11-15. ESTIMATION OF FLOTATION RATE CONSTANTS

Table 11-4. Flotation Rate Constants at Different Frother Concentrations

Frother concentration (kg/T of coal)	Flotation rate constant (per min.)
0.20	0.1148
0.30	0.1355
0.40	0.2503
0.45	0.2599
0.50	0.1910

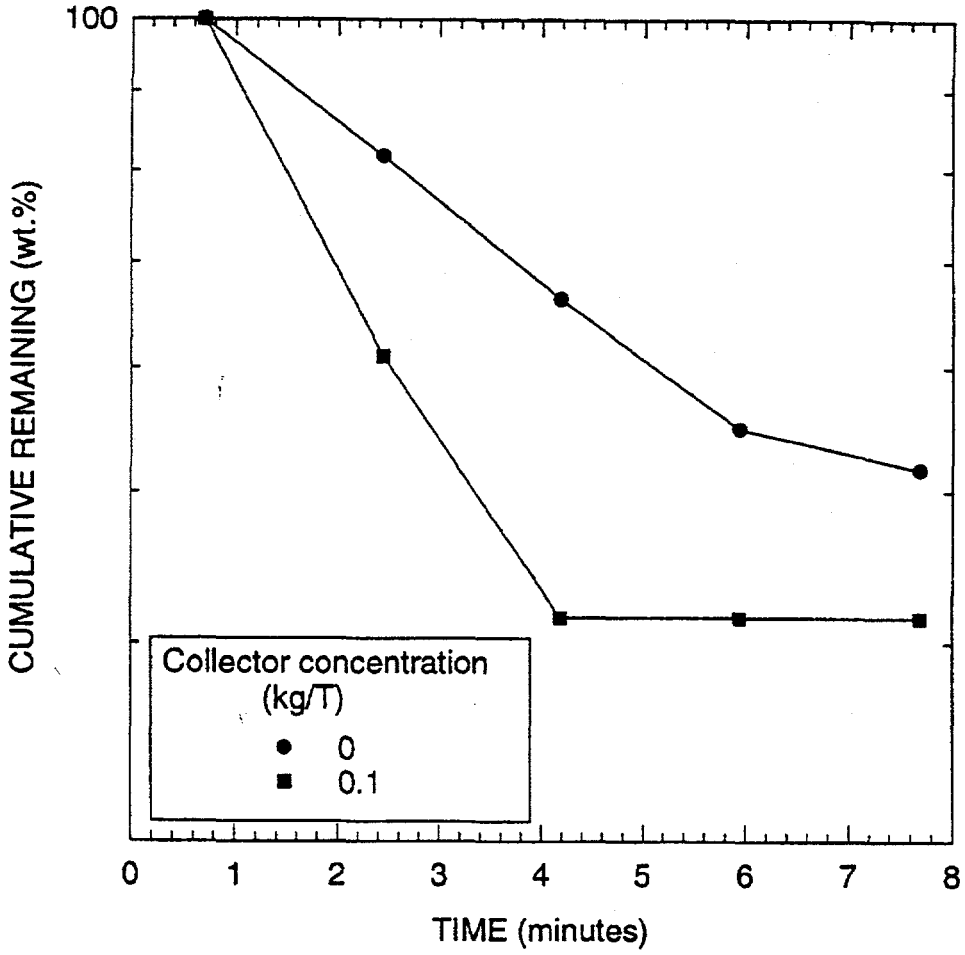

Figure 11-16. KINETICS PLOTS AT DIFFERENT COLLECTOR CONCENTRATIONS (frother conc. = 0.3 g/T)

Table 11-5. Flotation Rate Constants at Different Collector Concentrations.

Collector concentration (kg/T) (frother : 0.3 kg/T)	Flotation rate constant (min^{-1})
0	0.1152
0.1	0.2520

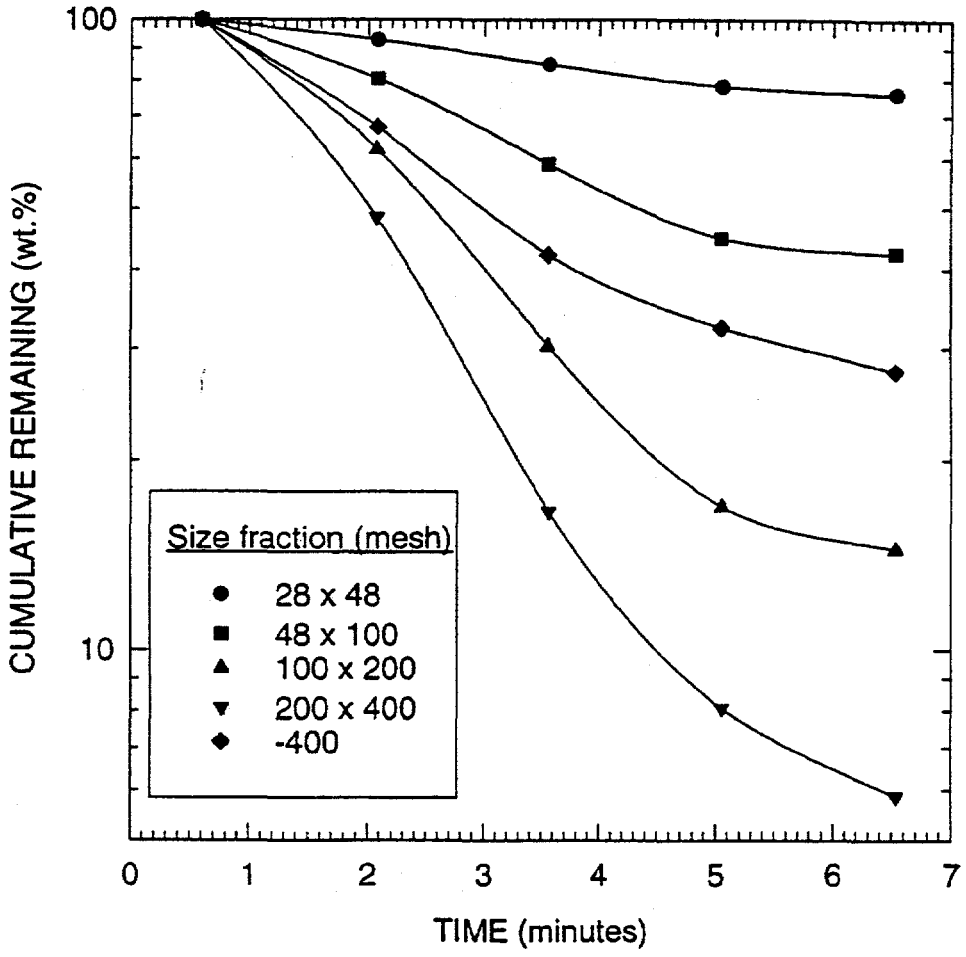

Figure 11-17. KINETICS PLOTS FOR DIFFERENT SIZE FRACTIONS FOR TESTS CONDUCTED AT A FROTHER CONCENTRATION OF 0.3 kg/T

and recovery were lower for the -400 mesh size fraction. The 200 x 400 mesh fraction had the highest flotation rate and final recovery.

The flotation rate regression lines are plotted in Figure 11-18. The flotation rate for each size fraction was calculated from the slope. The flotation rate constant values are given in Table 11-6.

The flotation rate constants for different size fractions plotted in Figure 11-19 show that the flotation rate of coal particles increases as the size decreases to about 400 mesh, and decreases with further decrease in size.

The cumulative recovery of each size fraction from the four cells is shown in Figure 11-20. The recovery was maximum for the 200 x 400 mesh fraction. The expected increase in the recovery of the coarser material in cells 3 and 4 was not observed probably because the level in these cells could not be controlled independent of cells 1 and 2. The froth mobility in cells 1 and 2 was very different from that in cells 3 and 4. It might be possible to increase 3 and 4 by using a frother which is more affective for coarse particles.

Evaluation of Vortactor Bubble Generator in Column Flotation

The Vortactor is a bubble generator that is under development at Penn State. A schematic representation of the Vortactor bubble generator is shown in Figure 11-21. A hydrodynamic study of the bubble generator has been recently completed (Ityokumbul, 1995).

In order to demonstrate the effectiveness of the present bubble generator in fine particle beneficiation, flotation experiments were carried out using -100 mesh Upper Freeport coal. The column was operated in the semi-batch mode with tailings recirculation. The recirculated tailings was the feed to the bubble generator and was maintained at a flow rate of approximately 4.5 L/min (0.27 m^3/h). The column had an overall height of 1.5 m. However, provision was made for the slurry-air mixture to be introduced at 0.33 m, 0.64 m, 0.89 m and 1.14 m from the base of the column. For the experiments reported here, the slurry-air mixture was introduced at a height of 0.33 m or 0.64 m from the base of the column.

A 5-, 10- and 15 wt. % coal slurry was prepared and transferred into the column using a peristaltic pump. The required amount of MIBC was added to give a frother concentration of 50 ppm (v/v). After allowing for the frother to be properly mixed with the slurry, the air was turned on to the desired value (2.24 L/min) and the chamber pressure adjusted to approximately 103 kPa. The choice of a chamber pressure of 103 kPa and a tailings recirculation rate of 0.27 m^3/h were based on hydrodynamic studies which indicated that finer bubble were created under these conditions. The froth overflowing the cell lip was collected as a function of time, filtered, dried and weighed. During the course

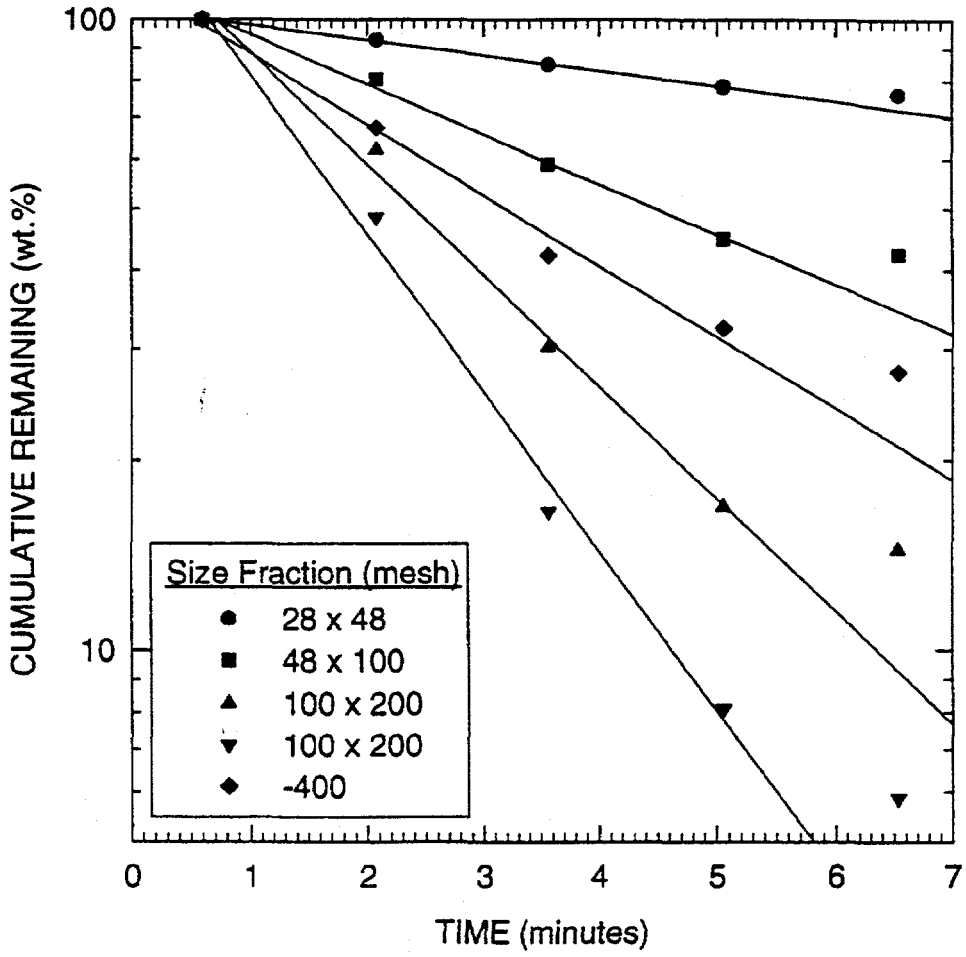

Figure 11-18. ESTIMATION OF KINETIC RATE CONSTANTS FOR EACH SIZE FRACTION

Table 11-6. Flotation Rate Constants for Different Size Fractions

Size fraction (mesh)	**Flotation rate constant (min^{-1})**
28 x 48	0.0557
48 x 100	0.1829
100 x 200	0.4079
200 x 400	0.5801
-400	0.2595

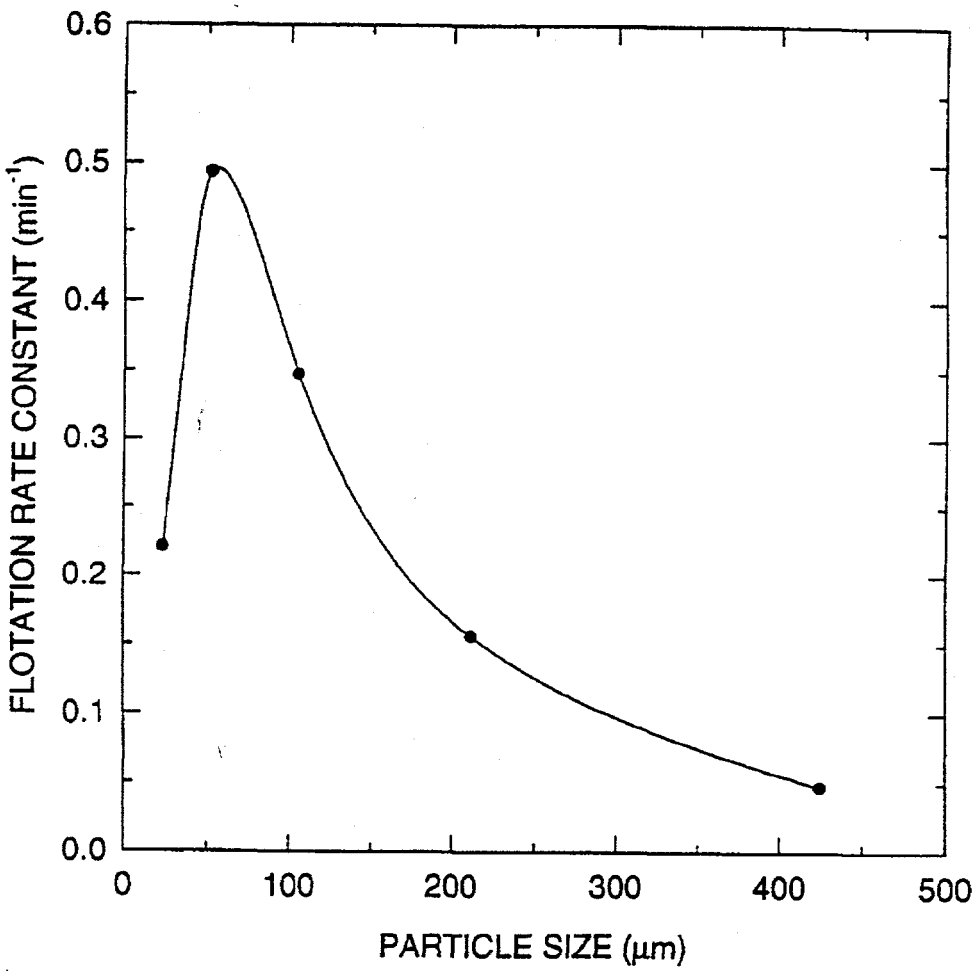

Figure 11-19. VARIATION OF FLOTATION RATE CONSTANT WITH PARTICLE SIZE

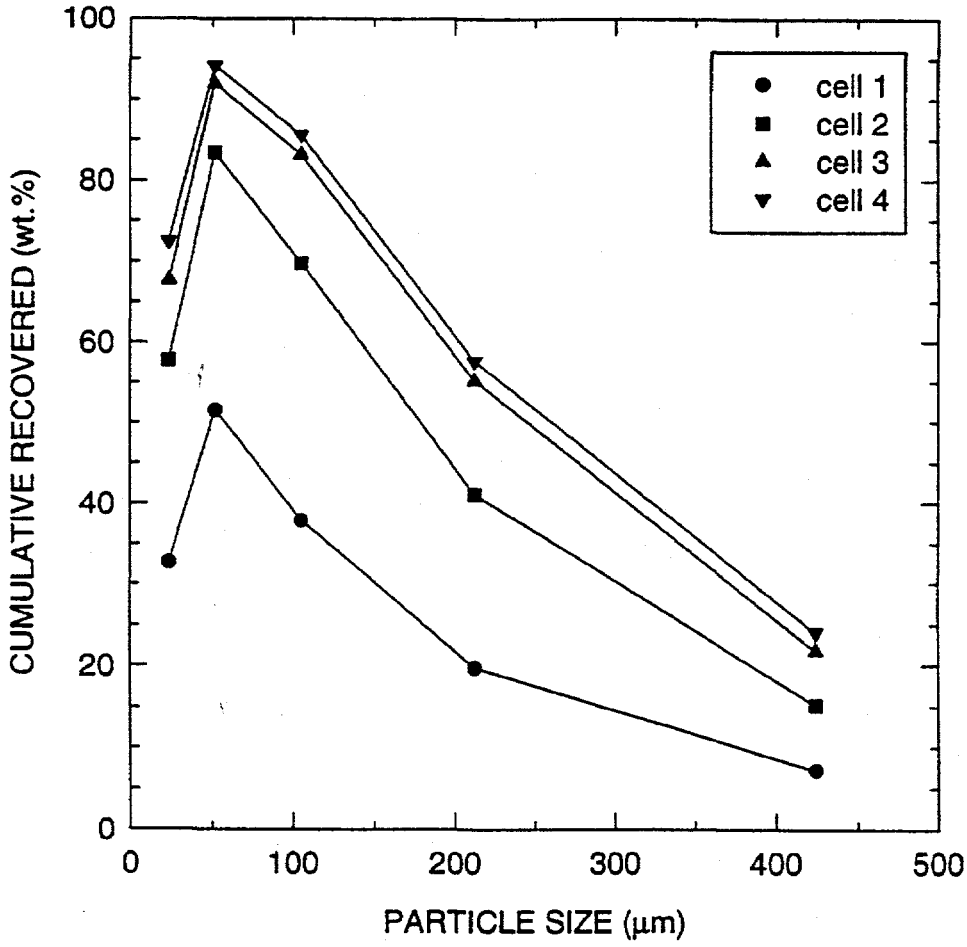

Figure 11-20. CUMULATIVE RECOVERY OF EACH SIZE FRACTION FROM EACH CELL

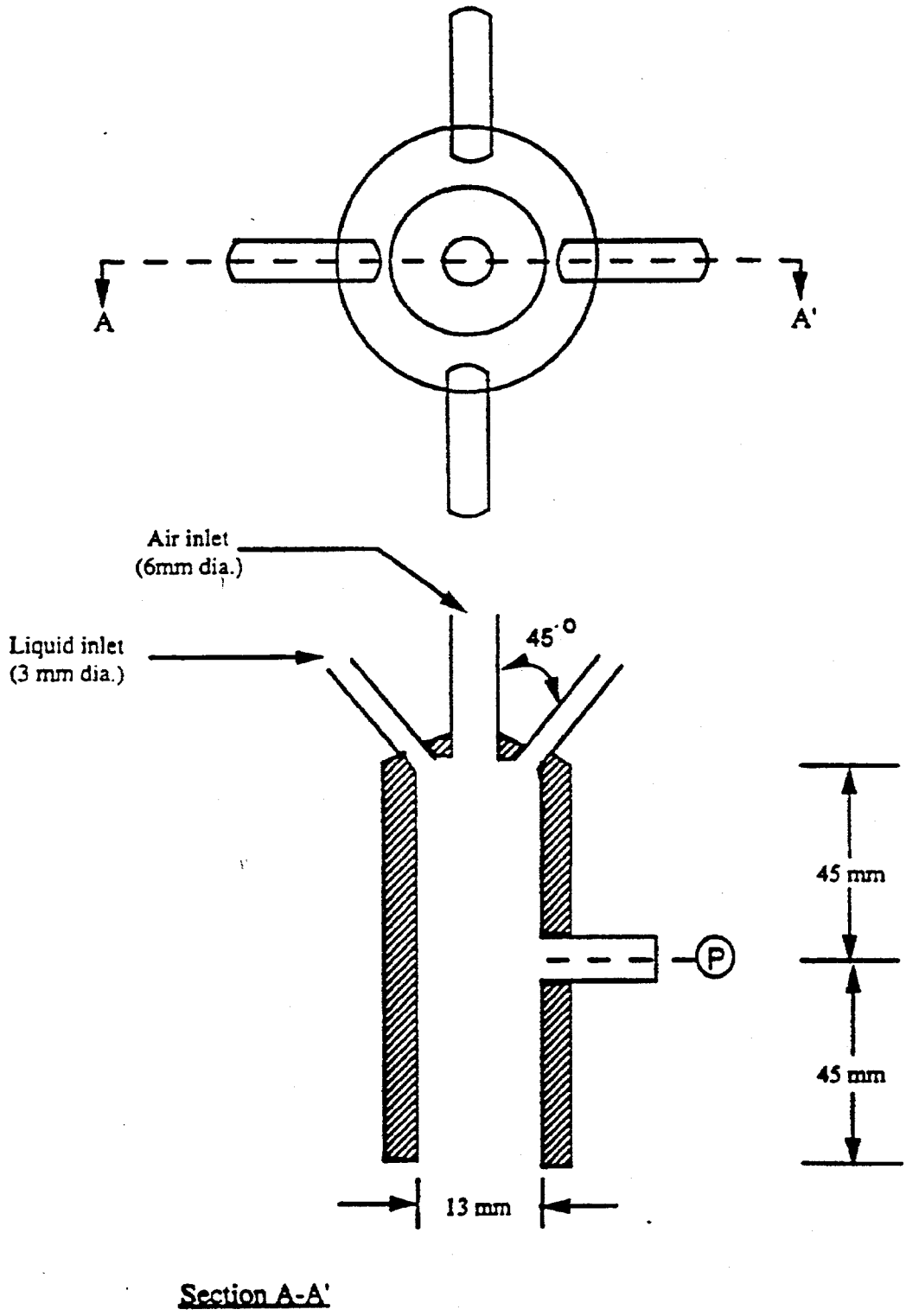

Section A-A'

Figure 11-21. DETAILED DRAWING OF THE VORTACTOR TURBULENT CONTACT CHAMBER

of the flotation experiments, it was determined that at high feed solid concentrations (≥ 10%), froth removal from the column was not satisfactory. In order to enhance froth removal, a ring spray was mounted at the outer periphery of the cell lip.

The ash content of the different fractions were determined in a Thermogravimetric Determinator (LECO TGA 501). From the weight of recovered coal and ash content, the cumulative yield, grade and ash rejections were calculated. The results obtained with the Vortactor bubble generator were compared with those reported previously with a Mott metallurgical (porous) sparger.

Results and Discussion

Figure 11-22 shows the effects of feed location and bubble generator type on the flotation response of Upper Freeport seam coal. In general, the product ash increases with initial solid concentration. This is attributed to increased loading of the bubbles, a process which tends to prevent adequate drainage of the resulting froth. For 5- and 10% solids in the feed slurry, the product grade does not appear to be dependent on the feed location. However, at 15% solids, the lower feed point gave better separation, thus making it the preferred feed location.

In comparison with the Mott Metallurgical (porous) sparger, the Vortactor bubble generator gave better grade-yield data. This observation is supported by the improved yield index-ash rejection data shown in Figure 11-23. The yield index is the product of the yield and the ash rejection. Since in separation processes, it is usually desirable to maximize both the yield and the rejection of unwanted material, optimization of the separation process using this index is preferred. In Figure 11-23, it can be seen that the use of the Vortactor bubble generator moves the optimum of the separation from the conventional/Mott Metallurgical (porous) sparger towards the washability data (which represents the most efficient separation possible). Since wash water was not employed for froth washing in the present study, these results clearly illustrate the effectiveness of the new bubble generator in fine particle separation.

11.4 Subtask 1.4 Dry Processing

Preliminary testing of the continuous rotating plate separator, which was described in the previous report, was initiated. During operation, it was found that arcing occurred between the drive pulleys and the rotating plates. This limited the operating voltage to approximately ±15 kV.

The separation tests were carried out using -100 mesh Upper Freeport seam coal. Tests were run to establish an operating procedure for the device. Ideally, the coal and refuse would be collected onto the rotating plates and then removed as the material passed by the scraper. This material would fall into the collection trough where it would be drawn

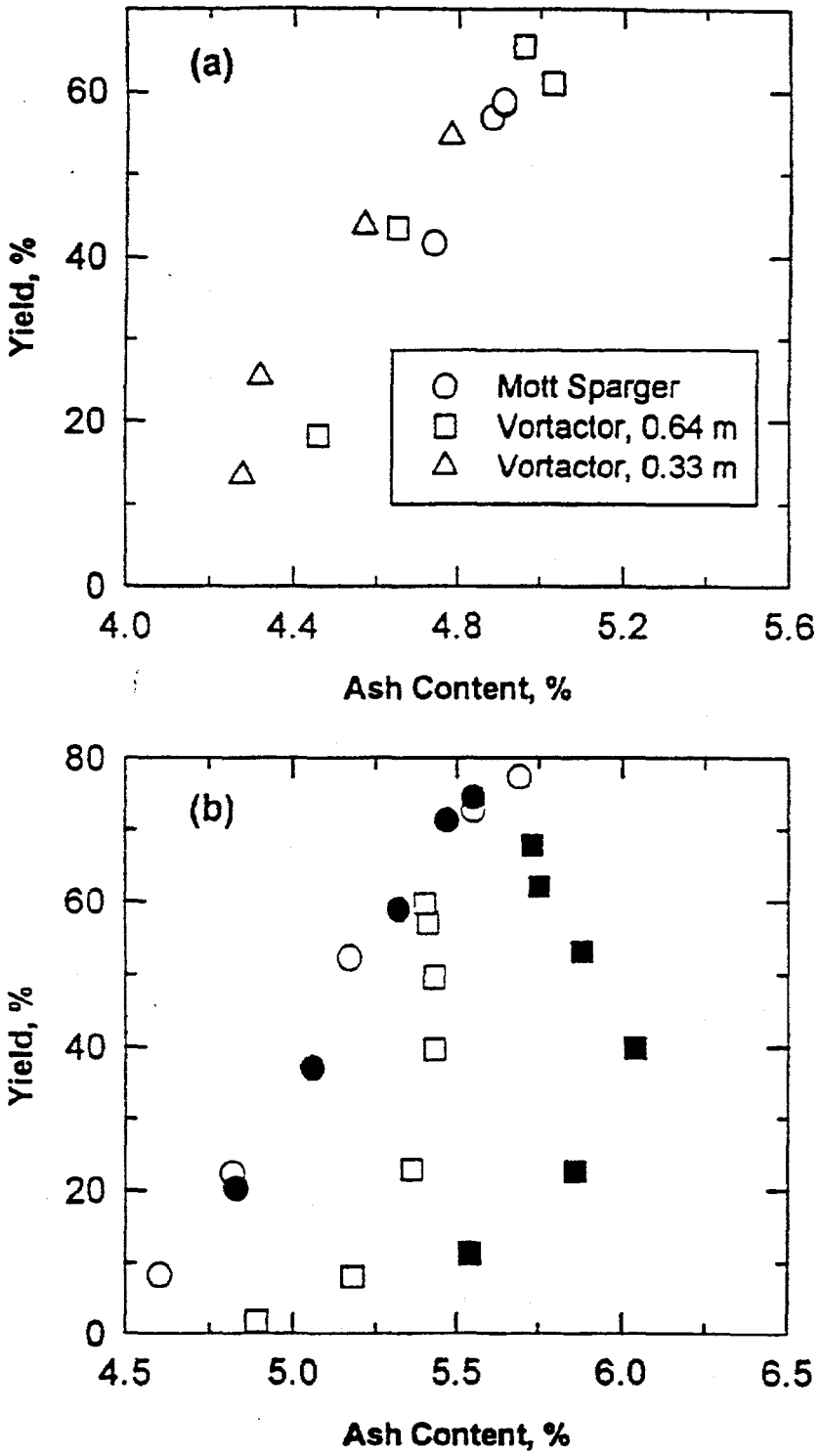

Figure 11-22. EFFECTS OF SPARGER TYPE, FEED LOCATION AND SOLID CONCENTRATION ON FLOTATION RESPONSE OF UPPER FREEPORT COAL; (a) EFFECTS OF SPARGER TYPE AND FEED LOCATION (5% solids); (b) EFFECTS OF SOLID CONCENTRATION AND FEED LOCATION
(○, ●) 10% solids, (□, ■) 15% solids; open and closed symbols are for feed locations of 0.33 m and 0.64 m respectively

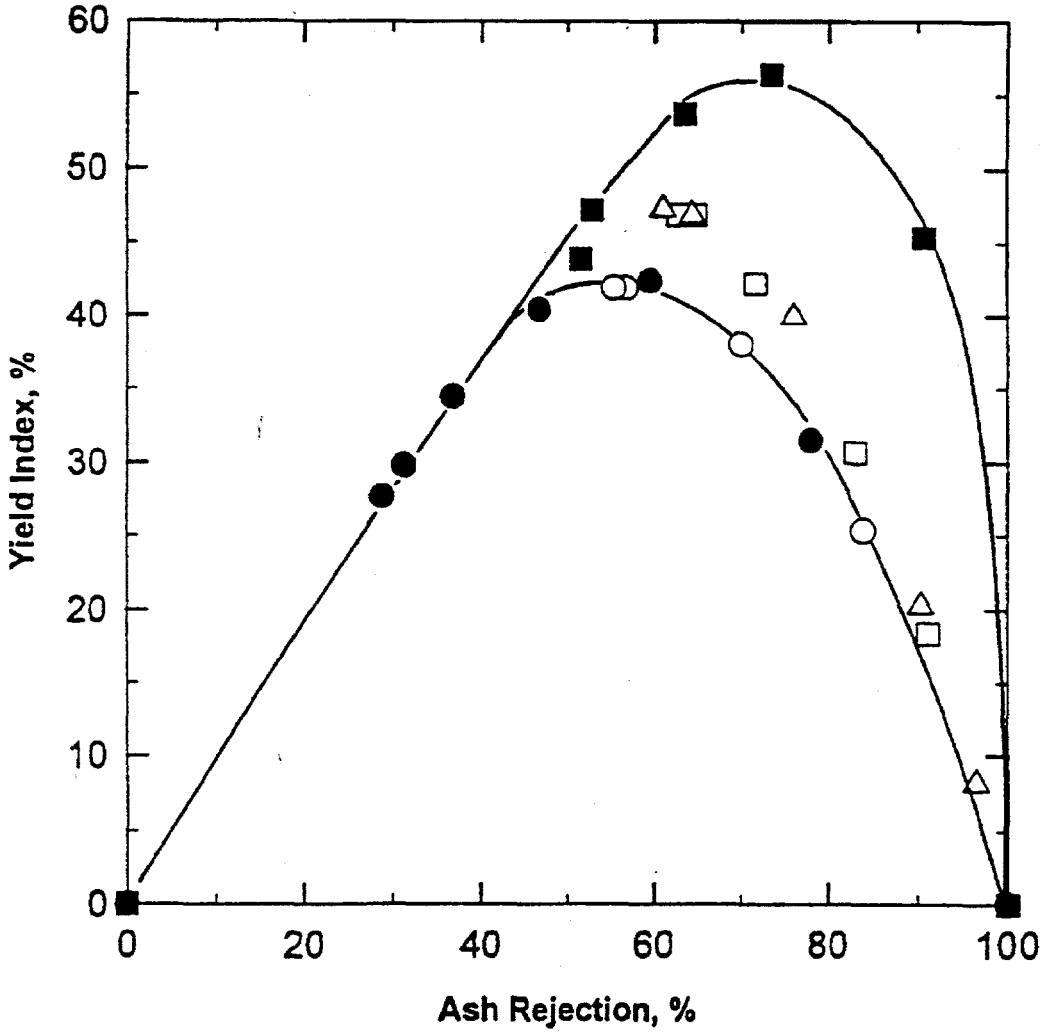

Figure 11-23. COMPARISON OF SEPARATION EFFICIENCIES FOR DIFFERENT UNIT OPERATIONS
(●) conventional flotation sell; (■) washability data; (○) column flotation equipped with Mott Metallurgical (porous) sparger; (□, Δ) Vortactor sparger data

through the cyclones and then collected. However, several problems occurred during operation of the separator.

As the material was scraped from the plates, cross contamination occurred between the clean coal and refuse as the products fell toward their respective collecting troughs. The center splitter was extended to minimize this effect. Also, part of the recovered material was not carried into the cyclone collectors but remained in the collecting troughs. Higher sweep air velocities should alleviate this problem.

A set of results, giving the distribution and ash values for the material collected from various parts of the separator, is shown in Table 11-7. As can be seen, the results indicate that the device was able to separate the coal selectively. However, the overall separation was not as efficient as the batch separation because of the limitations discussed previously.

11.5 Subtask 1.5 Stabilization of Coal-Water Mixtures

Overview

The purpose of this part of the project is to obtain an understanding of the hydrodynamic properties of coal-water mixtures in order to:

a) obtain stable slurries;
b) calculate the viscosity of a slurry, given its particle size distribution; and
c) specify blend compositions that will give optimal loading at a chosen viscosity.

In addition, the effect of air oxidation on slurry behavior was investigated using FTIR as a probe of chemical change.

In past reports, various elements of the theoretical approach have been presented and described:

a) a universal equation for viscosity that applies to concentrated slurries;
b) the problems with the older (Furnas) model of packing; and
c) a new model for the packing of slurries.

As stated in the previous semiannual report[14], these initial theories and arguments needed to be refined and modified and this has been accomplished during the last few months. In addition, a simple-to-use computer program was developed for the calculation of slurry viscosity and optimal blend compositions. This "hides" the underlying mathematical machinery and is simple enough to be used by plant personnel.

In the following sections, the details of this work are described. First, some additional arguments concerning the form of the viscosity equation will be presented. The modified theory of the packing of polydisperse particles will then be described, followed by a description of how this theory can be used as a practical guide for optimizing slurry

Table 11-7 Results from the Continuous Electrostatic Separator when Separating -100 Mesh Upper Freeport Seam Coal (clean coal yield = 50.2%).

	Clean Coal		Refuse	
Product	Weight, %	Ash, %	Weight, %	Ash, %
Electrode	56.7	4.0	41.7	24.1
Collecting Trough	18.2	9.4	22.3	22.6
Cyclone	25.1	10.4	36.0	13.0
Total	100.	6.6	100.	19.8

composition using the computer program developed. Finally, the work on coal oxidation will be presented.

The Viscosity of Highly Concentrated Slurries

The viscosity of complex systems like concentrated slurries is highly sensitive to how this property is defined and measured and also on the rate at which stress is applied. Only the simplest variant has been considered, the effective shear viscosity at zero frequency shear rate. Nevertheless, analogous results can be obtained at fixed shear stress or shear rate.

For dilute suspensions the classical result of Einstein shows that the effective viscosity depends only on the loading:

$$\eta = \eta_0\left(1+\frac{5}{2}\phi\right), \phi << 1 \qquad (11\text{-}1)$$

where η is the effective viscosity, η_0 is the viscosity of the solvent, and ϕ is the loading (volume fraction of the solid phase). As loading is increased, the universality of Equation (11-1) is lost, and the effective viscosity depends on the details of interparticle interactions, particle shapes, etc. The surprising fact is that in the limit of large ϕ, universality is recovered. This was first recognized by Dougherty and Krieger [15] (and references therein), and the validity of this conclusion will be shown here in a slightly more general framework than originally proposed.

The viscosity of a suspension is usually expressed in the form of a power law, which takes account of the fact that beyond a certain value of the loading, ϕ_{max}, the viscosity of the slurry is effectively infinite, and flow ceases. Dougherty and Krieger obtained an equation of the following form:

$$\eta = \eta_0\left(1-\frac{\phi}{\phi_{max}}\right)^{-[\eta(\phi)]\phi_{max}} \qquad (11\text{-}2)$$

where $[\eta(\phi)]$ is the intrinsic viscosity and is supposed to be a 'well-behaved' function of ϕ. If ϕ is close enough to ϕ_{max}, the main contribution to Equation (11-2) is from the singularity at $\phi \rightarrow \phi_{max}$. Accordingly, the unknown function $[\eta(\phi)]$ will be substituted by the intrinsic viscosity $[\eta] = [\eta(\phi_{max})]$. To determine the error of such an approximation, the log of Equation (11-2) can be taken and differentiated to obtain:

$$\frac{1}{\eta}\frac{d\eta}{d\phi} = \frac{[\eta(\phi)]}{1-\frac{\phi}{\phi_{max}}} - \phi_{max}\ln\left(1-\frac{\phi}{\phi_{max}}\right)\frac{d[\eta(\phi)]}{d\phi} \qquad (11\text{-}3)$$

The first term in Equation (11-3) describes the influence of the divergent factor $1-\phi/\phi_{max}$ in Equation (11-2), while the second term describes the influence of the variation in the function $[\eta(\phi)]$. If $[\eta(\phi)]$ is substituted by the constant value $[\eta]=[\eta(\phi_{max})]$, an error of the order of the ratio of the second and first terms in Equation (11-3) can be made. This error is negligible as long as:

$$\frac{1}{[\eta(\phi)]}\left|\frac{d[\eta(\phi)]}{d\phi}\right| << -\left[\phi_{max}\left(1-\frac{\phi}{\phi_{max}}\right)\ln\left(1-\frac{\phi}{\phi_{max}}\right)\right]^{-1} \qquad (11\text{-}4)$$

Experimental data [1] indicate that when ϕ changes from 0 to ϕ_{max}, $[\eta(\phi)]$changes from 2.5 to 2.7. Therefore, $\left|d[\eta(\phi)]/d\phi\right|/[\eta(\phi)] \sim 0.1$. On the other hand, the minimal value of the right hand side of Equation (11-4) is $e/\phi_{max} \approx 4$, and is achieved at $\phi = \phi_{max}e/(e-1) = 0.63\phi_{max}$. It can be seen that the condition described by Equation (11-4) is always satisfied. Therefore

$$\eta = \eta_0\left(1-\frac{\phi}{\phi_{max}}\right)^{-[\eta]\phi_{max}} \qquad (11\text{-}5)$$

where the intrinsic viscosity $[\eta]$ is a *constant* coefficient approximately equal to 2.7.

This simple argument shows why the Dougherty-Krieger correlation, Equation (11-5), is so successful for concentrated slurries and why other equations suggested for the concentration dependence of viscosity $\eta(\phi)$ give essentially the same result[16]. Since Equation (11-5) has the simplest form, this is what will be used for the calculation of viscosity.

If the slurry is polydisperse, $[\eta]$ and ϕ_{max} depend on the distribution of sizes and shapes of the solid particles. Repeating the preceding considerations, it can be concluded that Equation (11-5) is still valid, but the parameters $[\eta]$ and ϕ_{max} are now some functions of the composition of the solid phase. The variations in $[\eta]$ will be neglected and the contribution of the $1-\phi/\phi_{max}$ term will be concentrated on.

The recipe for the calculation of slurry viscosity is therefore the following:

- Calculate the maximal random packing loading ϕ_{max}.

- Use the generalized Dougherty-Krieger correlation Equation (11-5) to calculate η at a given loading ϕ.

It is evident that the only way to decrease the viscosity at a given loading is to increase ϕ_{max}. This is the problem of *optimal packing of particles* and is discussed in the following sections.

An Aside on Definitions

In the following paragraphs, the expressions "optimal packing" (or loading) and "maximal packing" (or loading) will be frequently used. It is important to make clear their meanings. For a monodisperse system of particles the maximal packing corresponds to the close packing limit, $\phi_{max} = \phi_0 \approx 0.637$. In a binary mixture of large and small particles one can have different loadings, depending on the arrangement of large and small spheres. One such arrangement will give the greatest loading at a given composition of the mixture. We will call this loading *the maximal packing* ϕ_{max}. If the fraction of small particles is low enough, the maximal loading is achieved by placing the small particles in the voids between the large ones. It is obvious that in the general case

$$\phi_{max} \geq \phi_0 \qquad (11\text{-}6)$$

Suppose that the composition of the binary mixture can be changed. The maximal loading ϕ_{max} will change with the composition. There is a special *optimal* composition at which ϕ_{max} achieves the greatest value, $\phi_{optimal}$. This value is called the *optimal loading*. It will be shown below that the optimal binary mixture has "just enough" small particles to fit in the voids between the large ones.

In the general case of polydisperse mixtures, the nomenclature will be analogous. This will be called the *maximal loading* ϕ_{max} the greatest loading achievable at a given composition of the mixture. In a typical situation, the composition of the mixture subject can be changed within some constraints. The mixture that satisfies these constraints and has the greatest ϕ_{max}, *is called the optimal mixture,* and the corresponding loading the *optimal loading.*

Modified Theory of Packing of Polydisperse Particles

Binary Mixtures

In previous reports, it was argued that the main disadvantage of the Furnas' theory is caused by the fact that it is based on conclusions drawn from an unrealistic "ideal case", namely, from a binary mixture of spheres of infinitely different radii. An alternative approach was employed from the "opposite end", a binary mixture of particles of close radii. Let us discuss a volume V filled by particles with sizes D_L and D_S such as

$D_L > D_S$. Suppose the space is completely filled with the large particles. Their overall (solids) volume is $V_1 = \phi_0 V$, where ϕ_0 is the maximal loading for the monodisperse mixture. Now add the smaller particles. If the overall volume of the smaller particles is smaller than some value V_{max}, they will fit in the space between the larger particles. Note what is being stated. There will be a distribution of void sizes between the large particles. A proportion of these will be large enough to accommodate particles of size D_S. The total volume of these particular voids is the quantity V_{max} and this will be proportional to the volume of voids $(1-\phi_0)V$ and will also depend in some unknown fashion on the ratio $x = D_S / D_L$ (for a simple binary mixture x= the Furnas K parameter). This relationship can be written as:

$$V_{max} = \phi_0(1-\phi_0)VY(x) \tag{11-7}$$

where $Y(x)$ is an unknown function. As long as the size of the container is large enough to neglect surface effects, $Y(x)$ will not depend on V. $Y(x)$ is then a universal function (for a given particle shape) of the size ratio x. If x = 0, Y(x) = 1; this is the "ideal case of infinitely different sizes, where $V_{max} = \phi_0(1-\phi_0)V$. At the other extreme, if x = 1, Y(x) = 0; we have close packing of particles of diameter D_L and cannot fit any more particles of the same radius into the volume V. It is obvious that the function Y(x) introduced here is closely related to the Furnas' function y(x). Actually, it will be proved below that it *coincides* with the Furnas' function y(x).

Next the maximal loading ϕ_{max} of a binary mixture of particles having a fraction f_L of large particles and a fraction $f_S = 1 - f_L$ of small particles will be calculated. Returning to the container discussed above, it can be seen that it contains a volume $V_1 = \phi_0 V$ of large particles and a volume $V_2 = V_1 f_S / f_L = \phi_0 V f_S / f_L$ of small particles. Therefore the total volume of the solid phase is

$$V_{solid} = \frac{1}{f_L}\phi_0 V \tag{11-8}$$

If the total volume of all the smaller particles V_2 is less than V_{max}, then all smaller particles fit between the larger ones. Therefore the total volume of the blend (including both the solid phase and the voids) is V, and the maximal loading is

$$\phi_{max} = \frac{V_{solid}}{V} = \frac{1}{f_L}\phi_0, V_2 \le V_{max} \tag{11-9}$$

If the volume of the small particles is greater than V_{max}, they will not all fit between the larger particles. Therefore the total volume of the blend V_{total} is greater than V. It is difficult to obtain an *a priori* prediction for V_{total}, but we can estimate a value. Obviously, the volume V_{total} of the closely packed mixture is smaller than the volume of the following two-layered hypothetical structure:

- First layer - all larger particles and those small particles that can fit between the larger ones,
- Second layer - the remainder of the smaller particles packed with a loading ϕ_0.

It is easy to calculate the total volume of this two-layered structure, obtaining the following inequality:

$$V_{total} \le V + \frac{f_S}{f_L} V - \frac{1}{\phi_0} V_{max} \tag{11-10}$$

As a crude estimation of V_{total} the right hand side of Equation (11-10) can be used. Actually this estimation is not as crude as it seems at first glance and can adequately describe some modes of the "random" packing of particles. Therefore

$$\phi_{max} = \frac{V_{solid}}{V_{total}} = \frac{\phi_0}{1 - \frac{f_L}{\phi_0}\frac{V_{max}}{V}}, V_2 \ge V_{max} \tag{11-11}$$

Using Equations (11-7, 11-9, and 11-11), the loading is:

$$\phi_{max} = \begin{cases} \dfrac{\phi_0}{1-f_s}, f_s \le \dfrac{(1-\phi_0)Y(x)}{1+(1-\phi_0)Y(x)} \\ \dfrac{\phi_0}{1-(1-f_s)(1-\phi_0)Y(x)}, f_s \ge \dfrac{(1-\phi_0)Y(x)}{1+(1-\phi_0)Y(x)} \end{cases} \tag{11-12}$$

Now it will be shown that the function $Y(x)$ coincides with the Furnas function $y(x)$. Suppose that following the Furnas treatment we consider closely packed large particles in a volume $(1-\phi_0)V$, and mix them. The maximal loading of this mixture, according to Equation (11-12) is

$$\phi_{\text{Furnas}} = \frac{\phi_0(2-\phi_0)}{2-\phi_0-(1-\phi_0)Y(x)} \tag{11-13}$$

The volume of the solids in this mixture is $\phi_0(2-\phi_0)V$, and the total volume of the mixture is:

$$V_{\text{Furnas}} = \frac{\phi_0(2-\phi_0)}{\phi_{\text{Furnas}}}V. \tag{11-14}$$

Accordingly, the volume gain upon mixing is

$$\Delta V = V + (1-\phi_0)V - V_{\text{Furnas}} = \frac{(2-\phi_0)(\phi_{\text{Furnas}}-\phi_0)}{\phi_{\text{Furnas}}}V. \tag{11-15}$$

The ideal volume gain is $\Delta V_{\text{ideal}} = (1-\phi_0)V$. The Furnas function $y(x)$ is therefore given by:

$$y(x) = \frac{\Delta V}{\Delta V_{\text{ideal}}} = \frac{(2-\phi_0)(\phi_{\text{Furnas}}-\phi_0)}{\phi_{\text{Furnas}}(1-\phi_0)} \tag{11-16}$$

Substituting ϕ_{Furnas} from Equation (11-13) gives $y(x) = Y(x)$ and using the notation $y(x)$ for the empirical function $Y(x)$, describes the maximal fraction of small particles that fit between the large ones.

An analytical expression is needed for the function $y(x)$. It is tempting to use the Furnas' correlation. Unfortunately, this correlation has an unphysical region of negative y at $x \geq 0.62$, as shown in Figure 11-24. Using the same data as Furnas, the following correlation for the function $y(x)$ (also shown in Figure 11-24) is obtained:

$$y(x) = \frac{1-x}{1+2.68x+3.98x^2} \tag{11-17}$$

This has the correct behavior at $x = 0$ and $x = 1$, and has the advantage of being monotonous in the interval $0 \leq x \leq 1$. The correlation Equation (11-17), strictly speaking, only applies to spherical particles, but it is customary to neglect the non-universality of $y(x)$ for particles close to spheres. It is assumed that the correlation Equation (11-17) is universal.

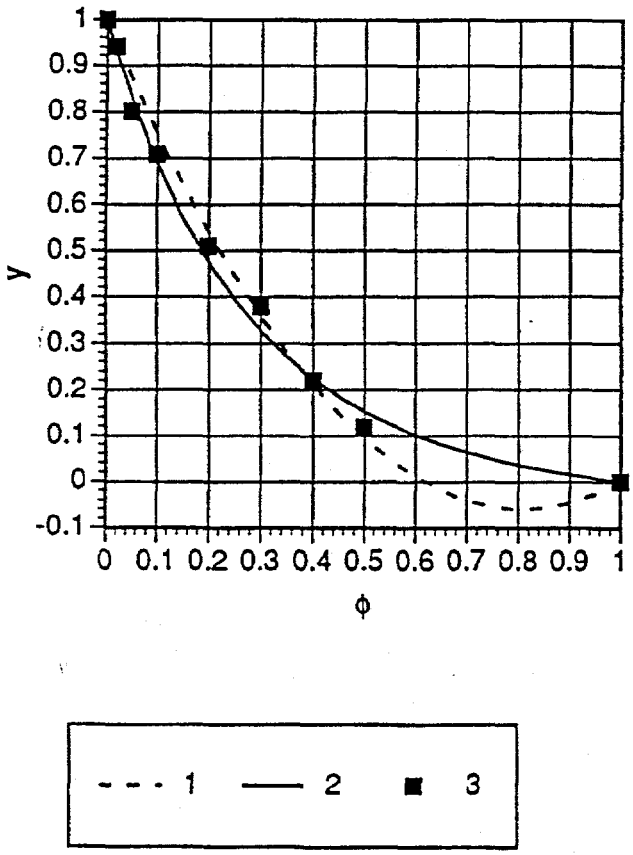

Figure 11-24. CORRELATIONS FOR THE FUNCTION $y(x)$.
1-Furnas correlation Equation 11-12
2-new correlation Equation 11-23
3-experimental data

Now consider the optimal mixing ratio for binary mixtures. Furnas suggests the composition $1:(1-\phi_0)$, with a loading given by Equation (11-13). However, Equation (11-12) indicates that the optimal composition is $1:(1-\phi_0)\,y(x)$, and the loading for this composition is

$$\phi_{optimal} = \phi_0\left[1+(1-\phi_0)y(x)\right] \tag{11-18}$$

In the limit $x \to 0, y(x) \to 1$, and these formulas coincide, giving $\phi_{optimal} = \phi_{Furnas} = \phi_0(2-\phi_0)$. In the other limit, $x \to 1$, $y(x) \to 0$, so that $\phi_{optimal} = \phi_{Furnas} = \phi_0$. However, in between these limits these formulae differ, and Equation (11-18) always gives a higher maximal loading than the Furnas' recipe (see Figure 11-25). This difference is quite small (and this explains the success of the Furnas' recipe over the last 60 years), but it can be seen that it becomes more important for polydisperse mixtures.

The new theory is potentially more useful than the classical Furnas theory. Its main advantage is not just the higher loading predicted by Equation (11-18) than by the Furnas recipe, the gain is quite small. The most important feature is that it can predict maximal loading for any composition.

Polydisperse Blends

Suppose there are n set of particles of consecutive sizes $D_L = D_1, D_2, ..., D_n = D_S$. Let the volume fractions of the particles of the corresponding sizes are $f_1, f_2, ..., f_n$, where

$$f_i = \frac{v_i}{\sum_{k=1}^{n} v_k} \tag{11-19}$$

Next, calculate the maximal volume fraction of solids after having mixed the particles. This problem will be solved iteratively. Suppose there are mixed particles in the groups 1, 2, ..., i, and particles of the group i + 1 are to be added. Suppose the mixture has the maximal loading ϕ_i after the i th step. The volume of solids in the resulting blend, the total volume of the blend and the volume of voids are:

$$V_i^{solid} = \sum_{k=1}^{i} v_k, V_i^{total} = \frac{1}{\phi_i}\sum_{k=1}^{i} v_k, V_i^{voids} = \left(\frac{1}{\phi_i}-1\right)\sum_{k=1}^{i} v_k \tag{11-20}$$

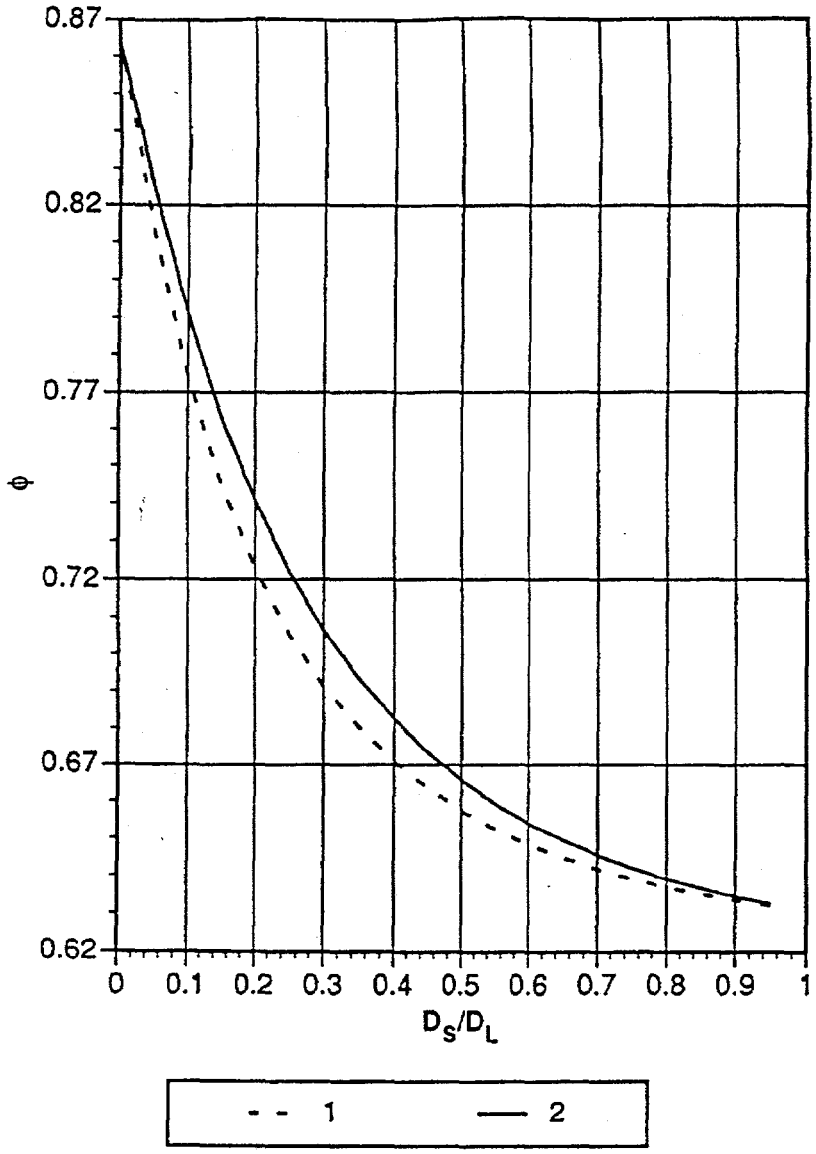

Figure 11-25. MAXIMAL LOADINGS FOR BINARY BLENDS
1-Furnas recipe, Equation 11-19
2-optimal recipe, Equation 11-24

D_i^{eff} is the *effective minimal diameter of the mixture*, if it is impossible to add any particles of size D_i^{eff} and larger without changing the volume of the mixture. In order to understand the meaning of D_i^{eff} consider a special case of polydisperse mixtures: Furnas' "telescopic tube" blend. Take particles of size D_1 and fill the volume V with them. The effective minimal diameter of the resulting system is D_1. Then add exactly as many particles of diameter D_2 as will fit in the void between the larger particles. The effective minimal diameter of the resulting blend is D_2. Then add exactly as many particles of diameter D_3 that can be fit between the previously placed particles. The effective minimal diameter of the blend after this becomes D_3. This process can be continued with particles of gradually decreasing sizes, and the effective diameter of the blend will decrease accordingly. Now an assumption about the packing of these particles must be made. This assumption is called the *basic hypothesis*. Assume that the amount of particles that can be added to any blend without increasing its total volume depends only on three parameters: the volume of voids, the added particle size and the effective minimal diameter of the blend. This assumption means that all information about a polydisperse blend can be (for our purposes) mapped into two numbers: the volume fraction of voids and the minimal effective diameter. Actually this assumption (as well as many other things in the packing of particles) was originally made implicitly but not explicitly by Furnas. It allowed the use of data obtained on binary blends to be applied to polydisperse mixtures. An explicit formulation of this underlying assumption allows one to exploit its deep consequences.

The maximal volume of particles of the $(i + 1)$th group that can be fitted into the blend after the i th step can now be written as

$$V_{i+1}^{max} = \phi_0 \left(V_i^{total} - \sum_{k=1}^{i} v_i \right) y\left(\frac{D_{i+1}}{D_i^{eff}} \right) \tag{11-21}$$

and the total volume of the particles in the system after the $(i + 1)$th step is

$$V_{i+1}^{total} = \begin{cases} V_i^{total}, v_{i+1} \le V_{i+1}^{max} \\ V_i^{total} + \frac{1}{\phi_0}\left(v_{i+1} - V_{i+1}^{max} \right), v_{i+1} \ge V_{i+1}^{max} \end{cases} \tag{11-22}$$

D_{i+1}^{eff} can be calculated provided that D_i^{eff} is known. If $v_{i+1} \ge V_{i+1}^{max}$, the result will be $D_{i+1}^{eff} = D_i^{eff}$. Consider the case $v_{i+1} \le V_{i+1}^{max}$. To calculate D_{i+1}^{eff} note that the

volume of particles of size D_{i+1} that can be fitted in the system without changing its volume after the $(i + 1)$th step is $\Delta V_{i+1} = V_{i+1}^{max} - v_{i+1}$. On the other hand, according to the basic hypothesis, the volume is $\Delta V_{i+1} = \phi_0 \left(V_i^{total} - \sum_{k=1}^{i+1} v_i \right) y\left(D_{i+1} / D_{i+1}^{eff} \right)$.

Therefore

$$D_{i+1}^{eff} = \begin{cases} \dfrac{D_{i+1}}{x(y_i + 1)}, v_{i+1} \le V_{i+1}^{max} \\ D_{i+1}, v_{i+1} \ge V_{i+1}^{max} \end{cases} \tag{11-23}$$

where

$$y_{i+1} = \frac{V_{i+1}^{max} - v_{i+1}}{\phi_0 \left(V_i^{total} - \sum_{k=1}^{i+1} v_i \right)} \tag{11-24}$$

and $x(y)$ is the inverse of the function after the $y(x)$. Using the correlation Equation (11-17) for the function $y(x)$, the following analytical formula for the function $x(y)$ can be obtained:

$$x(y) = \frac{1 - y}{1 + 2.68y + 3.68y^2} \tag{11-25}$$

Equations 11-21 to 11-24 allow the calculation of the maximal loading of a given blend if the initial conditions V_1^{total}, D_1^{eff} are known. These initial conditions are:

$$V_1^{total} = \frac{v_1}{\phi_0}, D_1^{eff} = D_1 \tag{11-26}$$

The problem of computing the maximal loading of a given blend is now solved. Indeed, for any given composition $v_1, v_2 ..., v_n$ of a blend with particles sizes $D_1, D_2 ..., D_n$ we can use the following step-by-step algorithm starting from the initial values of Equation (11-26).

1. Provided that D_1^{eff} and V_1^{total} are known, calculate V_{i+1}^{max} and y_{i+1} using Equations (11-21 and 11-24).

2. With these values of V_{i+1}^{max} and y_{i+1}, calculate V_{i+1}^{total} and D_{i+1}^{eff} from Equations (11-22 and 11-23).
3. Return to Step 1.

Having calculated V_n^{total}, the resulting maximal loading is obtained

$$\phi_{max} = \frac{\sum_{k=1}^{n} v_i}{V_n^{total}} \tag{11-27}$$

Actually the calculations depend only on the ratios of the partial volumes v_i, so we can substitute the corresponding volume fractions f_i instead of the volumes v_i in the Equations (11-21 to 11-24, and 11-26).

A Practical Guide to Optimization of Slurries

In this final section, a simple hypothetical example of how the equations work will be presented. Experimental studies that will allow a more detailed comparison of theory and experiment are underway. The results will be presented in the next semiannual report.

Consider the common situation where there are two grinders producing "fine" and coarse "particles". The output slurry consists of a mixture of the particles produced by both grinders. Given the size distributions of the particles from each grinder, one must find the mixing ratio that gives the slurry with the lowest viscosity. The methods described in this report allow one to solve this problem.

The information about the slurries can be represented as a pair of histograms $\left(f_1^{fine}, f_2^{fine}, \ldots f_n^{fine}\right)$ and $\left(f_1^{course}, f_2^{course}, \ldots f_n^{course}\right)$, where $f_i^{fine,\ course}$ is the volume fraction of particles with sizes between $D_i - \Delta D/2$ and $D_i + \Delta D/2$, ΔD being a step in a histogram. This histogram is the natural result of the size distribution measuring device commonly used in industry. At any given composition $\xi:(1-\xi)$ of the resulting mixture, we can calculate the histogram of the mixture as

$$f_i = \xi f_i^{fine} + (1-\xi) f_i^{coarse} \tag{11-28}$$

Using the algorithm developed in the previous section, the maximal loading $\phi_{max}(\xi)$ at any given composition can be determined. Then the viscosity $\eta(\xi)$ of the mixed slurry using Equation (11-5) can be calculated. The minimum of the function $\eta(\xi)$ (that coincides with the maximum of the function $\phi_{max}(\xi)$) gives the optimal slurry composition for this system.

A typical histogram of a micronized coal after grinding is shown in Figure 11-26a. Since a typical loading used in the transport of coal-water slurries is above 60%, the viscosity of the slurry is about thirty times greater than the viscosity of water. In order to lower the overall viscosity at the same loading (61.7%), consider adding a controlled amount of coarse coal. The histogram of the coarse component is shown in Figure 11-26b. A plot of the viscosity as a function of the composition of the mixture is shown on Figure 11-26c. It can be seen that the calculated viscosity of the mixture is much less that the viscosity of the components.

A computer program *Coal Viscosity Calculator* was developed that allows an optimization of the slurry composition in the working conditions of a power plant. This software can be also used for other industrial problems where powder packing optimization is needed.

Coal Oxidation Study

The goal of this study was to determine the effect of low temperature (38 °C) oxidation on the properties of a coal and, in turn, a coal-water slurry fuel. Oxidation was induced in a humidity chamber and the coal was allowed to oxidize for a period of 16 weeks. Fourier transform infrared spectroscopy (FT-i.r.) was used to determine the relative amount of oxidation in the sample by comparing the unoxidized baseline sample to the oxidized sample. The results demonstrated that low temperature oxidation of an Indiana #7 coal does not significantly affect the surface of the coal within the detectable limit of the FT-i.r.. For the entire time period of 16 weeks, it was shown that there were no significant changes in the region of 1600-1800 cm^{-1}, characteristic of oxidation products, between the oxidized and unoxidized samples. However, at higher temperatures, such as 130 °C, oxidation occurs very rapidly and is easily noticeable.

The data shows no evidence that the coal in question is easily oxidized at ambient conditions. This is important in that the coal necessary for the formulation of coal water slurry fuels can be prepared from the same coal seam without concern as to how long, within reason, that the coal has been weathered.

12.0 PHASE III, TASK 2 STOKER COMBUSTION PERFORMANCE ANALYSIS AND EVALUATION

12.1 Subtask 2.1 Determine DOD Stoker Operability and Emissions

No work was conducted in Subtask 2.1.

12.2 Subtask 2.2 Conduct Field Test of a DOD Stoker

No work was conducted in Subtask 2.2.

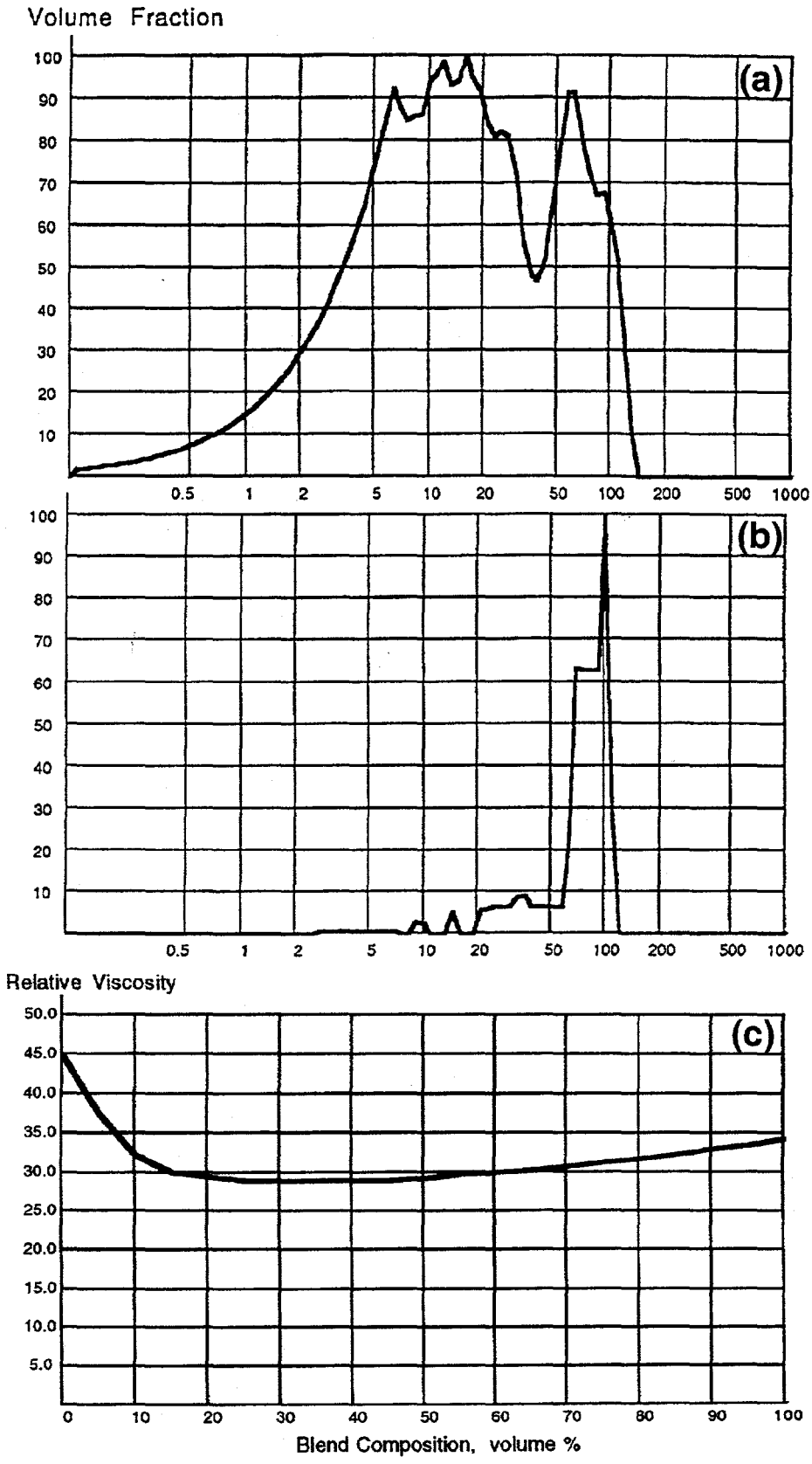

Figure 11-26. VISCOSITY OF A MIX OF COAL POWDERS OBTAINED FROM TWO GRINDERS
(a) Histogram of "fine" powder
(b) Histogram of "coarse" powder,
(c) Relative viscosity of the mixture at the loading ϕ = 60.1%

12.3 Subtask 2.3 Provide Performance Improvement Analysis to DOD

No work was conducted in Subtask 2.3.

12.4 Subtask 2.4 Evaluate Pilot-Scale Stoker Retrofit Combustion

No work was conducted in Subtask 2.4.

12.5 Subtask 2.5 Perform Engineering Design of a Stoker Retrofit

No work was conducted in Subtask 2.5.

13.0 PHASE III, TASK 3 EMISSIONS REDUCTION

13.1 Subtask 3.1 Demonstrate Advanced Pollution Control System

No work was conducted in Subtask 3.1.

13.2 Subtask 3.2 Evaluate Carbon Dioxide Mitigation and Heavy Metal Removal in a Slipstream System

No work was conducted in Subtask 3.2.

13.3 Subtask 3.3 Study VOC and Trace Metal Occurrence and Capture

No work was conducted in Subtask 3.3.

14.0 PHASE III, TASK 4 COAL-BASED FUEL WASTE COFIRING

14.1 Subtask 4.1 Coal Fines Combustion

No work was conducted in Subtask 4.1.

14.2 Subtask 4.2 Coal/Rocket Propellant Cofiring

No work was conducted in Subtask 4.2.

15.0 PHASE III, TASK 5 ECONOMIC ANALYSIS

15.1 Subtask 5.1 Cost and Market Penetration of Coal-Based Fuel Technologies

No work was conducted in Subtask 5.1.

15.2 Subtask 5.2 Selection of Incentives for Commercialization of the Coal Using Technology

Due to some unanticipated data problems, a significant portion of the period between February 1995 through September 1995 was allocated for double-checking of data, data correction, and cleaning.

The cross-reference performed in the previous period had revealed 128 corporations (or their subsidiaries) that have water tube boiler locations in the Commonwealth of Pennsylvania. A closer inspection of the individual characteristics of these boilers revealed

the result that only 63 boilers (firms) were falling into the category of boilers for which the new technology is being developed.

The data analysis (which is not conclusive) reveals that under the assumption of profit-maximization, firms under consideration should respond to changes in depreciation allowances, capital subsidies (which are to be used for covering fixed cost expenses), and reduced interest loan policies. Interestingly, a change in taxes does not reveal a significant response in the short run.

Except the turnover ratios, financial ratios are not significant in explaining short-run changes in net income, i.e., firms' after-tax profits. In the remaining period, the data analysis will be completed where the effects of incentives will be analyzed in a semi-dynamic setting: in this section, each firm's historical trends will be taken into account.

15.3 Subtask 5.3 Community Sensitivity to Coal Fuel Usage

During the reporting period, steady progress was made on the Community Sensitivity to Coal Fuel Usage component of Phase III. The examination is being focused on the issues of community risk perceptions and responses to planned non-utility generators. These facilities can entail a variety of fuel types which will allow the examination of specific sensitivity to coal versus other fuel types (e.g. oil, natural gas).

Industry representatives have been met or are scheduled to be met to discuss their experiences in responding to community sensitivity. During the Summer of 1995, two focus groups were conducted at Penn State which examined individual's perceptions and language associated with small energy generating facilities. Two focus groups have since been conducted in Williamsport, Pennsylvania to examine these issues further and to gather information necessary for developing a survey instrument. A primary purpose of these groups was to examine alternative methods of presenting risk information and scaling to subjects. The Williamsport focus groups are currently being transcribed prior to qualitative analysis. The demographic information is currently being compiled on the focus groups and entering data from the debriefing surveys.

A draft survey instrument will be ready by the end of October, and pre-testing and refining will begin during November and December. Additional focus groups and initiate verbal protocol analysis will be implemented during this period. The survey instrument will be refined to the point of implementing a pre-test by the end of January, 1996. At that point, the feasibility of larger scale implementation, which depends on the complexity and scope of the survey instrument, will be determined.

15.4 Subtask 5.4 Regional Economic Impacts of New Coal Utilization Technologies

Introduction

In addition to efforts to improve the economic and environmental efficiency of coal combustion technologies, future coal utilization will probably be equally, if not more greatly, impacted by environmental regulations. Probably the most profound of these would stem from alternative policies to prevent potential global warming.

Energy conservation is almost universally considered a prime strategy for mitigating greenhouse gases. At present, for example, 97.9% of the CO_2 emitted from industrial countries, and 70.6% emitted from developing countries, stems from fossil fuel combustion[17]. With any potential major shift to renewables many years away, outright reduction in the utilization of coal, oil, and natural gas is an obvious strategy. It appears even more appealing when one considers that a good deal of conservation can be attained at a cost-savings when less energy is used outright, or at a zero net cost when, for example, energy-saving equipment must be installed. These factors have led to energy conservation being placed in the category of "no regrets" strategies, which refers to measures that do not incur added costs even if projected warming trends are not forthcoming[18].

Clearly, production cost-savings and preservation of our energy resources are pluses. However, to date, very few studies have focused on the potential down-side. For example, there are jobs and profits at stake in the energy industries. Moreover, declines in fossil fuel sectors will lead to declines in output in successive rounds of upstream suppliers (e.g., mining equipment, fuel service companies), as well as some downstream customers (e.g., railroads, electric utilities). It is not clear whether these negative effects will be offset by the increased efficiency of the economy, various factor substitutions, purchasing power improvements for consumers, or any multiplier effects stemming from increased production of energy-saving equipment.

In this subtask, the effects on the U.S. economy and its energy sectors of conservation strategies to reduce CO_2 emissions are estimated. The analysis is undertaken with a 20-sector computable general equilibrium (CGE) model by simulating various responses to command and control, carbon tax, and carbon emission permit policies.

The results indicate that the characterization of energy conservation as a "no regrets" strategy is too strong. In all of our simulations, energy sectors stand to lose, though, in some cases, not anywhere near as much as would be expected. Each of our simulations of mandated conservation also leads to a decline in output and employment for the U.S. economy. In contrast some of the price-induced conservation response strategies we also simulate have a neutral impact on the overall economy.

This discussion is divided into five sections. In the following section, the basic features of the conservation strategy and some overlooked issues are discussed. Then the model used in the simulations is summarized. Next, basic results, as well as some sensitivity tests are presented. These are concluded with a summary and a discussion of policy implications.

Basic Features of the Conservation Strategy

Many proposals have been put forth to combat potential global warming. One that has received considerable attention calls for a 20% reduction in current greenhouse gas (GHG) emission levels for industrialized countries and a stabilization of developing country emissions at current levels. Several policy instruments are available to implement this reduction, the carbon tax being the most widely supported and most thoroughly analyzed[19, 20]. In the U.S., however, strong support exists for a marketable permits approach[21].

Actually, the conservation response to a carbon tax and a marketable permit system can be modeled in the same manner. First, the optimal carbon tax rate would be equivalent to the equilibrium permit price[22, 23]. Second, the two instruments would result in the same efficient response, in which each polluter equates its marginal cost of abatement to the tax rate or permit price. Third, even though polluters must pay for each unit of GHG emissions under a tax regime, but these emissions are usually free (entitlements) under a permit system, this does not affect the response in the short-run. That is, the tax payments or permit revenues/expenditures affect a firm's average cost but not its marginal cost and thus only bear upon long-run considerations such as exit and entry. Moreover, these conclusions pertain to the application of these instruments at both the international level in relation to total GHG reductions and within national boundaries.

In a recent study, Rose and Stevens[24] estimated an equilibrium permit price of $38.35 that would be associated with an agreement to limit *global* CO_2 emissions at 20% of year 2000 levels. The optimal response of the U.S. to this price is a reduction of 12.8% of baseline emissions. Moreover, given the uniqueness of the outcome of the Coase Theorem, this abatement level is not sensitive to how the permits are initially distributed across countries. Also, internally within the U.S., there would be a unique optimal response, though, given differences in marginal abatement costs, control levels would vary across polluters (e.g., economic sectors).

The various tactics that can be applied to the mitigation of CO_2 are depicted in Figure 15-1, utilizing a step function to highlight their usual relative marginal cost positions. The first step of the cost function refers to *no regrets* (cost less or even cost-saving) conservation. This could stem from either a technological innovation or a move toward the

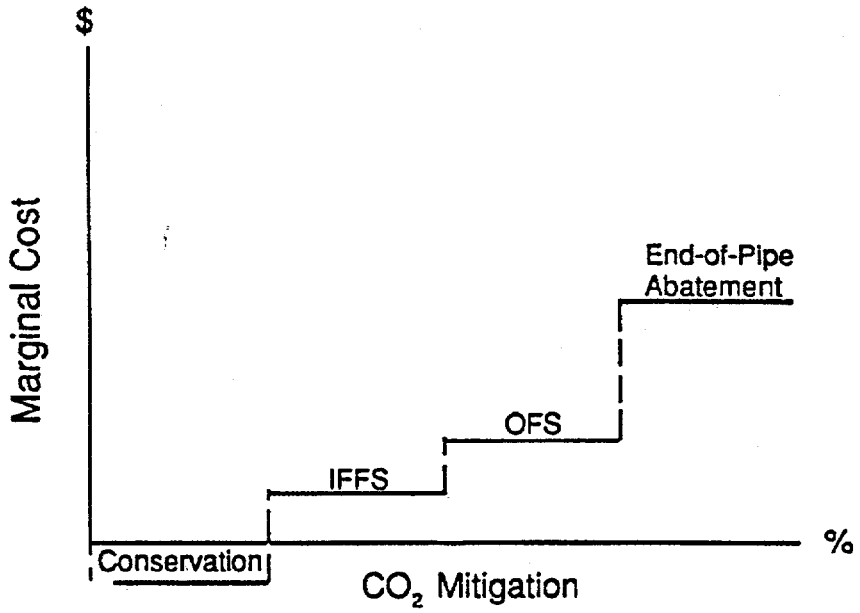

Figure 15-1. CO_2 COST FUNCTION

efficiency frontier as a result of correcting a misallocation (e.g., eliminating energy-wasting practices). There is considerable disagreement in the literature about the extent of conservation potential. Manne and Richels[19] refer to it as *autonomous energy efficiency improvement* (AEEI), which they estimate to be on the order of 0.5% to 1.0% per year. More optimistic estimates of costless conservation—in the range of 20% to 30% total for the near term— are offered by OTA[25], NAS[26], Lovins and Lovins[27], and Jaccard et al.[28]. This holds open the possibility that the optimal U.S. CO_2 emission reduction could be met entirely by this tactic.

Another major form of conservation is *price-induced*, e.g., decreasing energy use in response to a change in the price of energy relative to the price of other inputs, as would be caused by a carbon tax or permit regime. There are several types of input substitutions that could take place and we categorize them under the headings below following Cline[18]:

OFS—Other factor substitution
IFFS—Inter-fossil fuel substitution
NFFS—Non-fossil fuel substitution
PMS—Product mix substitution

Thus, if the tax is based on carbon content of fuels, there are optimal substitution responses within the class of fossil fuels (coal emits approximately 1.26 times as much carbon per unit as oil and 1.86 times as much as natural gas) and between the class of fossil fuels and other sources (e.g., nuclear, hydro, solar). All of these responses incur some costs unless the elasticity of substitution is infinite.

The final category of mitigation tactics shown in Figure 15-1, though limited in the near-term, is "end-of-pipe" abatement, such as CO_2 scrubbers. Of course other measures, such as climate engineering and carbon absorption through tree planting, might be used but are beyond the scope of this discussion.

The discussion above pertains only to a first set of adjustments for any decision-maker. If the price of energy inputs decreases because of improved efficiency, ironically energy then becomes more attractive, and there will be some offsetting increase through substitution of energy for other inputs. There is also the question of whether cost-savings will be passed along to industrial and/or final consumers or whether they will increase the returns to labor and/or capital. Similar possibilities arise with respect to responses that incur positive costs, though in terms of price increases and decreases in profits and wages.

The presentation thus far has been limited to partial equilibrium analysis, but a host of general equilibrium effects could potentially further enhance or offset these effects. First, if energy conservation savings are passed on to other industrial customers, there would be the possibility of further rounds of price reductions. This could potentially change the mix of material inputs in favor of those that are energy-intensive. The overall price reduction

would increase the purchasing power of consumers and provide a stimulus to the entire economy. This would also take place, but to a different degree, if price decreases were foregone in favor of increasing wages or profits.

At the same time, the reduction in energy use would lower production levels in the coal, oil, gas, refined petroleum, and electric and gas utility industries. This will touch off a chain of negative multiplier effects to upstream suppliers, such as mining equipment, field service, and finance industries, as well as downstream customers, such as railroads, pipeline companies, and electric utilities. These negative impacts would be reinforced by declines in wages and profits in all of these sectors as well. Interestingly, all of these negative effects engender additional energy conservation, though through reduction in economic growth rather than an improvement in energy efficiency. On the positive side, the resources released from the energy industries would stimulate economic activity elsewhere, though it is unlikely that they would be fully employed. Also, any increased demand for energy-saving equipment will have positive multiplier effects analogous to those mentioned in the previous paragraph. At the same time, this increased economic activity will result in increased energy use, partially offsetting conservation efforts.

Obviously, there are a sizable number of expansionary and contractionary influences. It is impossible to ascertain the net outcome a priori, and hence the need for empirical analysis based on a general equilibrium model.

The U.S. CGE Model

An updated version of a 20-sector CGE model developed by Lin[29] similar in nature to most SAM-based CGE models was utilized[30]; [31]. Limitations of journal space only allow us to provide a brief summary; however, details of the model are available from the authors upon request. Domestic producers, being profit-maximizers, produce goods and services using two primary factors, labor and capital, and intermediate goods as inputs. Intermediate goods are either produced domestically or imported, and are assumed to be qualitatively different (the Armington assumption). The utilization of inputs follows a two-stage decision process, and intermediate goods are modeled as a nested function of aggregates and components. Specifically, the energy aggregate consists of individual fuels (both primary and secondary energy), while the materials aggregate consists of goods such as plastics, glass, metals, etc., and the remaining input aggregate consists of all other intermediate goods. Inter-fuel and inter-material substitutions are allowed within their respective aggregates, which is a feature that is fundamentally required in evaluating environmental quality regulations[32]. The two-stage decision involves finding the optimum combination of components within energy and material aggregates, and then optimizing the levels of capital, labor, energy, and materials.

To take account of inter-fuel and inter-material substitution and substitution among aggregates, a flexible functional form cost functions was utilized to represent the technology of production sectors and assume these functions are homothetically weakly separable. The relationships between aggregates, and within the energy and material aggregates were specified with flexible functional forms, and the relationship between other intermediate inputs in terms of fixed proportions. For the current application, the Generalized Leontief (GL) functional form is used for all the flexible cost functions.

The demand component of the model includes both intermediate and final demands. Intermediate demand is determined by the cost-minimizing process discussed above. Final demand includes private consumption, government expenditures, and investment.

The modeling framework is general enough to incorporate several alternative views of equilibrium. In one version of the model, total employment is exogenously given, so full employment is achieved. Furthermore, the investment level is determined by savings, with savings rates being fixed. These specifications would have the model belong to the "classical" category. However, in the analysis below we also invoke an alternative (Keynesian) formulation of the labor market, in which the wage rate is fixed and labor supply adjusts to possibly less than a full-employment equilibrium. In addition, other components of the flow-of-funds account, such as the current account balance and government deficit, are considered in conjunction with the above for policy analysis purposes.

The core of the base year equilibrium data set of the model in this study is a SAM of the U.S. economy for 1987, constructed by Hanson and Robinson[33]. This data set contains both *make* and *use* versions of the U.S. Input-Output Table to capture the production and utilization of commodities. The SAM, in addition to providing the basic data set for model calibration, also provides initial values for endogenous variables and levels for exogenous variables. In this study, a 20-sector version of the model was used, including five mining sectors and two energy utility sectors (see Table 15-1).

Some key parameters of the empirical model—Allen elasticities of substitution between aggregate inputs—are presented in Table 15-2. They represent a synthesis of estimates available in the literature. Sensitivity tests are performed on these values below.

Simulation Results

In this section, we present simulation results for both autonomous and price-induced conservation strategies to be implemented in the Year 2000. The first set of simulations represents our best estimates of the effects of these responses on major economic indicators for the economy in general and the energy sectors in particular. Other simulations examine the sensitivity of the results to key parameters and behavioral considerations.

Table 15-1. Sector Definition

Sector	Name	BEA Code
1	Agriculture	1-4
2	Iron Mining	5
3	Non-Iron Mining	6
4	Other Mining	9,10
5	Coal Mining	7
6	Petroleum Mining	8
7	Construction	11,12
8	Manufacturing	13-30,33,34,39-64
9	Petroleum Refining	31
10	Plastics	32
11	Glass	35
12	Stone	36
13	Steel	37
14	Metal Manufacturing	38
15	Transportation	65
16	Communication	66,67
17	Electric Utilities	68.01
18	Gas Utilities	68.02
19	Trade & Finance	69,70
20	Services (including Water & Sanitary Services)	71-79,68.03

Notes: Sectors 5, 6, 9, 17, and 18 form the energy aggregate.

Table 15-2. Allen Elasticities of Substitution for Selected Sectors

Sector	σ_{KE}	σ_{KL}	σ_{KM}	σ_{LE}	σ_{LM}	σ_{EM}
Construction	.70	.20	.55	-.25	.89	.77
Petroleum Refining	.25	.90	.35	.20	.50	.05
Manufacturing	.70	.20	.55	-.25	.89	.77
Transportation	.70	.90	.35	.25	.10	.05
Utilities	.70	.90	.02	-.10	.01	.01

[a]The symmetry properties of our production function require $\sigma_{ij} = \sigma_{ji}$.

Table 15-3. Transformation of a Carbon Tax to an Ad Valorem Tax

	Fuel		
	Coal (ton)	Oil (bbl)	Gas (tcf)
Heat Content (million Btu per unit)	21.94	5.80	1.03
Emission Rate (kg per million Btu)	26.90	21.40	14.50
Conversion Factor (tons per unit)	0.59	0.12	0.02
Carbon Tax (1990 $ per unit carbon)	38.35	38.35	38.35
Ad Valorem Tax (1990 $ per physical unit)	22.63	4.76	0.57
Fuel Price, Year 2000 (1990 $ per physical unit)	26.64	26.40	2.72
Price Increase (percentage change)	85.12	18.02	20.83

Energy policy responses are simulated in two ways. First, to analyze *autonomous* conservation, or the *mandated* response to a command-and-control policy, the energy use parameters in the model are reduced by 12.8% across-the-board (recall the U.S. response to a global policy regime discussed above). The model then analyzes sectoral (partial equilibrium) and multi-sectoral (general equilibrium) responses. Also, sensitivity tests are performed to ascertain the possible offsetting effects of energy-saving equipment needed to implement the policy goal. Note that in actuality, abatement cost curves will vary across sectors and the least-cost no regrets level will thus vary. Due to the lack of data on sectoral conservation potential, a uniform level is simulated. Given the fact that command and control policies are typically applied across the board, this exercise may not in fact represent too much of a departure from reality.

The direct application of a carbon tax or permit trading to examine *price- induced* conservation is also simulated. This is modeled as a price increase in primary energy (tax on fossil fuel production), as indicated in Table 15-3. Note that in this case the optimal response calls forth differential reductions in energy use and differential levels of interfuel substitution across sectors.

Specifically, the following four cases will be simulated:

1. Simple conservation—a 12.8% cutback in purchases of all fossil fuel energy, including utilities, in all intermediate and final demand sectors.
2. Conservation, but with the entire cost-savings in each sector being assigned to increased purchases of energy-saving equipment.
3. Price-induced substitution, but with the carbon tax being imposed only on domestic use of domestically produced primary energy.
4. Price-induced substitution, but with the carbon tax being imposed on domestic use of both domestic and imported primary energy.

Note that, in effect, the optimal response to CO_2 mitigation policies is likely to be a combination of autonomous conservation and various types of substitution, which we have separated to isolate unique features of each. The overall outcome will thus be some weighted average of the two strategies. Referring to Figure 15-1, the exact combinations would be determined by the intersection of the carbon tax level (or equilibrium permit price) and the marginal cost of abatement.

Basic Results

The prime simulations are presented in Table 15-4 in terms of their impacts on five major economic indicators. The basic conservation case (line 1 of Table 3) is estimated to yield an overall decrease in GDP of 1.44% and a reduction in employment of 2.05%. Economywide investment decreases by 4.41%, with exports actually increasing by 2.75%

Table 15-4. Economywide Impacts Of CO_2 Mitigation, Year 2000: Base Cases
(percentage change from baseline)

Case	Real GNP	Employment	Investment	Exports	Imports	Welfare[a]	Energy Use	CO_2 Emissions
1. Conservation (100% cost-saving)	-1.44	-2.05	-4.41	2.75	-3.63	-0.84	-3.32	-3.44
2. Conservation (100% equipment offset)	-3.65	-3.94	-4.11	0.84	-3.02	-2.25	-9.16	-8.96
3. Interfuel Substitution (no tax on imported oil)	-1.56	-2.02	-3.59	-1.79	-1.93	-1.39	-24.17	-26.07
4. Interfuel Substitution (tax on all oil)	-1.77	-2.28	-3.37	-2.60	-3.38	-1.64	-25.49	-27.22

[a]As measured by compensating variation.

and imports declining by 3.63%. The difference in the GDP and Employment results indicates that there is proportionally greater substitution away from labor and labor-intensive goods than is the case for other inputs. Note also that the impact of this case (and all others) in terms of a welfare measure such as compensating variation, are also negative, though by a smaller percentage than the macro indicators.

Aggregate energy use declines as do CO_2 emissions, but startlingly less than expected. As expected, coal and electric utilities suffer the largest declines. Even though direct effects are proportional, general equilibrium effects allow for substitution away from these sectors. At first pass, one would expect declines of greater than 12.8% in each energy sector given the direct response and subsequent multiplier effects. However, it appears that the price decrease for each fuel causes energy to be more attractive to the point where there is a significantly offsetting substitution effect toward it. This has been pointed out in a number of studies that warn of the unintended side-effects of autonomous or mandated conservation[34]. Other general equilibrium effects are operative as well but are too difficult to sort out without further experimentation (see below). Overall, the downside effects are not overcome by stimuli from increased purchasing power, international competitiveness, or multiplier effects. The results for the energy sectors are presented in Table 15-5.

Note also the irony of this policy response. In effect, the initial willingness of industry to decrease energy consumption by 12.8% results in offsetting factors that would not enable the U.S. to meet its CO_2 reduction target. That is the overall average decline of energy use of 3.32% would mean that CO_2 emission reductions would only be one-fourth of those intended. This is somewhat disconcerting, and, using rough rules of thumb, indicates that energy users on the average might need to undertake several times the amount of initial energy conservation to yield the intended overall 12.8% reduction.

The results of a modified conservation response is presented in row 2 of Table 15-4. When the entire cost savings is offset by increased costs of energy-saving equipment, the negative impacts are even greater than in the base case. From Table 15-4, it can be seen that GDP declines by 3.65% and employment by 3.94%. The key to understanding the decline is the reduction in economywide investment. It would appear that the *crowding-out* effect of investment in energy-conserving equipment is substantial and has a dampening effect on the economy[35]. However, there is bias in the model and its application. The investment equations are specified for more general cases. The model thus views the earmarking of investment funds for energy conservation as sub-optimal (as do the vast majority of the models in the literature). On the other hand, if the rate of return on this investment specifically reflected the gains that could be brought about, it might very well be

Table 15-5. Energy Sector Impacts of the Conservation (100% Savings) Response, Year 2000: Base Case
(percentage change from baseline)

Energy Type	Gross Output	Employment	Exports	Imports
Coal	-3.85	-4.64	0.39	-6.52
Oil/Gas Extraction	-1.03	-2.75	4.36	-4.43
Petroleum Refining	-2.28	-2.84	2.61	-5.16
Electric Utility	-4.21	-5.36	1.99	-7.18
Gas Utility	-2.49	-3.07	3.37	-5.33

Table 15-6. Energy Impacts of the Conservation (100% Equipment Offset) Response, Year 2000: Base Case
(percentage change from baseline)

Energy Type	Gross Output	Employment	Exports	Imports
Coal	-8.05	-9.12	-13.01	-4.73
Oil/Gas Extraction	-9.63	-12.07	-1.34	-13.66
Petroleum Refining	-11.35	-12.10	-34.42	3.47
Electric Utility	-6.92	-9.30	-12.06	-4.24
Gas Utility	-10.05	-11.32	-30.66	2.48

that energy-saving equipment would be one of the better uses of investment funds. The otherwise expansionary effect of this increased investment might cause overall investment and output declines to be lower than Case 1. To be positive overall, however, would require considerable impetus. The 12.8% decrease in energy costs in most sectors translates into a 0.1 to 1.0% cost savings in each sector. This presents a relatively minor advantage to investment in energy-saving equipment over other alternatives.

The effect of Case 2 on individual energy sectors is presented in Table 15-6. The reductions come close to the 12.8% due in great part to investment considerations, which represent a type of forced substitution of capital for energy, in addition to other responses. Whereas in Case 1, energy intensity declines were below 0.2% for all sectors, here several sectors wind up with declines of greater than 2.0%.

In Cases 3 and 4, the response to a carbon tax or permit trading is simulated in terms of direct inter-fossil fuel substitution (IFFS) and other factor substitution (OFS), i.e., the increased cost of the energy aggregate leads to substitution between it and other aggregate input categories. These responses are further affected by various other general equilibrium interactions that take place, including product mix substitution (PMS). The results of simulations for these responses are presented in rows 3 and 4 of Table 15-4. In Case 3, the tax applies only to domestic use of energy produced in the U.S., while in Case 4 it applies to imported energy (primarily oil) as well.

Case 3 also yields a negative impact on the economy in terms of GDP and employment. The economic impacts of this case are quantitatively and qualitatively similar to Cases 1 and 2, except that exports decrease. The negative impacts on the economy are more pronounced in Case 4 because more inputs (i.e., imported oil) suffer price increases. These impacts are not offset by relatively more favorable terms of trade in Case 4 vs. Case 3.

The effect of Case 3 on individual fuels is presented in Table 6. As would be expected from Table 15-3, coal bears the brunt of the carbon tax, as reflected in a reduction in the sector's gross output of over 44%. Domestic crude oil production declines by 6.77% and imports decline by 8.77%. Sectoral results for Case 4 are very similar to Case 3, except that crude oil import reductions are much greater in the latter.

Perhaps the major differences between the mandated and incentive-based conservation responses are the energy and CO_2 reductions. Referring to the last two columns of Table 15-4, we see that under Case 3 aggregate energy use decreased by 24.17% and total CO_2 emissions decreased by 26.07% (both figures are slightly higher for Case 4). First, the nearly 2.0% differential between energy use and CO_2 emission reduction reflects a significant amount of fuel switching. The majority of the emission

reduction, however, stems from a relatively much greater decrease in energy use in Cases 3/4 vs. Cases 1/2 (compare also Tables 15-5 to 15-7). Some energy intensive sectors are the hardest hit by the general equilibrium effects, e.g., steel, stone (cement), and transportation.

Apparently declines in the energy sectors do contribute to the overall negative effect on the economy in the various simulations, but there are some offsetting effects in the carbon tax/permits cases, since decreases in GDP are only slightly higher despite a 7-8 fold decrease in energy production vis-a-vis Case 1. The relatively greater labor intensity of non-energy industries is one part of the explanation (compare the economywide employment decreases between Cases 1 and 3). Other explanations include the relatively lower negative impact on investment and the spending impetus of carbon tax revenues (though only to a slight degree as will be shown below).

Sensitivity Analysis

The CGE model is based on a calibration method with less than ideal statistical properties, and contains several facile assumptions. Therefore, it is not unreasonable to question the robustness of the results. This is tested by examining the effects of utilizing alternative estimates of capital-energy substitution elasticities and by invoking alternative CGE closure rules.

Recall the K-E elasticities of substitution for major sectors are presented in Table 15-2. They range from .250 to .700, which means capital and energy are considered substitutes. It is possible that these elasticities overstate the degree of the substitutability relationship. Moreover, it is also possible that capital and energy are complements.

Note that in addition to the elasticity values in Table 15-2, a further substitution relationship between capital and energy in Cases 2 and 3 of the previous subsection has been modeled. In effect, we inserted a direct decrease in energy and an increase in capital by an equivalent amount and by half the amount, respectively, essentially increasing the K-E elasticities by these quantities. Indirect effects are still modeled with the ordinary K-E substitution elasticities.

Two sets of sensitivity tests on elasticities were performed. The first reduced the K-E elasticity values by half. The overall results (not shown) yielded imperceptible differences for Cases 1 and 2 and only minor differences for Cases 3 and 4. The second set of sensitivity tests utilized elasticities for capital and energy that exhibit complementary relationships. This required recalibration of the production functions and mainly minor adjustments in other elasticities. The results of the application of these new parameters also had little affect on the results and are not presented here. In effect, the results are thus more

Table 15-7. Energy Sector Impacts of the Interfuel Substitution Response to Tax on Domestically Produced Energy, Year 2000: Base Case (percentage change from baseline)

Energy Type	Gross Output	Employment	Exports	Imports
Coal	-44.37	-37.43	-65.44	-19.31
Oil/Gas Extraction	-6.77	-8.76	-3.35	-8.77
Petroleum Refining	-7.72	-6.39	-32.05	8.74
Electric Utility	-7.85	-10.11	-34.49	9.32
Gas Utility	-1.69	-2.90	-18.94	8.34

Table 15-8. Definitions of Sub-cases of Simulation 5

Sub-cases	Government Expenditure	Total Labor Supply	Sectoral Labor Demand	Total Capital Stocks	Sectoral Capital Stocks	Characterization
5.1	NF	NF	M	F	M	UNEM
5.2	NF	F	M	F	M	FULEM
5.3	NF	NF	M	F	F	S-R
5.4	F	NF	M	F	M	UNEM
5.5	F	F	M	F	M	FULEM
5.6	F	NF	M	F	F	S-R

Note: F = Fixed; NF = Not Fixed; M = Mobile; UNEM = Underemployment equilibrium; FULEM = Full employment equilibrium; S-R = Short-run case

sensitive to substitution levels across input aggregates, than within them, even for the case of interfuel substitution.

The third set of sensitivity tests is based on alternative assumptions about the labor market, factor mobility, and fiscal balances. In order to achieve equilibrium in constructing the CGE model, one cannot over- or under-constrain any of the markets. For example, in the case of labor supply, both the labor supply and wage rate cannot be held constant, nor can both of them vary. The specification of which aspect is fixed and which is variable in this and in other markets is known as a *closure rule*.

In the simulations above, a fixed real wage rate was assumed. The implications of an alternative closure rule that sets labor supply fixed and allows the wage rate to adjust was examined. This forces full employment of resources directly and indirectly released by the decrease in energy production. In addition, the implications of our assumption about the perfect mobility of capital was examined. Finally, the sensitivity of the result to whether carbon tax revenues are used to expand government expenditures or used for deficit reduction (with government expenditures being fixed) was examined. The conditions underlying the various sensitivity tests are presented in Table 15-8.

The results of these sensitivity tests applied to Case 4 (Interfuel Substitution/Tax on All Oil) are presented in Table 15-9 (note that Case 4.1 is the same as Case 4 listed in Table 3). As in our original simulations, the impacts on real GDP are negative in all cases, though they are negligibly so in Cases 4.2 and 4.5 because of the employment forcing. In only two of the cases (4.1 and 4.4) are the negative impacts on GDP and employment greater than in Case 1, and then only marginally so. It appears that using carbon tax revenues for deficit reduction, rather than expanding government expenditures, does enhance negative impacts but only slightly. It also appears that a fixed capital stock assumption reduces the negative impact somewhat (Case 4.3). The explanation would appear to be that capital is prevented from leaving the U.S. (also compare the export and import figures for Cases 4.1 and 4.3).

Results for individual energy sectors (not shown) are reasonably similar for all cases. The only significant difference is that crude oil imports decrease slightly in Cases 4.1 and 4.6.

Conclusion

The general equilibrium impacts of a conservation strategy to reduce CO_2 emissions have been examined. There is a negative impact on GNP, employment, and other macroeconomic indicators. Not surprisingly, the impact on the energy industries was found to be strongly negative. Potentially positive ramifications of conservation, such as cost savings, increased consumer purchasing power, and multiplier effects of investment in

Table 15-9. Interfuel Substitution Impacts, Year 2000: Sensitivity Tests
(percentage change from baseline)

Case	Real GNP	Employment	Investment	Exports	Imports	Welfare[a]	Energy Use	CO_2 Emissions
4.1	-1.77	-2.28	-3.37	-2.60	-3.38	-1.64	-25.49	-27.22
4.2	-0.14	—	-2.24	-1.36	-1.60	-0.65	-24.09	-25.82
4.3	-1.34	-1.75	-3.71	-1.64	-3.20	-1.39	-22.45	-23.93
4.4	-1.79	-2.34	-1.83	-2.53	-3.25	-1.66	-25.55	-27.27
4.4	-0.08	—	2.97	-1.03	-0.99	-0.63	-24.13	-25.86
4.6	-1.50	-2.00	-1.67	-1.62	-3.17	-1.48	-22.59	-24.08

energy-saving equipment, were not able to offset the partial and general equilibrium downside effects of decreased energy use. Moreover, the results were robust to alternative assumptions on the degree of cost savings associated with conservation, the ease of substitution between energy and other inputs, and various macroeconomic closure rules. Finally, the results are in the ballpark of estimates undertaken by others, such as Manne and Richels[19, 36] and Jorgenson and Wilcoxen[35], though these studies placed a lesser emphasis on conservation. Thus, it is concluded that conservation should not be characterized as a "no regrets" strategy.

This does not, of course, mean that conservation is a poor strategy, but simply that it should not be oversold as costless. In addition, the scope of this section has been limited to one side of the ledger, and the existence of reasonable estimates of net benefits of reducing CO_2 emissions in the tens of billions of dollars per year for the U.S. alone[20, 37] is acknowledged. It should be pointed out, however, that a 3% decline in GNP in the Year 2000 translates into nearly $200 billion per year of opportunity costs.

Finally, the results pertain only to the short term. This, however, is the time period for which "no regrets" strategies apply, i.e., measures that can be taken until uncertainties about global warming are resolved. If predictions about the onset of warming are verified, a strategy need not be costless to be viable. Moreover, conservation may be able to play an expanded role in the longer term. Rather than the limited range of short-term options we have analyzed, some researchers have proposed more sweeping "eco-restructuring" for both industrialized and developing economies[38]. It is likely that these strategies would not bode well for traditional energy industries. However, their goal is to integrate innovative approaches to resource utilization into the economy so as to establish a path of sustainable development. Thus, further research is warranted to examine the long-term impacts of conservation.

15.5 Subtask 5.5 Economic Analysis of the Defense Department's Fuel Mix

Abstract

This subtask examines US military fuel consumption and describes alternative technologies that could be currently or potentially applied to the military in order to comply with US government directives to lower emissions, lower dependence on imported oil and to become more energy efficient.

Introduction

The DOD is responsible for approximately 2% of US energy consumption. The DOD is a more important market player with respect to some types of fuel, however. For example, in 1990, DOD consumed approximately 34% of all aviation fuel and 33% of all

distillate used for shipping[39]. To provide perspective, Table 15-10 contains the breakdown of US military fuel consumption with US government usage and total consumption for the USA as a whole. It is clear that defense consumption makes up the vast majority of US government use, though this is only a few percent of the total US consumption in all of the major source fuel markets (petroleum, electricity, natural gas and coal).

The EIA has made forecasts regarding certain types of fuel consumption for the years 2000, 2005 and 2010. Table 15-11 also shows breakdown of usage of various fuels in the military and their relative importance in terms of US consumption. The military is a major user of shipping and aviation fuels which are predominantly petroleum based.

DOD energy use is divided into two major user types for the purposes of this report: 1) power and heat generation users at military installations representing fairly large expenditures on energy and; 2) transport users which represent smaller absolute amounts but larger relative amounts in terms of percentage of US usage. These two categories will be used as the basis for organization of this report.

Power Generation Technologies That Could Lead to Changes in Fuel Consumption Patterns in the Military

A large percentage of military fuel consumption is due to the needs of military bases in terms of space heating and electricity generation for other purposes. The US military has around 275 bases split between the Army, Navy and Air Force. The fuel needs for these are split between coal, gas and petroleum products such as distillate and heavy fuel oils.

Alternative methods to reduce fuel costs, decrease dependence on imported oil and to improve environmental quality of emissions are discussed below with respect to improvements in energy management, new technologies and alternative fuels.

Energy Management Initiatives

The DOD uses approx. $2.9 billion annually in energy at installations. The US government's "Energy 2005" initiative calls for a 10 % reduction in installation's use of energy by FY 1995 and a 20 % reduction by 2005 (1985 is the base level). Industrial energy use is also aimed at being 20 % lower than 1985 levels in 2005.

Since the late 1970's the army has been installing Energy Monitoring and Control Systems (EMCS) at its installations. These are computer systems designed to keep track of and adjust if necessary, energy usage in order to minimize energy costs. Their development is evolutionary and implementation on large scale of the newer technologies in this field would bring significant savings in energy use due to advances in control technologies and software. MacDonald and Gettings[40] have studied military use of such systems and concluded that "dramatic changes (in the technology) are possible in the next decade".

Table 15-10. Consumption of Energy (1992) (trillion Btu)

Fuel / Energy Type	Defense	US Government	USA
Motor Gasoline	12	35	13980
Distillate / Residual Fuel	214	236	8870
Jet Fuel	765	775	3080
Other	2	5	7540
Total Petroleum Based	993	1050	33470
%	3%	3%	100%
Electricity	117	190	9440
%	1%	2%	100%
Natural Gas	109	154	20320
%	1%	1%	100%
Coal & Other	51	65	19140
%	0.0%	0.0%	100%
Total	1269	1460	82360
% of US Consumption	2%	2%	100%

Source : EIA. 1992. Annual Energy Review.

Table 15-11. Military Fuel Use Forecasts

Transportation Sector Energy Use by Mode and Type - Military Use
(trillion Btu per year)

Year	1990	2000	2005	2010	Annual Growth 1990-2010	1990 % of total market use
Total Military Use	902.1	656.2	660.3	670.4	-1.50%	
Aviation fuel	795	570.1	573.7	582.5	-1.50%	34.05
Residual Fuel Use	15.6	12.7	12.7	12.9	-0.90%	1.54
Distillate Fuel Use	91.5	73.4	73.9	75	-1.00%	33.11

Transportation Sector Energy Use by Mode and Type Within a Mode
(trillion Btu per year)

International Shipping					
Distillate (diesel)	62.2	81.74	92.27	102.06	2.50%
Residual oil	920.24	1209.7	1356.11	1509.33	2.50%
Domestic Shipping					
Distillate (diesel)	214.19	231.25	246.36	262.96	1.00%
Residual oil	94.37	101.92	108.55	115.82	1.00%
Air Transport					
Jet Fuel	2334.55	3147.5	3509.52	3856.3	2.50%
Aviation Gasoline	45.36	42.56	42.26	42.14	-0.40%
Military Use					
Jet Fuel (Kerosene)	451.55	334.13	336.23	341.44	-1.40%
Jet Fuel (Naphtha)	343.4	235.95	237.43	241.11	-1.80%
Residual Fuel	15.58	12.66	12.74	12.94	-0.90%
Distillate	91.52	73.41	73.87	75.02	-1.00%

Source: EIA 1994.

Flue Gas Desulfurization : "e-scrub technology"

The SERDP (Strategic Environmental Research and Development Program) (US Senate, 1992) allocated $160 m for financial year 1994 for the development for military and commercial use of the "e-scrub" flue gas desulfurization devise adapted from other military technology; according to the DOD (1994 annual review) this device "may be able to efficiently turn dirty, high sulfur coal emissions into a fertilizer, resulting in cleaner water, air and a commercial product." This is but one of many flue-gas desulfurization technologies now available.

Dry Micronized Coal and Coal / Water Slurry Technology - New Boiler and Handling Technologies

The defense FY86 Appropriations Act (Public Law (PL) 99-190, Section 8110) directed the DOD to rehabilitate and convert its existing domestic power plants to burn a higher percentage of coal. By FY 1994 coal consumption by the military was to have increased to 1.6 m tons per year above the level of consumption in 1985. The FY 87 Defense Authorizations Act directs that the primary fuel source used in any new heating system installed be the most life-cycle cost effective. Thus the DOD cannot install new coal fueled plants without making sure the plant is the most cost effective over the life of the plant. These laws, together with a directive canceling the restriction that oil or gas heating systems be built on a scale smaller than 50 million Btu / hr have provided impetus for the military to look at conversion of boilers at military installations to coal

US military coal consumption from 1985 - 1991 is listed in Table 15-12. It can be seen that the army is the largest user of coal with the navy second largest and air force is the smallest user. It was recommended by the US Army Construction Engineering Research Laboratories (USACERL) in 1991 that the Navy has the highest potential for increasing its coal consumption after a study in 1987 identified bases where conversion to coal would be most advantageous.

Work by USACERL[41] indicates that there are several choices in achieving this goal once sites for increased coal use have been identified. These include the choice to build new plants to replace old ones, or to retrofit oil and gas boilers for coal firing or to build third party coal fired cogeneration plants in conjunction with commercial power companies. Various technologies are available for retrofit projects; these were under investigation by other contributors to this report[42]. Briefly these are : coal/water slurry fuels, dry micronized coal, coal gasification, retrofit fluidized-bed combustors and slagging combustors.

Table 15-12. DOD Coal Consumption (short tons)

Year	Army	Air Force	Navy	DOD Total
1985	704190	452242	162095	1336261
1986	733490	491122	168689	1409446
1987	734457	472086	163891	1384984
1988	802218	478092	178227	1471240
1989	768962	448945	222888	1453444
1990	867690	439512	178490	1498740
1991	766725	435563	167232	1381155
(% of DOD)	56 %	32 %	12 %	100 %

Source: Adapted from Lin (1993)

So far USACERL work as concluded that the building of new coal fired plants to replace old oil/gas fired plants is economic at only one site. Retrofitting heavy oil plants for coal firing was found to be an attractive strategy for 38 plants of 88 studied.

Fuel Cell Technology

The underlying principle of fuel cells has been known about for over a hundred and fifty years but the technology has only been proposed recently for commercial use. The principle is similar to how a battery works, but, unlike a battery, it continues to provide power so long as fuel and oxidant are supplied. It works by chemically reacting air / oxygen with a fuel such as hydrogen processed, using a reformer, from natural gas, for example; this produces a direct chemical transfer of energy as a DC current which is then transformed to an AC current for use. The method of reaction means that energy efficiency is extremely high relative to thermal power plants. Newer plants are expected to produce efficiencies of 50-60 % compared to 30-40 % at thermal plants. Other advantages are flexibility due to their modular construction, quietness, reliability (allowing reduction in backup systems required), and environmental advantages such as extremely low NO_X, CO and unburned hydrocarbons emissions.

Fuel cells require a feed stock that enables release of hydrogen. Alternatives include all fossil fuels. Coal gasification is among those methods currently being investigated for fuel production. Natural gas is probably the most convenient feed stock. Research and development is currently going on with respect to 4 types of technology: each referring to the type of electrolyte used in the cell (see Table 15-13).

Canada's military has made a strategic decision to investigate fuel cell technology and has contracted Ballard Power Systems, Inc. to investigate polymer electrolyte fuel cells and their operation on air and reformate fuels. The results of the program are a demonstration program with power outputs up to 5 kW and hydrogen-oxygen and hydrogen-air low kW units have been delivered to customers. The Canadian department of defense is also sponsoring a program to demonstrate the use of 100 MWh and 300 kW Ballard fuel cells for submarine propulsion to replace diesel engines currently used. A 50 kW scaled version is being developed by Ballard which will operate on methanol and oxygen or methanol and air (on surface). The Royal Military College of Canada continues its analysis of fuel cell systems.

At present, units range from very low output (<10 kW) to 200 kW. In the very near future units will be available up to 10 MW. This range will probably find many uses in the military. US military research has been active since the 1980's by participating in DOE, GRI (Gas Research Institute) and utility companies' field tests of 40 kW phosphoric acid fuel cell units produced by International Fuel Cells Corporation. In FY 1993 the DOD

Table 15-13. Summary of Worldwide Fuel Cell Development Progress

	<---------- Fuel Cell Status ---------->						
Country	**Phosphoric Acid (PAFC)**	**Molten Carbonate (MCFC)**	**Solid Oxide (SOFC)**	**Proton Exchange (PEFC)**	**Operating Capacity (kW)**	**Reformer made ?**	**Approx. Funding ($ U.S. Million / yr)**
Austria	Dn[1]				200		-
Australia			R,Dt				5 Total
Canada	Dn[1]			R,Dt,Dn	325		Unknown
Denmark	Dn[1]	R,Dn[1]	R,Dt	R	200	Y	4 Total SOFC
Finland	Dn[1]			R	200		-
France		R	R	R			2 Total PEFC
Germany[2]	Dn[4]	R,Dt	R,Dt	R,Dt	800		6 Gov., No PAFC
Italy	R,Dn[1]	R,Dt	R	R,Dt	1500		4 Gov
Japan	R,Dt,Dn[4],C	R,Dt	R,Dn[5]	R	+/- 40,000	Y	46 Gov.
Korea	R,Dn[4]	R,Dt	R		200	Y	Unknown
Netherlands		R,Dt	R				10 Gov.
Norway			R,Dt				2
Spain	Dn[3]	R,Dt			200		1 No PAFC
Sweden	Dn[1]	R			200		2 Gov., No PAFC.
Switzerland	Dn[1]		R,Dt		200		2 Gov., No PAFC
United States	R,Dt,Dn,C	R,Dt,Dn	R,Dt,Dn	R,Dt,Dn	+/- 4500	Y	104 Gov. & Institutes

R Research
Dt Development
Dn Demonstration
C Near Commercial or Commercial Sales

Notes:
1. U.S power plant(s)
2. Germany demonstrated a 100 kW alkaline fuel cell system in a submarine
3. Japanese power plant(s)
4. U.S and Japanese power plants
5. Westinghouse (U.S) SOFC modules
   Belgium is demonstrating an alkaline fuel cell unit in a bus.

Source: After USDOE report prepared by Gilbert / Commonwealth Inc.(1993)

initiated a program to demonstrate and use commercially produced fuel cell power plants at sites located at military bases. DOD has also initiated a program to develop fuel cell power plants for defense applications; particularly in order to develop units fueled by standard logistic diesel or jet fuel.

Conclusion

The technology seems to be rapidly developing. It has a wide variety of applications due to the different scales it is offered at. Environmentally, the technology provides extremely low emissions energy. It is deemed more reliable and flexible than conventional thermal power / boilers. It is also more fuel efficient; implementation would result in lower fuel consumption. Its major drawbacks are that it is still very high cost technology. Current capital costs for natural gas fueled plants are estimated at between $ 600 - 1000 / kW, and for coal fueled plants are $1000 - 1200 / kW[43].

Combined Cycle Gas Turbine

The waste heat generated in burning oil or gas in a boiler is used to run a separate turbine to increase energy efficiency. The technology has been used for many years. As such it is proven technology, but represents an option for new plants because it is suited to utilization of gas (now more abundant at low cost) and also because of recent advances in this technology. With respect to coal, gasification prior to burning can allow this technology to be employed[44].

Other Clean Coal Technology Programs

The Office of Clean Coal Technology (part of the US DOE) sponsors, in partnership with industry, a wide range of clean coal technology programs which apply to research and demonstration at various levels in the processing of coal to energy such as preparation (e.g. coal washing process developed for Phase 1[42]), transformation (e.g. production of "Syncoal" by the Rosebud Syncoal Partnership[45]), combustion[42]), post-combustion (the SNOX process[46]) and other relevant areas.

The Federal Government has invested $ 2.5 billion in the Clean Coal Technology Program; other contributions from industry and individual states have amounted to more than $ 4 billion[47]. As a result, 45 new demonstration projects are underway[45]. Advanced technologies are being tested in emissions reduction using scrubbers for NO_X and SO_X gases, clean coal fuels, clean coal fluidized-bed technologies, integrated combined cycle gasification projects and other innovations. Earlier demonstration results are now being used in the design and construction of larger scale commercial facilities. It is expected that most of the 45 projects will have provided sufficient data for full scale commercialization decisions in the early years of the next century (i.e. in 5 - 15 years time)[48].

The current drive to commercialize these technologies could affect military choice of fuel in favor of coal as the military may place more urgency on strategic considerations.

Transport : Technology That Could Lead to Changes in Fuel Consumption Patterns in the Military

The consumption of various types of fuels could be affected by technological change in two main ways : 1) Fuel economy changes and; 2) Substitution to other fuels. Table 15-14 presents the types of transportation used in the military that are considered in this analysis. The currently used fuels are noted as well as possibilities for conversion either physically or by re-equipping the fleet with new engines / vehicles.

Alternative fuels

Currently, conventional fuels are those most widely in use including gasoline and diesel for land based vehicles and residual oil and distillate for ships and kerosene / naphtha for aircraft. The DOD is now under pressure to have their consumption reduced for two main reasons : 1) to reduce reliance on imported oil ; a strategic issue; and 2) to reduce harmful emissions caused by their use, especially those used in land-based applications, for environmental reasons.

Alternative fuels have characteristics that make them more attractive than conventional fuels on strategic and / or environmental grounds. Table 15-15 lists currently known alternative "fuels" in the broad sense (including nuclear and electric technologies), the conventional fuels that they replace and the technologies that are now being developed to exploit them ; either in the military or private / civilian sectors.

In terms of projects already under way the DOD has undertaken to convert a portion of its 200,000 administrative vehicles (assumed to include all buses, trucks, LDV's, automobiles and other such) to "alternative fuels". By FY 1995 the DOD has undertaken to acquire 10,000 alternative fuel vehicles.

State and Federal Government Initiatives and Legislative Aspects

1970's oil price increases and current environmental concerns have lead to governmental sponsoring of and influence over efforts to introduce alternative fuel use. The Clean Air Act Amendments of 1990 set goals for improvement of air quality especially concerned with CO (carbon monoxide) and O_3 (ozone) emission reduction in the transport sector. The law is viewed as favorable towards alternative fuels such as chemically simpler fuels (e.g. methanol and methane).

The Energy Policy Act of 1992 (EPACT) was passed in the wake of the Persian Gulf War of 1990-1991. This act set out to decrease independence of the US on imported oil. The act targets fleets of vehicles for increased use because of the costs of conversion,

Table 15-14. Possibilities for Conversion of Vehicles to Alternative Fuels

Mode of transport	Main Fuel	Possibilities for Conversion
Light vehicles	diesel / gasoline	CNG,LNG,LPG,M-85,M-15,E-95,E-100,M-100, electricity, H-Fuel Cell
Buses	diesel / gasoline	CNG,LNG,LPG,M-85,M-15,E-95,E-100,M-100, electricity, H-Fuel Cell
Trucks	diesel / gasoline	CNG,LNG,LPG,M-85,M-15,E-95,E-100,M-100, electricity, H-Fuel Cell
Ships	distillate residual fuel - oil ? nuclear	Fuel cells, CNG,LNG,
Jet aircraft	jet fuel JP-8, JP-4, (kerosene, naphtha)	Coal gasification derived JP-8
Helicopters / prop aircraft	kerosene	Coal gasification derived JP-8
Tanks & other armored vehicles	diesel ?	

Table 15-15. Alternative Fuels and Technology Developments for Transportation

Alternative fuel	Conventional fuel replaced	Technologies available	Development stage
Compressed natural gas (CNG)	Gasoline Diesel	Light Duty vehicles: Buses and other heavy duty vehicles.	Demonstration
Liquefied natural gas (LNG)	Gasoline Diesel	Light Duty vehicles: Buses and other heavy duty vehicles.	Demonstration
Liquefied Petroleum gas (LPG) (Propane)	Gasoline Diesel		Demonstration
Methanol / gasoline (M-85)	Gasoline Diesel	Cars, trucks, heavy duty vehicles	Demonstration/ Commercial
Methanol (M-100)	Gasoline Diesel	Cars, trucks, heavy duty vehicles	Demonstration / Commercial
Ethanol (E-95, E-100)	Gasoline Diesel	Cars, trucks, heavy duty vehicles	Demonstration / Commercial
Ethanol / Gasoline (E-10[1], E-15[1], E-85)	Gasoline	Cars, trucks, heavy duty vehicles	Demonstration / Commercial
Electricity	Gasoline Diesel	Cars, trucks, heavy duty vehicles	Demonstration / Commercial
Reformulated gasoline[2]	Gasoline Diesel	Cars, trucks, heavy duty vehicles	Demonstration / Commercial
Fuel cell	Gasoline Diesel	Methanol fueled bus - Mercedes, GM, Chrysler - also cars, trucks and plans for locomotives	Demonstration

Notes:

[1]These fuels are statutory not defined as "alternative" in EPACT but are defined as "replacement"
[2]These fuels are aimed at lowering emissions regardless of source (and thus strategic influence).

Source: EIA. June 1994.

refueling and fuel storage facilities. EPACT mandates acquisition targets for alternative fueled vehicles for Federal and State agencies.

Table 15-16 illustrates how, under EPACT, the federal government (including the DOD) will be required to increase the numbers of alternative fuel vehicles rapidly in the next 5 years. 75 % of all new federal vehicles acquired in 1999 will have to be alternative fuel powered vehicles. New military vehicles will undoubtedly be affected by these regulations.

Conclusions

It is shown that for both power / heat generation and transport applications there is a wide variety of possible alternatives that could be applied for military use. Many new coal technologies such as dry micronized coal, fluidized bed, flue-gas desulfurization, coal gasification, combined cycle and advanced combustors are currently being implemented and designed[42].

Energy use in the military could also be significantly affected by new energy management systems and implementation of modified, more efficient , conventional technology.

Fuel cells appear to be a fast emerging technology for both generation and transport applications, with small scale power applications currently closest to proven commercial use. Numerous commercial and demonstration programs are underway regarding use of alternative fuels in transportation. Many of these, including fuels for fuel cell use, could use coal as a feed stock if processed by gasification or liquefaction either on site or at processing plants prior to distribution.

15.6 Subtask 5.6 Constructing a National Energy Portfolio which Minimizes Energy Price Shock Effects

Progress has been achieved in two areas: data collection and fundamental theory. Price series have been obtained for natural gas and petroleum. Preliminary studies of petroleum prices show the existence of GARCH disturbances in this series, indicating that modeling the portfolio in a GARCH model is appropriate. Portions of the prices series for coal have also been obtained. The prices series for coal will either be the spot price paid by electric utilities for Power River Basin coal (Colorado source) or the spot price paid for Appalachian coal. These price series are being gathered from reports to the FERC by electric utilities. The use of contract prices of coal is avoided to get better estimates of the true coal price volatility in the market. Other issues that may be addressed are external environmental costs of energy that perhaps should be included in a price analysis and the size and existence of a security premium on oil. These issues should be addressed when

Table 15-16. Alternative Fueled Vehicle Targets for the Federal Fleet as proposed in Two Pieces of Legislation.

Fiscal Year	EPACT Requirements	Executive Order 12844
1993	5,000	7,500
1994	7,500	11,250
1995	10,000	15,000
1996[1]	25% of acquisitions	-
1997[1]	33% of acquisitions	-
1998[1]	50% of acquisitions	-
1999[1]	75% of acquisitions	-

Source : EIA .June 1994.

Notes:
[1]Percentage of acquisitions in these years is based on light duty vehicle acquisitions. The Executive Order did not provide AFV targets or percentage acquisition for these years.

the actual portfolio is created because they affect energy return on investment but are not important to the GARCH analysis.

The theory side of the problem is challenging. Fundamental theory provides the objective function that the user will to maximize or minimize. The original goal of finding a portfolio that minimized the risk of an energy price shock due to potential macroeconomic effects of such a shock was naive, and many other factors should be considered. If a group of series all have positive covariances, then the minimum variance portfolio will simply be the price series with the lowest variance. Such an analysis ignores the price of that commodity. If pure price stability was the goal we could transfer to coal or synthetic renewable fuels. Therefore the goals of energy policy must be further defined. Two fundamental goals may be low volatility and low prices. The benefit of such a policy should be increased economic efficiency and growth. Currently, the problem of formally modeling such a theory so that after the GARCH variances and covariances are calculated is being worked on so that the portfolio can be determined.

15.7 Subtask 5.7 Proposed Research on the Coal Markets and their Impact on Coal-Based Fuel Technologies

Two Ph.D. theses were competed in Subtask 5.7. The first was completed by Jørn Aabakken and entitled, "Fuel Use in United States Electric Utilities, Developments 1947-1993." This research is summarized as follows:

Fuel use in the United State Electric Utility industry has varied across time as well as within the regions of the United States.

Coal is identified as the single largest energy source in the electric utility industry, with nuclear power emerging as the next largest fuel source.

Fuel use within the regions varied greatly, with the eastern states being the most dependent on coal and nuclear power. The western states were less dependent on coal and used more hydroelectric and gas as inputs to energy. This is especially true for the pacific region.

The history of power plant additions by fuel show that coal has been the single most popular energy source. Oil was a significant input to electricity production until the middle of the 1950s, then experienced a revival in the 1970s for a decade. At the end of the 1970s, oil was no longer popular, but has seen a revival since 1990.

Nuclear power emerged rapidly as a major fuel in the 1970s and is currently responsible for nearly a quarter of electricity production. Regulatory pressures slowed down nuclear power to no additions since 1990.

The second thesis, was conducted by Yuliang Li and was entitled, "Market Structure and Reorganization of the U.S. Electric Utility Industry: A New Proposal." This research is summarized as follows:

Although the organizational structure of the electric utility industry has been well-established, development of the economy and technologies, both on the consumption side and on the supply side, demand the old system be chained. Several restructuring proposals have emerged in recent years. The purpose of this thesis is to design a more realistic and practical one. Through a theoretical model, this thesis first points out that it is the cost of electricity transmission that determines the potential of market competition. By analyzing the actual capability of long distance transmission,, this thesis demonstrates the feasibility of making this sector competitive. Further cost analysis also supports this conclusion, at least for populated metropolitan areas. On the other hand, similar analysis derives the opposite conclusion for the distribution sector. Based upon these findings, technological reality and constraints, the structure of this industry, configurations of the existing transmission system, and in reference to other proposals, this thesis proposes a new market-oriented approach. Given the feasibility of transmission competition, once the restrictions imposed by regulations are removed, transmission competition will occur automatically among neighbor utilities. Consequently, generation competition and competition between transmission and distribution will also take place; organizational structure will evolve. All these changes are based upon market force.

15.8 Subtask 5.8 Integrate the Analysis

No work was scheduled in Subtask 5.8

16.0 PHASE III, TASK 6 FINAL REPORT/SUBMISSION OF DESIGN PACKAGE

No work was scheduled in Task 6.

17.0 MISCELLANEOUS ACTIVITIES

Two project review meetings were hosted at Penn State. The first was held on May 11, 1995 and was attended by representatives from DOE, the Department of Navy, U.S. Corps of Engineers, Construction and Engineering Research Laboratory, and Penn State. The second was held on September 21, 1995 and was attended by representatives from DOE and Penn State.

A paper was presented at the 20th International Technical Conference on Coal Utilization & Fuel Systems held at Clearwater, Florida on March 20-23, 1995. The title of the paper was "A Comparison Between Firing Coal-Water Slurry Fuel and Dry, Micronized Coal in an Oil-Designed Industrial Watertube Boiler" and was coauthored by Bruce G. Miller, David A. Bartley, Roger L. Poe, and Alan W. Scaroni.

A paper was prepared and presented at the Eleventh Annual Coal Preparation, Utilization, and Environmental Control Contractors Conference held at Pittsburgh, Pennsylvania on July 12-14, 1995. The title of the paper was "Developing Coal-Based Fuel Technologies for DOD Facilities" coauthored by Bruce G. Miller and Alan W. Scaroni.

18.0 NEXT SEMIANNUAL ACTIVITIES

During the next reporting period, the following will be done:

- The Phase I final report draft will be submitted to DOE.
- Appropriate commercial NO_x and SO_2 technologies for installation on an industrial boiler will be identified, the systems will be designed, and component procurement will begin for installing them on the demonstration boiler.
- Work will continue on designing and installing a ceramic bagfilter on the demonstration boiler.
- Bench-scale and pilot-scale emissions activities will continue with algal capture of trace metals and CO_2, and will begin with low-temperature NO_x and SO_2 catalyst development.
- Work will continue in the refinement and optimization of coal grinding and MCWM preparation procedures.
- Work will continue on determining cost and market penetration, selection of incentives, and regional impacts of coal-based fuel technologies. In addition, work will continue in developing a national energy portfolio.

19.0 REFERENCES

1. Davidson, J. E., Hartsock, D. K., Conley, A. D., Hein, R. L. and Schanche, G. W., Overview of Slagging Coal Combustor Systems as Applied to Army Central Heat Plants, Technical Report, USACERL, E-91/04,

2. Miller, B. G., Bartley, D. A., Hatcher, P., Knicker, H., McConnie, J., Moulton, B., Morrison, J. L., Pisupati, S. V., Poe, R. L., Sharifi, R., Shepard, J. F., Xie, J., Xu, G., Scaroni, A. W., Hogg, R., Chander, S., Cho, H., Ityokumbul, M. T., Klima, M. S., Luckie, P. T., Rose, A., Addy, S., Chidley, P., Considine, T. J., Gordon, R. L., Harley, K., Jung, G. C., Kocagil, A. E., Lazo, J., Li, P. C., McClain, K., Schaal, A. M., Painter, P. C., Veytsman, B., Morrison, D., Englehardt, D. and Sommer, T. M., The Development of Coal-Based Technologies for Department of Defense Facilities, Semiannual Technical Progress Report for the Period 09/28/1994 to 03/27/1995, U.S. Department of Energy Pittsburgh Energy Technology Center, DE-FC22-92PC92162, April 28, 1995.

3. Knicker, H., Hatcher, P. G. and Scaroni, A. W., Solid-State ^{15}N NMR spectroscopy of coal, *Energy & Fuels*, 1995, 9, pp.999-1002.

4. Knicker, H. and Ludemann, H. D., N-15 and C-13 CPMAS and solution NMR studies of N-15 enriched plant material during 600 days of microbial degradation, *Organic Geochemistry*, 1995, 23, pp.329-341.

5. Knicker, H., Ludemann, H. D. and Haider, K., Investigation about the Incorporation of NH+4 during composting of Organic Residuew by Means of ^{15}N-CPMAS-NMR-Spectroscopy, *European Journal of Soil Science*, 1996a, sunmitted, .

6. Knicker, H., Hatcher, P. G. and Scaroni, A. W., A solid-state ^{15}N NMR spectroscopic investigation of the origin of nitrogen structures in coal, *International Journal of Coal Geology*, 1996b, in press, .

7. Berkaloff, C., Casadevall, E., Largeau, C., Metzger, P., Peracca, W. and Virlet, J., The resistant polymer of the walls of the hydrocarbon-rich alga *Botryococcus braunii*, *Phytochemistry*, 1983, 22, pp.389-397.

8. Hatcher, P. G., Spiker, E. C., Szeverenyi, N. M. and Maciel, G. E., Selective preservation and origin of petroleum-forming aquatic kerogen, Nature, 1983.

9. Knicker, H., Scaroni, A. W. and Hatcher, P. G., ^{13}C and ^{15}N NMR spectroscopic investigation of the formation of fossil algal residues, *Organic Ceochemistry*, 1996c, submitted, .

10. Maillard, L. C., General reaction between amino acids and sugars: the biological consequences, *C.R. Soc. Biol.*, 1917, 72, (599-601), .

11. Boon, J. J. and de Leeuw, J. W., Amino acid sequence information in proteins and complex proteinaceous material revealed by pyrolysis-capillary gas chromatography-low and high resolution mass spectrometry, *Journal of Analytical and Applied Pyrolysis*, 1987, 11, pp.313-327.

12. Yildirim, K., On the Mathematical Modeling and Optimization of Grinding Circuits, M.S. Thesis, 1987, The Pennsylvania State University.

13. Miller, B. G., Bartley, D. A., Morrison, R., Poe, R. L., Sharifi, R., Shepard, J. F., Xie, J., Xu, G., Scaroni, A. W., Hogg, R., Chander, S., Cho, H., Ityokumbul, M. T., Klima, M. S., Luckie, P. T., Rose, A., Addy, S., Considine, T. J., Gordon, R. L., Lazo, J., Li, P., McClain, K., Schaal, A. M., Szczesniak, P., Walsh, P. M., Painter, P. C., Veytsman, B., Morrison, D., Englehardt, D. and Sommer, T. M., The Development of Coal-Based Technolgoies for Department of Defense Facilities, Semiannual Technical Progress Report for the Period 03/28/1994 to 09/27/1994, U.S. Department of Energy Pittsburgh Energy Technology Center, DE-FC22-92PC92162, April 14, 1995a.

14. Miller, B. G., Bartley, D. A., Morrison, J. L., Poe, R. L., Sharifi, R., Shepard, J. F., Xu, G., Scaroni, A. W., Hogg, R., Chander, S., Cho, H., Ityokumbul, M. T., Klima, M. S., Luckie, P. T., Rose, A., Addy, S., Considine, T. J., Gordon, R. L., Lazo, J., Li, P. C., McClain, K., Englehardt, D. and Sommer, T. M., The Development of Coal-Based Technologies for Department of Defense Facilities, Semiannual Technical Progress Report for the Period 03/28/1994 to 09/27/1994, Semiannual Technical Progress Report, DOE/PETC, DE-FC22-92PC92162, April 14, 1995.

15. Krieger, I. M., *Adv. Colloid Interface Sci.*, 3, pp.111-136 (172).

16. Shook, C. A. and Rocko, M. C., Slurry Flow, Principles and Practice, 1991, Boston, Butterworth-Heinemann.

17. (WRI), W. R. I., World Resources: 1993-94, 1994, New York, NY: Oxford University Press, .

18. Cline, W., The Economics of Global Warming, 1992, Institute for International Economics: Washington, DC.

19. Manne, A. and Richels, R., Global CO2 Emission Reductions: The Impacts of Rising Energy Costs, *Energy Journal*, 1991, 12, pp.87-107.

20. Nordhaus, W., Rolling the DICE: The Optimal Transition Path for Controlling Greenhouse Gases, *Resource and Energy Economics*, 1993, 15, (27-50), .

21. Change, T. F. o. t. C. A. t. C., A Comprehensive Approach to Addressing Potential Climate Change, U.S. Department of Justice, Environment and Natural Resources Division,

22. Weitzman, M., Prices vs. Quantities, *Review of Economic Studies*, 1974, 41, pp.447-91.

23. Pezzey, J., The Symmetry between Controlling Pollution by Price and by Quantity, *Canadian Journal of Economics*, 1992, 25, pp.983-91.

24. Rose, A. and Stevens, B., The Efficiency and Equity of Marketable Permits for CO2 Emissions, *Resource and Energy Economics*, 1993, 15, pp.117-46.

25. (OTA), O. o. T. A., Changing by Degrees: Steps to Reduce Greenhouse Gases, Office of Technology Assessment,

26. (NAS), N. A. o. S., Policy Implications of Greenhouse Warming, National Academy Press,

27. Lovins, A. and Lovins, H., Least-Cost Climatic Stabilization, 1991, 16, pp.433-531.

28. Jaccard, M., Nyboer, J. and Fogwill, A., How Big Is the Electricity Conservation Potential in Industry, *The Energy Journal*, 1993, 14, pp.139-56.

29. Lin, S., A Computable General Equilibrium Model for U.S. Mineral Policy Analysis, unpublished Ph.D. dissertationw, 1991, West Virginia University.

30. Dervis, K., de Melo, J. and Robinson, S., General Equilibrium Models for Development Policy, 1982, Cambridge, MA: Cambridge University Press, .

31. Shoven, J. B. and Whalley, J., Applying General Equilibrium, 1992, New York, NY: Cambridge University Press, .

32. Hazilla, M. and Kopp, R., Social Cost of Environmental Quality Regulations: A General Equilibrium Analysis, *Journal of Political Economy*, 1990, 98, (853-73), .

33. Hanson, K. and Robinson, S., U.S. Social Accounting Matrix, 1987, Economic Research Service, USDA,

34. Khazzoom, D., Economic Implications of Mandated Efficiency Standards for Household Appliances, *Energy Journal*, 1980, 1, pp.21-39.

35. Jorgenson, D. and Wilcoxen, P., Reducing U.S. Carbon Emissions: An Econometric General Equilibrium Assessment, *Resource and Energy Economics*, 1993, 15, pp.7-25.

36. Manne, A. and Richels, R., Buying Greenhouse Insurance, 1992, Cambridge, MA: MIT Press, .

37. Boyd, R., Krutilla, K. and Viscusi, W. K., Energy Taxation as a Policy Instrument to Reduce CO2 Emissions: A Net Benefit Analysis, *Journal of Environmental Economics and Management*, 1995, 29, pp.1-24.

38. Ayres, R. and Simonis, U., Industrial Metabolism: Restructuring for Sustainable Development, 1994, New York: United Nations University Press, .

39. EIA, Alternatives to Traditional Transportation Fuels: An Overview, DOE/EIA-0585/0,

40. MacDonald, J. M. and Gettings, M. B., Military EMCS: Implications for Utilities, Cities and Energy Services, *Energy Engineering*, 1991, 88, (No. 4), pp.20-35.

41. Lin, M. and al., e., Development and Economic Analysis of Army Coal Conversion Program, *Proceedings of the 19th International Technical Conference on Coal Utilization & Fuel Systems*, Florida, USA, 1994,

42. State, P., The Development of Coal Based Technologies for Department of Defense Facilities: Semiannual Technical Progress Report for the Period 09/28/93 to 03/27/94. (Unpublished),

43. DOE, Annual Review,

44. Rose, A. Z., Labys, W. and Torries, T., Clean Coal Technologies and Future Prospects for Coal, *Annual Review of Energy and Environment 1991*, 1991, 16, pp.59-90.

45. DOE, Clean Coal Technology Demonstration Program Update 1993, DOE/FE-0299P, March, 1994.

46. DOE, The Investment Pays Off, *Third Annual Clean Coal Technology Conference*, Chicago, 1994,

47. DOE, Clean Coal Technology: "The Investment Pays Off", DOE/FE-0291, January, 1994.

48. DOE, Comprehensive Report to Congress: Clean Coal Technology Program. "Completing the Mission", DOE/FE-0309P, May, 1994.

20.0 ACKNOWLEDGMENTS

Funding for the work was provided by the U.S. Department of Defense (via an interagency agreement with the U.S. Department of Energy) and the Commonwealth of Pennsylvania under Cooperative Agreement No. DE-FC22-92PC92162. The project is being managed by the U.S. Department of Energy, Pittsburgh Energy Technology Center (PETC). John Winslow of PETC is the project manager.

The following Penn State staff were actively involved in the program: Michael Anna, Glenn Decker, Howard R. Glunt, Samuel Gross, Robert Klemz, Ruth Krebs, Bradley Maben, and Ronald T. Wincek.